HIGH TEMPERATURE RESISTANCE OF REINFORCED CONCRETE BEAMS STRENGTHENED WITH

STEEL REINFORCED INORGANIC POLYMER (SRIP)

By

DANIEL CHIRSTOPHER GREK

A dissertation submitted to the

School of Graduate Studies

Rutgers, The State University of New Jersey

In partial fulfillment of the requirements

For the degree of

Doctor of Philosophy

Graduate Program in Civil and Environmental Engineering

Written under the direction of

P.N. Balaguru

And approved by

_____

_____

_____

_____

New Brunswick, New Jersey

October, 2017

ABSTRACT OF THE DISSERTATION

HIGH TEMPERATURE RESISTANCE OF REINFORCED CONCRETE BEAMS STRENGTHENED WITH

STEEL REINFORCED INORGANIC POLYMER (SRIP)

By DANIEL GREK

Dissertation Director:

P.N. Balaguru

Use of Fiber Reinforced Polymer (FRP) composite in infrastructures has steadily increased over the last two decades. The primary use is still for repair, rehabilitation and strengthening of structural elements made of reinforced or prestressed concrete. FRP has substantial advantage over classical structural materials such as steel in the area weight, strength, and durability against corrosion. Two major drawbacks of FRP are the lack of fiber resistance and brittle fracture of high strength fibers. The results presented in this dissertation address these two issues. High strength steel wire, commercially known as "Hardwire," was used in combination with inorganic matrix. The inorganic matrix, similar in chemistry to Portland cement matrix, is more compatible with steel than organic polymers. In addition, the matrix can withstand more than 2000°F with no smoke, or toxins. The larger fiber diameter, as compared to thin carbon or other high strength fibers, and non-simultaneous failure of wires provide better ductility as compared to classical FRP.

The experimental and analytical investigations were tailored to evaluate steel reinforced inorganic polymer (SRiP) composite at high temperatures. Rectangular reinforced concrete beams strengthened with SRiP on the tension side were tested with high moment section exposed to temperatures upwards of 1000°F. The beams were loaded in four point loading, and the maximum moment section at the midspan was heated using hot plates. Heating and cooling were repeated three times to establish the robustness of the repair at high temperature. After this cyclic exposure, Beams were tested to failure. Control beams with no strengthening and control strengthened beams that were not exposed to high temperature were also tested to compare the behavior of SRiP beams with carbon FRP strengthened beams. The results show that SRiP strengthened beams behaved similarly to classical FRP strengthened beams and can withstand higher temperatures without losing load capacity. Note that most polymers cannot withstand more than 300°F and carbon fibers start to oxidize around 800°F.

Overall results presented in the dissertation show that inorganic polymer-steel fiber, high strength composite is a viable FRP for strengthening and rehabilitation. The added advantages are high temperature resistance and improved ductility.

ACKNOWLEDGEMENTS

This work would not have been possible without the assistance and support of a great many

other people. First, and foremost of which I would like to thank my advisor Dr. P. N. Balaguru.

Your wisdom and patience has allowed me to move through this project while also continuing to

move through life. Your Advice over the years has been invaluable to my development as an

academic and is a major reason I find myself teaching as I am today.

I would like to extend a special thanks to my committee members: Dr. H. Najm, Dr Y. Yong, and

Dr. J. Yi. Not only did they play an integral part in the process of this doctorate research, but sat

through my proposal, which I consider to be a strong candidate for worst presentation I have

given in my entire life. Further thanks go to Dr. H. Najm, as an ever available consultant during

my time teaching in the Civil Engineering lab courses. Dr N. Gucunksi gave me opportunity make

my way in graduate school by teaching and for that I will always be grateful. I would be remised

if I did not thank Prof. S. Medlar who inspired the way I approached engineering and the way I

conduct myself in the classroom.

The staff of the Civil Engineering department provided a great deal of support for all manner of

things. Linda Szary and Gina Cullari were both guiding hands and sympathetic ears over the

course of this work. Ed Wass could always be found when the logistics started getting out of

hand.

I had a handful of student help as well, whether undergraduate assistants or graduate level

peers. Alicia Plinio, Nikhita Ganji, TJ Dembia, Abanda Abanda, and Justin Bewley were

indispensable in the collection of data and processing of samples. Brian Pailes helped make the

pouring of those initial beams possible. Matthew Klein, it was a pleasure to learn both from and

with you. Chris Mazzotta, you were perhaps the one person I could always get a hold of no matter what and a firm friend.

To all my coworkers who pushed me to finish, it was a tremendous help having you in my corner as the deadlines approached.

I have countless friends and family who have supported me along the way. My parents, Jeff and Mary, who allowed me to live rent free while all this work was going on. Gabrielle Moore, who followed along to help combat the black hole that is working on a dissertation while working full time. Geoff Ming, who I hope to support in his current PhD process as he did for me. For all those not named, I thank you all equally as well, I just fear giving you the pages you deserve would turn this dissertation into a novel.

And I leave for last Becca Dagnall, now Becca Grek, who since the start of my graduate program became my friend, partner, anchor, biggest fan, harshest critic, wife, mother of beagles, and the only thing that could mean more to me than completing this journey.

TABLE OF CONTENTS

LIST OF TABLES

LIST OF FIGURES

CHAPTER 1 – INTRODUCTION

This dissertation details the investigation into the use of Steel Reinforced Inorganic Polymer (SRiP) composite in strengthening of reinforced concrete beams and, more specifically, the ability of SRiP composite to maintain performance in the presence of extreme heat events better than its common fiber reinforced polymer (FRP) composite counterparts. The combination of high strength steel wires and alkali-aluminosilicate geopolymer creates a durable composite that exhibits similar strength to and improved ductility over carbon or glass fiber with an organic epoxy matrix. Heat testing was performed on reinforced concrete beams with SRiP to see the resilience of the inorganic matrix and steel to several cycles of extreme temperature. These beams were then tested to failure in four point bending along with control samples to determine the permanent damage to the composite due to high temperature exposure and compared load-deflection performance to the non-heated samples. Additional testing investigated the ability of inorganic polymers to bond to surfaces with little preparation or with previous polymer exposure and the effect of several additives that can aid with composite bonding.

Chapter 2 presents an overview of the history of FRP systems in Civil engineering as well as common installation techniques and some field practices for composite based repair systems. Recent increases in bridge and road fires will be addressed to highlight the most prominent flaw in classical FRP. Uses of both inorganic polymer and high strength steel wire will be detailed. At the conclusion of the chapter the combination of the two, forming what is now referred to as SRiP, will be explored.

Chapter 3 will focus on two major categories, the mechanical properties of the inorganic polymer, high strength steel wire, and SRiP composite and preliminary testing used to select the

inorganic polymer formula used for this dissertation. Details of the polymer selection will be given in this chapter, one of the most important criteria being the workability of the mix. The selection criteria for the high strength steel wire will also be stated. Results of preliminary tests will be listed to better illustrate the material selection process. These tests were designed to demonstrate the ability of different combinations of geopolymer matrix and steel wire to be easily and effectively bonded to a masonry surface.

Full scale testing of various control beams in four point deflection is described in Chapter 4. Manufacturing of beam samples and properties of the concrete will be reported early on in this chapter. Details on sample preparation methods used in this experiment appear first in Chapter 4. Comparisons will be drawn between normal surface preparation for organic epoxies and a less intensive process needed for inorganic polymers. Material installation and curing for the samples will be outlined but, discussions on adapting to a more commercial use will be done in a later chapter.

Chapter 5 introduces the effects of exposure to high heat on the SRiP repair materials. Two types of testing are addressed, the cycling of heat on the tension surface of a reinforced beam and the subsequent testing in flexural failure in an identical case to the controls in Chapter 4. Description of the experimental set up and qualitative and quantitative analysis of any damage from the high heat conditions will be reported in detail. After a brief refresher on the set up of the flexural tests, load deflection reactions of the heated beams will be compared to those of the control specimens to demonstrate the ability of the SRiP reinforcement system to maintain structural validity in the presence of extreme temperatures.

The discussion will be completed with a more thorough investigation into the analysis of data provided as well as recommendation for how to utilize the proposed system in a practical

setting. While a complete field investigation was not performed, insight was certainly gained

from laboratory testing in proper application methods and possible issues to look out for when

taking the system to a practical, structural application.

CHAPTER 2 – STATE-OF-THE-ART

2.1 Introduction

With the ever increasing age of structures and a similarly increasing cost of rebuilding them,

modern engineers have sought more economical methods to repair and retrofit existing

structures to enhance their lifespans. With the development of fiber reinforced polymer (FRP)

composites in the 1940's, Civil Engineers were presented with a strong and lightweight material

that could adhere easily to both concrete and steel surfaces. Over the next several decades and

continuing today, these composites have been adapted as a widely accepted method of repair

and retrofit for aging and damaged structures.

This chapter presents the State-of-the-Art, which focuses on: the history of FRP composites,

their main components (matrix and fibers), techniques used to apply FRP, the uses of FRP as a

strengthening tool, current issues found with traditional organic FRP systems, and Steel

Reinforced Inorganic Polymer (SRiP) systems. The latter subject, SRiP composites and systems,

will be the focus of this dissertation, specifically load/deflection behavior and response to high

temperature exposure.

2.2 History of Fiber Reinforced Polymer Composites

While structural applications of composite materials have been around since early man first

combined mud bricks with straw, the use of fiber reinforced polymer composites (FRP) for the

repair and retrofit of structures remains a relatively new technology. FRP are generally

composed of fiber tows or mats coated in and bound together with some kind of matrix. This

combination creates a strong but lightweight material seen today in everything from

construction, to vehicles, and even now phones. The journey to get to this material spanned

most of the 20th century and has revolutionized major commercial industries, most notably here, Civil Engineering.

2.2.1 Early Development of FRP Materials

Until the start of the 1900's the only adhesives and binding agents available were resins that could be obtained from organic material such as plants or animals (composite.about.com). The largest issue with simple organic resins is that as time passes the organic particles will deteriorate, causing the bonds the resins create to break down. The organic degradation forces users to repeat the repair expense and procedure with relative frequency in order to maintain a functioning item. With the boom of the Industrial Revolution, however, came the access to new technologies and manufacturing processes.

Around 1909, materials scientists started to develop thermosetting plastics, compounds that could be mixed in heat, molded, and then cooled to a set shape. The first of these plastics was phenolic plastic and in the coming years, vinyl, polystyrene, and polyester were created (Norwood et al, 1994). While these materials were not easily usable by the average citizen, commercially they allowed for cheaper production of some products and longer lasting resins. These plastics allowed much more freedom in the shapes they could be cast in and plastic parts greatly reduced the weights of manufactured objects, however, plastics proved to have nowhere near the strength of metals and heavier materials. This made plastics' use in the burgeoning automotive and aviation industries as well as military applications, the areas where decrease weight could make the largest difference, rather limited.

It wasn't until 1935 that two materials based inventions would pave the way for the creation of FRP as it is known today. That year, Dr. S.O. Greenlee of America and Dr. Pierre Castan of Switzerland both independently developed the first two part epoxy resins (Epoxy Chemical, Inc.

2013). Two part epoxy allowed for separate storage of chemicals that could be then mixed together in desired quantities either at a point of manufacture or in situ and then applied to a surface or mold. An exothermic reaction would then generate enough heat to cause the components to set as a solid resin. 1935 also saw Owens Corning, a company now prominently know for insulation, introduce the first glass fiber, which they simply termed "fiberglass" (composite.about.com).

Engineers of the 1940's learned that by encasing fiberglass in these new epoxy resins they could create a composite that is can be easily molded and then set to form a variety of shapes and contours. It had the moldability and weight of plastics but could resist much greater forces. Known as fiber reinforced polymers, the aforementioned "FRP," these composites found initial use in aviation and aquatics as parts for aircraft and boats. The demand for materials in World War II led to the use of FRP composites for a variety of Navy and Airforce equipment where lightweight and high strength were important. FRP was also found to allow radio frequencies to pass through with ease and was adapted to casings and shelters for radar equipment.

After the war, the new FRP techniques had to be adapted to commercial use and soon boat hulls were being created from fiberglass composites. A man by the name of Brandt Goldsworthy contributed a great deal to the creation of new manufacturing techniques, processes, and products including the first FRP surfboard and the method of "pultrusion," which is now used in everything from tool handles to pipes to medical devices. FRP composites eventually made a natural progression to the automotive industry in the late 1960's after the popularization of bulky muscle cars and the implementation of a federal highway system. Composite parts continue to be heavily used in all types of vehicles today as well as sports equipment and a variety of tools.

2.2.2 Adaptation of FRP to Civil Engineering

While after its creation, modern FRP was quickly adapted into aeronautical, nautical, and automotive applications, the transition to Civil Engineering was not as immediate. One of the first major uses of FRP in a structural engineering application more closely resembled the early nautical uses than current repair and retrofit uses seen in Civil Engineering. In 1950, an American company designed a house entirely out of FRP and called it, "The House of the Future." This structure gained a great deal of notoriety as part of Tomorrowland in Walt Disney's Disney World theme park. While full FRP homes became like several other of Tomorrowland's future technologies that never saw use as they were originally intended, the "House of the Future" did prove to be quite durable. In 1967, the house was scheduled for demolition and when the wrecking ball first struck it the house still stood. Workers were then forced to manually dismantle the house (March, November 2010. Throughout these early decades several conceptual or unique structures were developed with FRP, however, there was no major push as the materials were still relatively expensive to be used heavily in the construction industry, at least in the current FRP forms (Correia, March 2013).

So how did this technology become the structural FRP we know today? When engineers realized that the thermoset plastic resins could bond effectively to concrete surfaces the door opened for the application of fibers externally to structures in order to reinforce for flexure, shear, and seismic loading. FRP allowed engineers to add extra load capacity to existing structures with minimal increases in weight, FRP are known for having high ratios of strength increase to weight increase. To generate interest in the use of FRP for repair and retrofit of structures the National Science Foundation (NSF) and Federal Highway Administration (FHWA) issued grants and financial support to various research institutions. Throughout the 1980's these two

organizations helped further research into FRP practices (Dawood and Rizkalla, 2014). As the 1980's and 1990's rolled on, a need for faster construction and desire to rehabilitate existing structures increased. FRP proved to allow for faster construction speed due to a relatively simple installation process and the drastic increases in strength made retrofitting of existing structures a more viable option for construction companies. Acceptance of FRP by the construction industry increased and has since become more widely used and researched in recent years.

2.2 Matrix

The first component of a fiber reinforced polymer composite is the matrix that bonds the reinforcement fibers to the desired surface. A matrix can generally be characterized as either organic or inorganic. Organic matrices are more commonly utilized for FRP currently but do have some drawbacks when used to repair structures. Organic matrices can provide 100% permeability barriers when applied to a concrete surface. While low permeability is desired to prevent corrosion in reinforcing steel inside of concrete, in the case of a completely impermeable exterior coating, vapor pressure can be trapped and lead to spalling in the concrete beneath the coating and subsequent delamination. Organic matrices also deteriorate with exposure to UV light and high temperatures. Inorganic matrices, while not 100% permeable, prevent major penetration of materials but also allow for the release of vapor pressure. Inorganic matrices also show resistance to both UV light and high temperatures.

2.2.1 Organic Matrix

Organic matrices can be split into two basic categories based upon number of components, either single component or multi-component. Multi-component matrices are normally considered to have better adhesion to surfaces and mechanical properties than single

component matrices. The most common multi-component organic matrix is a two part matrix. These consist of a "Part A" component, normally a resin, and a "Part B" component, some kind of activator or hardening agent. When these components are mixed together they have a pot life that can range anywhere between 15 to 120 minutes at room temperature.

Different formulations of organic matrix are created depending on the desired application and material to be adhered to. The matrix must work with both the surface being repaired and the desired fiber reinforcement in order to properly function. The environment that the matrix can be used also depends on the type of organic matrix selected. Workability and pot life must be selected based on the requirements of of ACI 440. Surface preparation is also an intensive process with organic epoxies. For concrete applications surfaces must be ground to expose coarse aggregate and the surface must be dry, with no dust or loose particles. In addition, organic matrixes should not be applied in temperatures below 40°F.

The subsequent sections will provide further details on four major types of organic matrices: Epoxies, latexes, polyurethane resins, and polyester resins.

2.2.1.1 Epoxies

Epoxies are a two-component organic matrix consisting of a resin and activating agent as mentioned in Chapter 2.2.1. These materials are sensitive to changes in their mixing ratios, as such, manufacturer guidelines should be strictly followed and the ingredients should be fully mixed. The tensile strength of epoxies can range from 500 to 7000 psi, while the compressive strength can range from 500 to 12,000psi (ACI Committee 503). Elongation of an epoxy ranges drastically from 0.2 to 150 percent. Epoxies provide a variety of resistances to a variety of chemical issues, including: deicing salts, gasoline, oil, alkalis, muriatic acid, sulfates, and wet-dry

cycling. Table 2.1 below details the general performance of epoxy compared to concrete when exposed to certain chemicals, as outlined in ACI 503.

Type of Chemical Exposure	Expoy Performance	Concrete Performance
Wet-Dry Cycling	Excellent	Excellent
Chloride Deicing Salts	Excellent	Fair
Muriatic Acid (15% HCl)	Excellent	Poor
Foods Acids (Dilute)	Good	Poor
Sugar Solutions	Excellent	Fair
Gasoline	Excellent	Excellent
Oil	Excellent	Excellent
Detergent Cleaning Solutions	Excellent	Excellent
Alkalies	Excellent	Good
Sulfates	Excellent	Fair

Table 2.1 Chemical Properties of Epoxy and Concrete (Adapted from ACI 503)

Over the last few decades, epoxies have been used in many different fashions. The most prominent uses for epoxies tend to be as either a decorative or protective coating for an exterior surface, as the adhesive matrix in FRP composite systems, for various submerged applications, and in epoxy modified concretes. . Epoxy resins can be drastically affected by the surface they are applied to if it is not properly prepared. As with other organic matrices a solid, clean, and dry surface is require to insure a proper bond and surface and air temperature must be considered to properly cure the epoxy. Epoxies are commonly applied with a brush or roller; however, it is possible to also apply them to a surface via spraying equipment. Should the surface to be coated possess a large number of visible pores, multiple layers of epoxy may need to be applied.

2.2.2.2 Latexes

When talking about latexes, a wide array of organic matrices could actually be referenced, including the aforementioned epoxies. For the purposes of this dissertation, latex will be primarily used to reference thermoplastic and elastomeric latexes. Thermoplastics include: polyacrylic ester, styrene-acrylic, vinyl acetate, polyvinyl acetate, polyvinyl proponate, polypropylene, and also epoxies. Elastomeric latex is split into both natural rubber latex and a variety of synthetics.

Latexes see common use in situation that require: protecting reinforcement from corrosion, water resistance as a coating or a liner, repair of spalling concrete, leveling of floors, and bonding of fresh concrete with hardened concrete layers.

2.2.2.3 Polyurethane Resins

Polyurethane resins are another two-component organic matrix system that consists of a resin known as polyol and an activating agent known as isocynate. It is possible with some polyurethane resins to air cure in place of a using an activator. Polyurethane coatings are used to protect concrete from deicing salts and other chemicals, preventing the growth of fungus on concrete, or mixed with pigments and used as a decorative coating. Surfaces should be dry when this type of organic matrix is applied.

2.2.2.4 Polyester Resins

Polyester Resins are another popular two-component organic matrix, consisting of the base resin and a catalyst that speeds the curing process. There are many different formulations of polyester resins commercially available. The curing process of polyester resin is greatly inhibited by exposure to water or air. To prevent issues in curing two additional steps are added when a

polyester resin is used in an application. A base coat of a material that is unaffected by water must be applied before the resin and to reduce air exposure a material, such as paraffin wax, must be applied to the resin as a top coat.

2.2.3 Inorganic Matrices

While organic matrices have seen wide use for decades and over that period have proven effective in a variety of applications they still possess a set of negative features that can hinder their use in FRP systems. Beyond the weakness to UV light and heat mentioned earlier organic matrices are subject to natural deterioration and increase in brittleness from the presence of organic compounds. These issues can arise over a relatively short period of time, around a five to ten year period, which can result in the need for further repair and incurred costs.

The easiest way to circumvent the issues of organic deterioration is to avoid using organic material in your system. These matrices are commonly referred to as inorganic matrices and several types have been identified for use with concrete repair, the main material focus of this dissertation. The major benefit in most of these systems is that their properties closely resemble that of the concrete itself which can lead to a much more uniform composite structure. Inorganic systems also provide resistance to high temperatures, show stability when exposed to UV light, suitable hardness, and non-toxic properties.

The most common inorganic matrix is Portland cement; however, for FRP applications were thin coatings are often preferred the relatively large grain size of Portland cement is not ideal. Other inorganic systems include: dry-pack mortar, proprietary repair mortars, fiber-reinforced mortars, grouts, low-slump dense concrete, magnesium-phosphate concrete and mortar, preplaced-aggregate concrete, rapid setting cements, shotcrete, shrinkage-compensating concrete, silica fume concrete, and alumino-silicate polymers (ACI Committee 503 and 548,

2007). Alumino-silicate polymers, specifically Potassium alumino-silicate, will be detailed in the next section as they are one of the primary components of the research done for this dissertation.

2.2.3.1 Background of Potassium Alumino-Silicate

A severe outbreak of fires in France during the 1970's lead Joseph Davidovits, a French scientist, to research into the area of new fire resistant materials. From his research he developed a new type of inorganic "plastics" that proved to resist damage from fire and high temperature (Davidovits, Synthesis of New High-Temperature Geo-Polymers for Reinforced Plastics/Composites, 1979). Due to the geologic origin of several main components and the similar properties of the material to minerals such as feldspar, the new family of materials was called Geo-polymers. Geo-polymers possess smooth surfaces, relative hardness, weather resistance, and thermal stability and resistance potentially exceeding 2000°F. Though these materials share much in common with geological minerals, they are still polymers and therefore can be manipulated and molded with relative ease. Geo-polymers can be created and utilized in similar fashions to both organic resin systems and cementitious systems. Like their organic counterparts, geo-polymers can be manufactured with performance enhancing fibers or fillers should the application call for it. They also see use in the automotive, aerospace, civil engineering, and materials engineering industries like organic resins. Geopolymers have been tested with carbon glass, nylon, and steel fibers and fabrics and have been used in the creation of FRP systems for the strengthening of reinforced concrete elements (Balaguru et al., 1996, Lyon et. al., 1997, Foden et al,. 1997, Foden et al., 1996b, Foden et al., 1996c).

2.2.3.2 Chemical Make-Up and Properties

Potassium aluminosilicate is also referred to by term, polysialate or poly(sialate-siloxo). Sialate or sialate-siloxo is an acronym for silicon-oxo-aluminate of sodium, potassium, calcium, or lithium. Structurally, sialate is composed of tetrahedrals of silicate, SiO_4, and aluminate, AlO_4 sharing oxygen atoms. For potassium aliuminosilicates, the type of geopolymer considered in this dissertation, aluminum ions in the reaction gain a negative charge which is balanced out by positive K^+ ions. The formula for potassium polysialate can be written as:

$$Kn\{-(SiO_2) - AlO_2\} \cdot H_2O \qquad\qquad (2.1)$$

where z is normally 1,2, or 3 and z>>n, the degree of polycondensation. Polysialates are characterized as chain or ring polymers. Potassium polysialate has the chemical formula $Si_{32}O_{99}H_{24}K_7Al$. Potassium aluminosilicate resins harden into a glassy, amorphous solid. Figure 2.1 below shows a representative structure of the cured inorganic matrix as determine by Si magic angle spinning magnetic resonance spectroscopy (Si MAS-NMR), x-ray diffraction, and elemental composition (Davidovits, 1991).
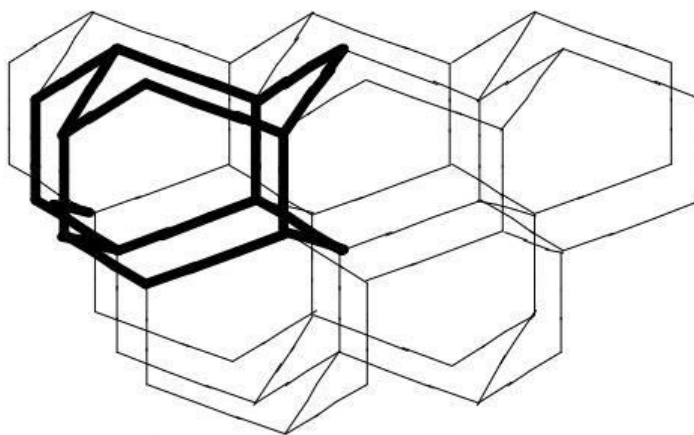
Figure 2.1 Chemical Structure of Potassium Polysialate (Klein, M.J., 2013)

Potassium Aluminosilicate matrix has two basic components, a liquid Part A and a solid

component blended from several powder materials. Filler materials can also be added in to

affect the properties of the matrix such as fibers, retarders, wetting agents, and water to

increase workability of the inorganic polymer. Mixing of the two components is performed in a

high shear mixer which is capable of blending the ingredients and reducing the particle size of

the constituent materials. The liquid component is first placed in the mixing apparatus and the

solid component is introduced carefully to avoid any loss of material. Ingredients are mixed for a

period of 60-90 seconds depending on the specific blend and then allowed to sit for a 30 second

rest in order to not overheat the equipment or material. The sides of the mixing container are

scrapped to ensure that no solid material remains unmixed and blending then occurs again for

30-60 seconds. Application of the polymer can be done with common painting tools such as

brushes, rollers, or sprayers, or in some cases with a trowel. Initial optimal curing was determine

to be around 12 hours at no less than 79°C, however, more recent blends will cure effectively

after 3 hours at 20°C. This is also far more practical for most applications and has little impact on

the properties of the material. The workability of potassium aluminosilicate has been found to

be up to 4 or 5 hours, though 3 hours is generally accepted to add a factor of safety. Should a

longer work time be required the pot life can be extended by placing the material in a cool

environment, a refrigeration unit or portable cooler depending on work environment.

Thorough, ongoing testing of potassium aluminosilictate's mechanical properties has been

carried out at Rutgers University under the guidance of Dr. P.N. Balaguru with support from the

National Science Foundation, Federal Aviation Administration, and the Connecticut Department

of Transportation. The results listed below represent testing efforts of Andrew J. Foden and

Ronald J. Garon in conjunction with Dr. Balaguru and was originally presented in their respective

Phd dissertations (Foden, 1999 and Garon, 2000). As part of the testing, different curing regimes

were used for different sets of samples which include curing in: 100°F for 6 hours, 140°F for 6 hours, and 175°F for 24 hours after completion of mixing and sample production.

Compression, Strain, and Modulus of Elasticity: Compression testing was performed under the guidelines of ASTM D695 Standard Test Method for Compressive Properties of Rigid Plastics (ASTM D695, 2010). Five cylinders of potassium aluminosilicate, measuring 1 inch in diameter and 3 inches tall, were tested in a 10kip capacity Sintech 10GL frame. Data from the samples was recorded and stored by a computer controlled data acquisition program. Testing rate was set at 0.05 inches per minute and average compressive strength was determined to be 5,665 psi. While compressive testing was performed, a separate Instron extensometer was used to record the strain capacity of the samples. This data not only identified the failure strain for potassium aluminosilicate, but also allowed for the determination of elastic modulus. These results were 0.49% and 1.4×10^6psi, respectively. It should also be noted the stress-strain graph remained linear until failure showing the potassium aluminosilicate to be a brittle, linearly elastic material.

Tension: Tensile strength of the matrix was determined in this case with ASTM C496 Standard Test Method for Splitting Tensile Strength of Cylindrical Concrete Specimens (ASTM C496, 2011). For this test, five samples measuring 1 inch in diameter and 1½ inch long were utilized. Again, the samples were tested in a Sintech 10GL test frame with 10kip capacity and a controlled rate of 0.05 inches per minute. From the testing an average split tensile strength of 530 psi was determined.

Strain Capacity and Surface Energy: The research lead by Dr. Balaguru utilized a technique developed by Detersa et al, that originally determined properties of Kevlar fibers (Deteresa et al, 1984). In the test one side of an elastic rectangular beam is coated and the beam is loaded as a

cantilever. The Bernouli-Euler beam theory can be used to find tensile and compressive strains by observing the time the beam first cracks and the corresponding load that produces the crack.

The equation used is:

$$\varepsilon_u = \frac{My}{EI} \tag{2.2}$$

Where:

ɛu is the ultimate strain capacity calculated

$M = L_c \times P$, and is the bending moment when cracking is first observed

Lc is the distance from the loading point to the initial crack

P is the load when the initial crack is observed

Y is half the thickness of the beam

E is the elastic modulus of the rectangular beam

I is the moment of inertia of the rectangular beam

Using fracture mechanics and conservation of energy principles, the surface energy of the inorganic matrix was also determined. The equation for this case was:

$$\gamma = \frac{1}{4}\varepsilon^2 E a \tag{2.3}$$

Where:

γ is the surface energy in joules per unit of area

ε is the strain

E is the elastic modulus of the inorganic matrix

A is the debonded distance perpendicular to the crack in the organic matrix

The testing regime involved the coating of three 1 inch wide by 8 inch long by 0.06 inch deep steel beams in the potassium aluminosilicate geopolymer. Two tightly spaced clamps were used to hold the beam in place and ensure that there is a zero slope. Tension was achieved by hanging loads directly on the end of the steel beam, compression was achieved with a pulley to change the direction the forces act. Average tensile strain capacity was found to be 743 μin/in. Average compressive strain was found to be 5,173 μin/in favorably compared to the 4,900 μin/in from the compressive testing mentioned earlier. The average free surface energy was determined to be 0.994 x 10^{-6} Btu/in^2.

Flexural Strength: Testing for flexural strength, modulus, and failure strain followed ASTM D790 Standard Test Methods for Flexural Properties of Unreinforced and Reinforced Plastics and Electrical Insulating Materials (ASTM D790, 2010). For cylindrical specimens of 1 inch diameter and 7 inch length Samples were tested with an MTS Teststar system using mid-point loading at a deflection rate of 0.11 inches per minute. Deflections were measured with a spring loaded LVDT and recorded by the MTS system. The following data was obtained:

- Average flexural strength: 1.17 x 10^6 psi

- Average flexural modulus: 1.36 x 10^6 psi (compared to 1.4 x 10^6 psi from
    compression testing and 1.57 x 10^6 psi from dynamic elastic modulus testing,
    mentioned next)

- Failure strain: 860 μin/in which correlates to the 743 μin/in mentioned earlier

Dynamic Elastic Modulus: To test for dynamic modulus, the compressive wave velocity was measured passing through a sample. The sample was 1 inch diameter and 12 inches long and was affixed to a large steel cylinder. An accelerometer was connected to a Krenz PO 5050 Dynamic Signal Analyzer and attached to the free end of the specimen. This testing set up was used to record the acceleration and time history throughout the testing. The specimens were impacted by six different spherical strikers of varying sizes, three of the strikers steel and three of the strikers copper. Two specimens were tested with each striker for a total of twelve specimens. Using a Fast Fourier Transformation, the data collected was transformed and graphed to identify the frequency at which the peak value was located. The modulus was then calculated using the frequency of the first three modes, which were then averaged, and applied to the following equation:

$$E^* = (4f_n \frac{L}{n})^2 \rho \tag{2.4}$$

Where:

Fn is the natural frequency of the nth mode of vibration

n is equal to 1, 3, 5,…

L is the specimen length

ρ is the density of the material

The elastic modulus was calculated to be 1.57 x 10^6 psi, which matches well with both the compression and flexural testing.

Dynamic Shear Modulus: Dynamic shear modulus was experimentally determined using methods governed by ASTM D4015 Standard Test Methods for Modulus and Damping of Soils by

Resonant-Column Method (ASTM D4015, 2007). This style of testing has procedures for Young's

modulus, shear modulus, and shear damping for solid cylindrical samples. To find the resonant

frequency of the sample a quasi-static torsional simple shear and resonant column apparatus

supplied by Soil Dynamics Instruments, INC. combined with an oscilloscope were both used.

Shear Modulus can be found using the dynamic modulus and the following calculation:

$$v = \frac{E^*}{2G^*} - 1 \qquad\qquad (2.5)$$

Where:

    E* is the dynamic Young's modulus as determined through testing

    G* is the dynamic shear modulus

    v is the Poisson's ratio of the material

Two glass rods of 1 inch diameter and 12 inch length were used for the test. The average

dynamic shear modulus was found to be 0.706 ksi. Entering this value into the equation above

results in a calculated Poisson's ratio of 0.244, which favorably compares to an expected

Poisson's ratio for glass of 0.245.

Durability Testing: In more recent testing at Rutgers University, the durability of aluminosilicate

geopolymer was investigated to better understand its repair potential of the inorganic coating.

Using a PosiTest AT-M Manual Adhesion Tester and the guidelines of ASTM D7234 Test Method

for Pull-Off Adhesion Strength of Coatings on Concrete using Portable Adhesion Testers, pull-off

tests were performed during various stages of freeze/thaw cycles and wetting. Samples showed

an average decrease in pull-off strength of 15-20% at the end of 30 cycles of freeze/thaw.

2.3 Fibers

The second component required for an FRP composite is fiber tows or mats. Fiber provides strength and stiffness to the composite which, for civil engineering applications, determines many of the design requirements for repair and retrofit applications. While traditionally in concrete reinforcement fibers of various types tend to be short, from 1-2 inches to 3-6 mm, FRP composites generally deal with much longer strands. This allows for better transfer of loads when applied to a beam for tension reinforcement or when wrapping a column to confine it. Fibers themselves can be applied as tows or as fabrics. Tows are bundles or individual fibers that are treated as one individual strand during application. Fabrics or mats are comprised of fibers and tows that are weaved together to create a larger reinforcement piece that can be easier in some cases to install. The main benefit to fabrics is the ability to orient fibers in various directions, allowing for easy multi-axial reinforcement or simple shear and torsion reinforcing (ACI 440R). Certain properties must be considered when selecting an FRP system as they greatly affect its performance. Those factors include (ACI 440R): Orientation of the fibers, shape, composition of the fibers, mechanical properties of the matrix, bond and adhesion between the fibers and matrix. There are several types of fibers commonly used in FRP systems, those being glass, carbon, aramid or Kevlar, basalt, and more recently steel.

2.3.1 Glass Fibers

Though molten glass fibers have existed in some fashion for over 3000 years, it wasn't until 1935 when Owens Corning introduced a commercially available glass fiber, fiberglass, that glass fiber showed value in structural applications. Glass fibers are some of the most economical available which is partly why they found the highest usage in early FRP composites of the 1940's and 1950's. Even today, glass fibers are still the most commonly used in composites (Balaguru,

Nanni, and Giancaspro, 2009). These composite systems are sometimes referred to as the shortened, "GFRP."

Individual glass fibers can be about 13 or 14 microns thick. Mono-filament E-glass has an elastic modulus of approximately 1.06×10^7 psi and remains elastic until fracturing at around 2.5 to 3.5% strain. The main issues that can arise when using glass fibers are microscopic voids that can develop in the glass itself during the manufacturing process. If manufacturers cannot remove these voids then stress concentrations can be generated within the voids and entrapped air inside the voids can contain carbon dioxide, which is corrosive to glass overtime. Glass fiber can also corrode in alkaline rich environments, which makes it necessary for glass fiber to be combined with a relatively impermeable matric when used to repair concrete (Balaguru and Shah, 1992).

Glass fibers can be divided into several subtypes based on the composition of the glass. These include E, S, AR, R, and C-glass (ACI 440R). The most common types of glass used in the composites industry are E-glass and S-glass, with E-glass making up 90% of glass fibers used (Balaguru, Nanni, and Giancaspro, 2009).

2.3.1.1 E-Glass

E-glass is mainly composed of calcium-alumina silicate glasses. 80-90% of commercially produced glass fiber is E-glass. This is due to E-glasses classification as electronic grade glass. A modified version of E-glass called ECR-glass can be manufactured in applications that require higher acid resistance, such as in the presence of acid batteries.

2.3.1.2 S-Glass

S-Glass is the most expensive type of glass fiber usable in GFRP systems due to its high strength
and performance in the presence of high temperature. It has the highest strength of all the
types of glass. S-glass is composed of magnesium alumina-silicate (Miller, 1987; Gurit Composite
Technologies, 2008).

2.3.1.3 AR-Glass

AR-Glass fibers possess a higher alkali resistance due to zirconium oxide content of potentially
19% or higher.

2.3.1.4 R-Glass

R-Glass is similar to E-Glass in make-up but the amounts of alumina are greater in R-Glass while
E-glass contains more calcium oxide and magnesium oxide. R-glass is stronger than E-glass and
has a decreased loss in strength due to temperature increases.

2.3.1.5 C-Glass

C-glass is also used when acid resistance is needed and is composed of soda-lime-borosilicate.

2.3.2 Carbon Fibers

The usage of carbon fibers dates back to Thomas Edison in the late 19th century who used
carbon fibers as filaments in early light bulbs. These fibers were cellulose-based and processed
from organic materials like cotton or bamboo. Today's fibers are generally petroleum-based and
have a much greater tensile strength. Modern carbon fibers were first introduced from rayon in
the 1950's (HJ3 Composite Technologies). These fibers are created from 3 different sources:
pitch, polyacrylonitrile (PAN), and rayon (Nazier, 2004). Rayon is avoided for modern carbon

fiber as the carbonization process can lead to a loss of 75% of the carbon's mass, making it very expensive. PAN is most frequently used as it can retain 50-55% mass. Pitch costs lower that PAN but there tends to be a lack of uniformity between batches, which can make pin pointing exact properties difficult without continuous testing. There are two distinct types of carbon fiber, Type I high modulus and Type II strength, which result from differences in microstructure of the fibers.

There are several major benefits to using carbon fiber for FRP and other structural applications that have resulted in carbon fiber being used whenever possible in FRP composites. Carbon fiber has a higher strength and modulus than normal steel at a fraction of the weight, about 70%. Carbon fiber also has a low elongation which helps greatly in reinforcing structures where rigidity is a key factor. Carbon fiber's stiffness to weight ratio is about 3 times higher than that of steel and aluminum (GW Composites). Depending on the type of carbon fiber, tensile modulus can range from $7.25x10^6$psi to $2.9x10^7$psi. Modulus can be increased by manufacturing at a higher temperature, above 1400°F. Carbon fiber, by itself, is capable of withstanding temperatures up to 750°F and 3600°F if protected from oxidation. Combined with a low, and sometimes negative, coefficient of thermal expansion carbon fiber can create a very stable composite. Carbon also proves more resistant to alkali environments that glass and possesses similar resistance to acids (Balaguru and Shah, 1992).

While carbon fiber properties are superior to many FRP materials' the major downside to carbon fiber is its relatively high cost compared to other fibers. Carbon fiber does see wide use, as previously stated, but in areas such as aviation and mass production of sporting goods where the cost is less important. For structural repairs, carbon fiber's cost can have less of an impact when it is compared to complete reconstruction or more intensive concrete or steel repair. In

some cases, however, cheaper glass can still be used effectively. Like glass, carbon fiber can be purchased in tows, fabrics, and short chopped fibers.

2.3.3 Aramid Fibers

Aramid is the most popular synthetic organic polymer fiber. Aramid is created by spinning the fibers from a blend of liquid chemicals. They have the highest tensile strength-to weight ratio and have more abrasion and impact resistance than the fibers previously mentioned. Aramid fibers have a large temperature range in which they are viable, from about -400°F to 400°F but will decompose in air at about 800°F. The two biggest drawbacks to aramid fibers are a difficulty in cutting or machining aramid samples and degradation from UV light. This means that aramid must be thoroughly coated to ensure it doesn't lose bond or strength.

2.3.4 Basalt Fibers

Basalt fiber is possibly the most interesting of the fibers mentioned thus far. Basalt fiber is extruded from inert rock and volcanic material that is found abundantly on Earth. It also possesses excellent strength, higher than the other fibers mentioned, durability, thermal properties, and hardness, 8 or 9 on the Mohs Hardness Scale (Balaguru, Nanni, and Giancaspro, 2009). Basalt fibers are better than glass for thermal stability, heat, sound insulation, vibration resistance, and durability which can make them the ideal fiber for certain applications such as geothermal well reinforcement, heat shields, or sound barriers. They are also cheaper to purchase than many other high temperature resistant fibers, though this does not mean they are cheaper than other less specialized fibers.

2.3.5 High Strength Steel Wires

Steel wire was not used in early FRP composites due primarily to their very low strength to weight ratios. Standard steel, while quite strong and capable of creating solid sections for structures, has a much lower tensile strength than glass, carbon, or aramid fibers. For FRP applications this makes a much larger difference as the applied fibers are required to have much lower cross-sectional areas. With the advent of high strength steel wires, however, the potential tensile strength of steel could compare with that of fiber glass, carbon, and aramid. High strength steel wires are primarily used in the steel belts for modern tires. These tires contain what are essentially piano wires bound together to form sturdier cords and help alleviate the stress on the tires' rubber due to internal pressure, vehicle weight, and normal driving wear.

High strength steel wire is made from pearlite steel filaments that are drawn into small diameters of 0.2 to 0.35mm. These wires are much thicker than traditional composite fibers but still allow for a relatively low profile and thin composite layers (Prota et al, 2006). Individual wires are then generally combined into larger strands which has a variety of benefits for use in composites. Wrapping wires together allows for easier lay-up of composite in field applications. Wires can be twisted to create a screw thread type effect that can enhance mechanical bonding with the matrix and lower development lengths while wires can be wound less tightly to allow for easier penetration by the matrix. Figure 2.2 shows an example of a steel strand bound with a single wrapped wire. Table 2.2 shows some basic properties of the fibers mentioned in this section.

	E-Glass	Carbon	Aramid	High Strength Steel
Tensile strength (Mpa)	1300-3400	2000-5600	2500-3620	1000-2200
Modulus of elasticity (Gpa)	22-62	150-325	48-76	185-200
Elogation (mm/mm)	0.03-0.05	0.01-0.015	0.02-0.036	0.04
Coefficient of thermal expansion (10-6m/m/K)	5.5	0	-0.5	6.5
Melting Point °C	1100	310	420	1300
Density (g/cm3)	2.5-2.6	1.7	1.4	7.9

Table 2.2: Basic material properties of common FRP fiber types (Adapted from

Papakonstantinou and Katakalos, 2009)

In addition to potentially increased mechanical bonding with a matrix, steel also possess a relatively high and more easily predictable elongation. This allows for engineers to enhance the strength of structural elements such as beams but still maintain a relatively ductile and safer failure.

Currently, research of steel reinforced inorganic polymer has been performed for both SRiP with specially manufactured steel cords and SRiP with commercially available steel cord solutions. Companies such as Hardwire LLC offer high strength steel wires as both individual strands and "tapes" of strands connected by a polyester scrim. These tapes are the most popular steel cord system to use for SRiP composites as they come with evenly spaced wires and allow for quicker installation; much like a carbon fiber mat requires less effort than a large collection of individual fiber tows. In the case of custom made steel cords, such as in experiments by Katakalos and Papkonstantinou, specially manufactured cords were also made into tapes similar to those commercially available and simply used more, smaller diameter wires in each cord and a zinc coating instead of brass (Katakalos and Papakonstantinou, 2009).

In depth discussion of the physical properties and details of the application of the steel wires will be provided in Chapters 3 and 4 in the discussion of the material selection and composite application.

2.4 Strengthening Techniques

One of the key concepts when designing a large structure is determining the desired life of the structure. Engineers must figure out based on trends and collected data how long structures can withstand the expected usage. If a structure's actual loads and use exceed the predicted amounts, or as it approaches the end of its lifecycle, owners may choose to have repairs or retrofits done to the structure to extend its life and maintain its functionality. Retrofitting of existing structures has become an increasingly popular alternative to constructing new structures as it reduces cost, time spent constructing, and time with the structure unusable.

There are two major strengthening techniques when dealing with preexisting structures. The first, utilizes externally mounted framework. These external structures are manufactured from concrete or steel and are affixed to the existing structure to provide extra support. Additional structural components such as these can be material intensive and thus have great cost. They also take up a great deal of space which can hinder maintenance or limit useable space inside or on a structure. Additional components can also lead to adjustments in a structure's foundation which also take a great deal of time and money.

The second type of strengthening technique is surface treatment. Surface treatments are less material, time, and cost intensive than adding on a frame to an existing structure. These techniques involve the bonding of additional structural elements to the exterior surface of a structure. This could include coring out concrete and replacing it with steel and a bonding agent, Affixing steel plates to a structure, or applying a layer or layers of FRP Composite.

FRP systems allow for the least amount of weight to be added structure while also providing a large increase in load capacity. FRP composites can be applied to provide assistance with flexure, shear, torsion, or a combination of the loads. These systems have been seen an increased use over the last few decades and a great deal of research has shown that a properly applied FRP composite can greatly enhance a structure's properties.

2.5 Application Techniques for FRP

Matrices can be applied using brushes, rollers, trowels, or sprayers. Often times a squeegee or spatula can be used to help move the matrix into the fibers used. Brushes and rollers have proven to be better for wetting of fibers with an organic matrix. Sprayers required thicker layers to guarantee an effective bond. If a sprayer is used, airless sprayers are preferred to make sure of a continuous, even spray. A number of commercial sprayers exist, some of which will mix components as spraying occurs, two component systems, and some are able to attach equipment that can incorporate chopped fibers into the spray.

This section will discuss the most important factors to consider while applying FRP systems.

2.5.1 Surface Preparation

Surface preparation is an extremely important step in the installation of FRP composites. Depending on the matrix selected, labor and subsequently cost can greatly increase. For organic matrices the surface must be free of dust, water, and loose materials such as aggregate to ensure a proper bound. Concrete surfaces are often ground down to barely reveal the aggregate, ensuring the matrix bonds well with the concrete and just not a thin external layer of cement paste. This too increases the cost as more equipment and labor are needed in the grinding process.

Inorganic polymers require a fair amount less preparation in order to guarantee a successful bond. While loose aggregate is still an issue, inorganic polymers still bond on a wet surface, though not soaking wet, and are not as hampered by the presence of dust and other small particles. Inorganic polymers have also shown in testing to not require as much surface grinding as organic matrices (Balaguru, NSF).

2.5.2 Pot Life and Temperature

Working time for organic matrices doesn't normally exceed two hours while some inorganic polymers such as potassium aluminosilicate can last three hours or even more if stored in low temperatures in between usage. Application should occur at temperatures greater than 40°F and if possible greater than 50°F. These numbers are accepted requirements for both organic and inorganic matrices and apply to ambient and surface temperature of the structure to be repaired.

2.5.3 Special Considerations During Application

When working with various matrices, any specific safety requirements should be strictly followed. This could include specific materials for gloves or the use of masks gloves or full protective suits. Repairs performed in crowded areas can require the addition of a protective enclosure to keep the public away from any components of the repair.

Applications involving chopped fiber as either the main reinforcement or filler in the matrix should require respirators to protect again fiber inhalation and full body coverage as the small fiber strands can get into the pores of the skin and cause irritation.

Mixing of inorganic matrices with solid components should also require respirators.

2.5.4 Curing Requirements

The majority of systems will require protection from weather and contamination for at least 24

hours while curing. In lower temperatures a heating blanket could be required. In the case of

potassium aluminosilicate, full curing can be achieved within 3 hours at 68°F.

2.6 Dangers of Fire with Organic FRP Systems

While research in FRP performance and retrofitting has occurred for decades and dealt with

numerous applications, the majority of all field use of FRP occurs in the reinforcement of flexural

members of bridges. These members are often reinforced along beams in order to help with

deflection, flexural load, and/or shear. During design, factors such as strength, deflection, and

adhesion are thoroughly considered in order to guarantee a successful and safe repair. And

depending on the materials used, protective coatings are added to prevent UV degradation and

damage from chemical exposure. Most FRP system designs do not account for, or initially

account for, exposure to high temperatures and fire (Bisby, Green, and Kodur, 2005). This can be

a major issue with bridge repairs, as over the late decade or so bridge fires have been a growing

problem in the United States.

2.6.1 Increased dangers from bridge fires

While environmental events such as earthquakes gain much more attention when causing

damage and collapse due to design flaws rightfully occupy the media and people's minds when

they occur, bridge fires are an increasing issue in the US and can cause catastrophic failures in

their own right. There are a variety of causes for bridge fires such as, vandalism, electrical

malfunctions, natural causes, and traffic collisions. The majority of these fires either burn out

due to lack of fuel or are fully extinguished by firefighting efforts, but some fires are able to

grow and rage to the point of damaging the structure (Kodur and Naser, 2013). More than likely, these fires are tied to traffic collisions, primarily those involving vehicles carrying combustible chemicals. This could be tankers, freight vehicles, or even multiple cars hitting other vehicles or parts of the bridge itself. In these cases, not only are combustible materials involved, but also pressurized containment systems. The combination of potentially high vapor pressures and flammable chemicals can lead vehicular based fires to be explosive. This issue has increased over the last 2 decades as shipping of combustible materials via trucks has shot up dramatically.

When a bridge fire does start, it can become a devastating force if not quickly controlled. Especially for fires started from collision, the combination of high vehicle speeds and low flash point materials can generate fires that reach upwards of 800°C in just a few minutes (Payá-Zaforteza and Garlock, 2012; Strutt, 2008; Stoddard, 2004). And within thirty minutes, a fire of such type can reach upwards of 1000°C. Exposure at those temperatures for such a time are devastating to structural components if not properly protected against fire damage.

A New York Department of Transportation (NYDOT) survey performed in recent years showed that during the fifteen year period of 1990-2005 fire caused three times as many bridge collapses as earthquakes did. Fire prevention is also a much more universal issue in the US than earthquakes as only certain locations in the United States experience seismic events on a semi-regular basis (NYDOT, 2008).

2.6.2 Major Bridge Fire Events

Several relatively recent bridge fires illustrate the importance of fire protection for bridges and FRP systems. These fires caused significant damage to infrastructure, contributed to major traffic rerouting and issues, and required large financial expenditure to repair. Overviews of those catastrophic events have been detailed below.

2.6.2.1 I-95 in Bridgeport, CT

On March 23, 2003, while driving on the I-95 Howard Avenue Overpass in Bridgeport, Connecticut a car crashed into a fuel tanker that at the time was transporting nearly 50,000 liters of heating oil. The tanker attempted to avoid the smaller vehicle but in doing so contacted the concrete barrier of the bridge and contacted two traffic light poles. The tanker's contents spilled over a 100m length and ignited causing a fire that lasted for two hours and reached a maximum temperature of near 1100°C. The bridge itself used 30 inch deep steel girders spanning approximately 72 feet. The fires generated significant buckling in these girders which lead to partial collapse of the overpass. Traffic going in both directions on I-95 had to be rerouted as well as, on the street below, for the duration of the $11.2 million repairs.

2.6.2.2 Bill Williams River Bridge

Another major bridge fire due to a fuel tanker on July 28, 2006 occurred on the Bill Williams River Bridge in Arizona. An overturned fuel tanker spilled out some of its 28,701 liters of diesel in the vicinity of the bridge. After ignition the fire burnt near spans 8, 9, and 10 of the bridge for several hours. During this time it spread to an adjacent wildlife area where it burned and spread for two weeks.

As for the bridge itself, the close to 80ft spans consisted of prestressed concrete girders supporting a cast-in-place slab. Spalling of concrete on the previously mentioned spans was detected but found to have no major impact on the capacity of the girders. Rehabilitation was required on the east overhangs of spans 8, 9, and 10 as these were closest to the fire.

2.6.2.3 I-580 Freeway Oakland, CA

On April 29, 2007 an overturned tanker truck once again lead to a major blaze. The truck, carrying 32,500 liters of fuel, overturned under a two span bridge of the I-580 freeway in Oakland, California. The steel girder bridge was subjected to temperatures in the area of 1100°C resulting in rapid strength loss in the girders and a drastic increase in girder deflection. The girders and joints became severely overstressed which resulted in collapse of the structure within 22 minutes. 9 million dollars in damage was done to the structure and significant traffic rerouting was in place for weeks during clean up and repairs.

2.6.3 Response of Organic FRP Matrix to Increased temperature

As stated above, bridge fires have been documented at temperature exceeding 1000°C and lasting in some cases for hours. The damage to steel and concrete structures can lead to capacity issues, costly repairs, and loss of use of a structure. But extra dangers can exist if that structure has already needed some kind of retrofitting. While adding external reinforcement is an efficient and relatively cost effective way to increase flexural or shear capacity, there is now an extra area of the beam that, if it were to fail, would lead to failure or significant damage in the structure. Furthermore, it is possible that the sudden loss of bond of an FRP system, or the brittle failure of fibers, specifically carbon, in the presence of extreme temperatures can result in a more sudden and catastrophic failure.

While the significant code exists for the design and application of FRP for both flexure and shear, no code exists that deals with the protection of FRP systems from fire damage. As with any material used in Civil engineering applications, a lack of standardization can lead to suboptimal conditions for a structure to maintain its integrity in a variety of negative event conditions. As

stated, this dissertation will focus primarily on high temperature events and in chapter 5, will address what current standards are considered in greater detail.

When looking at the impact of fire, or more specifically heat, on an FRP composite it is critical to look at both of the major components used in the composite. Various reactions of common fiber types to high heat will be discussed, followed by a look at the response of organic matrices to similar temperatures.

2.6.3.1 Response of Common Fibers to Increased Temperatures

Glass fibers are the most commonly used fibers in FRP systems and can be highly susceptible to increases in heat. While the melting point of glass is relatively high at 1100°C the strength of glass is greatly affected by increases in ambient temperature around the glass. The table below shows that even more heat resistant types of glass fiber loses load capacity very drastically at major increases in temperature.

Temperature °C	Residual Strength (%) E glass	Residual strength (%) R glass
-200	100	100
200	98	100
300	82	91
400	65	77
500	46	61
600	14	45
700	-	27

Table 2.3: Thermal Resistance of R and E glass filament (Adapted from Saint-Gobain Vetrotex Technical Sheet)

The most common type of glass, E glass, losses over half of its load capacity at a slightly below 500C, which a bridge fire could reach in mere minutes. In maximum bridge fire temperatures, those exceeding 1000°C, glass fibers lose all ability to support any significant loading. Aramid

fibers perform even worse under higher temperature conditions as they are organically based

and deteriorate at high temperature. As can be seen in the following graph by Bisby, Green, and

Kodur, of carbon fiber, glass fiber, and aramid fiber lose strength rapidly with temperature

increase in a relatively predictable fashion. It is also evident that glass composites too lose quite

a bit of strength as temperatures increase, the drop-off becoming more obvious after 300°C.

Glass fiber also have a less predictable decrease which can make designing for a specific load

during heat based failure difficult. While carbon fiber does prove to be very steady initially, as

temperature increase about 350°C the strength capacity of the carbon fiber becomes sporadic

but still high.
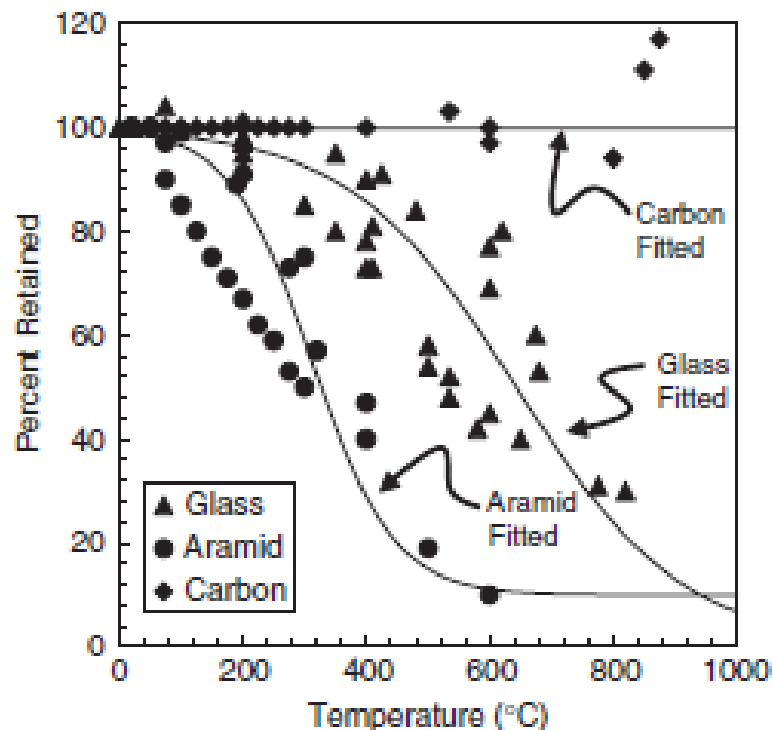
Figure 2.2: Variation of Tensile Stress with Temperature (Fibers) (Bisby, Green, and Kodur, 2005)

In a second test, Bisby, Green, and Kodur demonstrated the percentage of strength retained for

a carbon FRP composite in tension when exposed to similar temperature increases. Now with

the presence of an organic matrix the residual strength greatly decreased with an increase in

temperature and in a more scattered fashion. The results of this test are depicted in the graph

on the next page. To fully understand these results, however, the effect of increased

temperatures on the matrix in an FRP composite must also be explored.
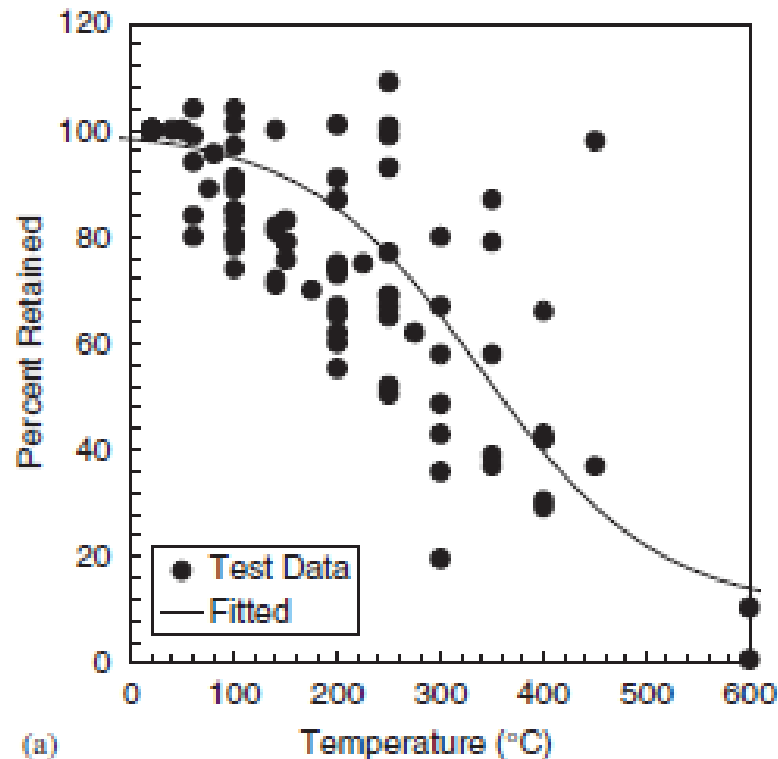
Figure 2.3: Variation of Tensile Stress with Temperature (Carbon FRP) (Bisby, Green, and Kodur,

2005)

2.6.3.2 Response of Organic Matrices to Increased Temperatures

When looking at the impact and dangers of fire on an FRP reinforced structure the matrix tends

to be the most critical component. As seen in Figure 2.3, the use of a Carbon FRP with an organic

matrix has a big effect on the residual strength of the system at higher temperatures, as

compared to a sample of carbon fiber in tension by itself. In addition to the normal damage that

occurs in the fibers the worry over a bonding agent becomes an issue as failure within the matrix can result in debonding of the elements granting additional strength. This is considered by many to be the largest drawback of using an FRP composite or FRP reinforcement bars.

Testing of externally bonded FRP systems using a traditional two part epoxy resin matrix has shown that epoxy is extremely susceptible to fire damage. In two separate testing regimes by Blontrock et al. it was shown that an epoxy could only maintain bond for 55 minutes in temperatures upwards of 47°C, which decreases to 40 minutes with temperatures in a range of 52-65°C (Blontrock et al., 2000&2001). These temperature ranges are an order of magnitude lower than the temperatures of a chemically fueled bridge fire after only 10 to 15 minutes of burning.

Kamal, Hamdy, and Abou-Atteya in testing of a set of reinforced concrete beams at different temperatures found that after extended exposure to 600°C temperatures, within the potential of a bridge fire, an FRP reinforced beam behaved similarly to a reinforced concrete beam with no FRP attached. This demonstrated that at temperature conditions similar to a fire, organic epoxy FRP loses its ability to support a load and can no longer function as a repair or retrofitting mechanism (Kamal et al., 2013).

Beam	Strengthening	Temperature (°C)	Protection layer	Failure load (kN)	Ratio to control (B_1, B_2) (%)
B_1, B_2	–	25	–	30	100
B_3, B_4	GFRP	25	–	38	126.67
B_5, B_6	–	100	–	30	100
B_7, B_8	–	200	–	27.1	90.33
B_9, B_{10}	–	300	–	22.8	76.00
B_{11}, B_{12}	–	400	–	18.7	62.33
B_{13}, B_{14}	–	500	–	15.6	52.00
B_{15}, B_{16}	–	600	–	10.3	34.33
B_{17}, B_{18}	GFRP	600	–	10.3	34.33

Table 2.4: Failure loads of unprotected RC beams (Kamal et al., 2013)

In 1994, a Swiss researcher named Deuring investigated the effect of fire on externally bonded

steel plates and FRP strips. Deuring found within minutes of exposure the adhesive matrix

holding the external reinforcement onto the concrete surface would deteriorate, unless the

external reinforcement system was protected by some type of insulation.

What is apparent from the work of these researchers and others is that in order to account for

the potential destruction brought on by bridge fires, precautions must be taken to protect FRP,

and specifically organic matrices, from any extended increases in temperature. In fact, fire is so

devastating to the bonding capabilities of organic resins that in ASTM 440.2R-02 Guide for the

Design and Construction of Externally Bonded FRP Systems for Strengthening Concrete

Structures, explicitly states that standard FRP systems should be considered completely

ineffective in the presences of fire (ASTM 440.2R-02, 2002). ASTM 440.2R-02 along with the

Concrete Society's TR55 code consider fire and accidental load that should be calculated with

reduced safety factors as in some cases FRP could fail without compromising the base

structure's integrity. This thinking can be dangerous, however, in the case of repair and retrofit

where the extra support provided by the FRP can be critical to maintaining the effectiveness of a

structure.

2.6.4 Combatting Fire Damage in FRP

Given the dangers that fire can pose to FRP and the growing use of FRP in infrastructure, it is

imperative that engineers and researchers work to identify ways to protect FRP systems from

becoming damaged and leading to failure in critical structural members. As discussed above, the

matrix has been shown to be the weak link when it comes to high temperatures. There are two

natural directions an engineer can move in to create a system that can maintain performance

during and after prolonged fire exposure. An engineer can insulate FRP from the damage by

using an additional material or coating or an engineer can modify the matrix holding the FRP together to reduce the likelihood of debonding.

Insulation is the most common form of fire protection for composite systems currently as the process of insulating FRP can be performed any point after the FRP has been installed and does not drastically alter the application methods developed for composites over the years. The goal of insulation is to completely coat the FRP system and decrease the amount of heat that is able to penetrate to the FRP. By creating a more drastic temperature gradient the insulation lowers the maximum temperature that the epoxy will reach which prolongs the time it takes for debonding to occur. Gypsum boards or powders are a common insulation component as their mineral based structure can handle the heat well. Blontrock et al. utilized a variety of insulations throughout years of testing including gypsum systems and found that the use of insulation can result in FRP strengthened beams showing a similar endurance to fire as beams with just concrete and internal steel bars (Blontrock et al., 2001).

Williams et al. used a vermiculite-gypsum insulation coated with a top layer of intumescent coating to insulate CFRP reinforced slabs. Williams proposed that with a proper 38mm (1.5 inch) thick layer of this type of insulation that FRP could achieve 4 hours of fire endurance rating. Testing showed for the samples, however, that the glass transition temperature, when the polymer goes from glassy to rubbery, was still reached within one hour of the testing (Williams et al., 2006, Williams et al., 2008).

Other types of Insulation include:

- Portland cement mortar
- Perlite (siliceous volcanic rock) mortar
- Vermiculite (phyllosilicate) mortar

- Clay mortars, such as Aswan clay

- Ceramic fiber blankets

There are downsides to using insulation to protect against fire. Insulation requires an additional step in the application process. Insulation may also need to be thick, over an inch, in order to provide proper protection which may not work with a client's aesthetic desires. If the insulation were to be damaged in any way the underlying composite will become susceptible to fire and increased temperatures. Such was the case in research by Ahmed and Kodur, whose insulated FRP reinforced beam developed cracks in the Vemiculite-Gypsum coating. The FRP was then exposed to the applied fire from their testing and debonded severely, as shown in Figure 2.4 below.
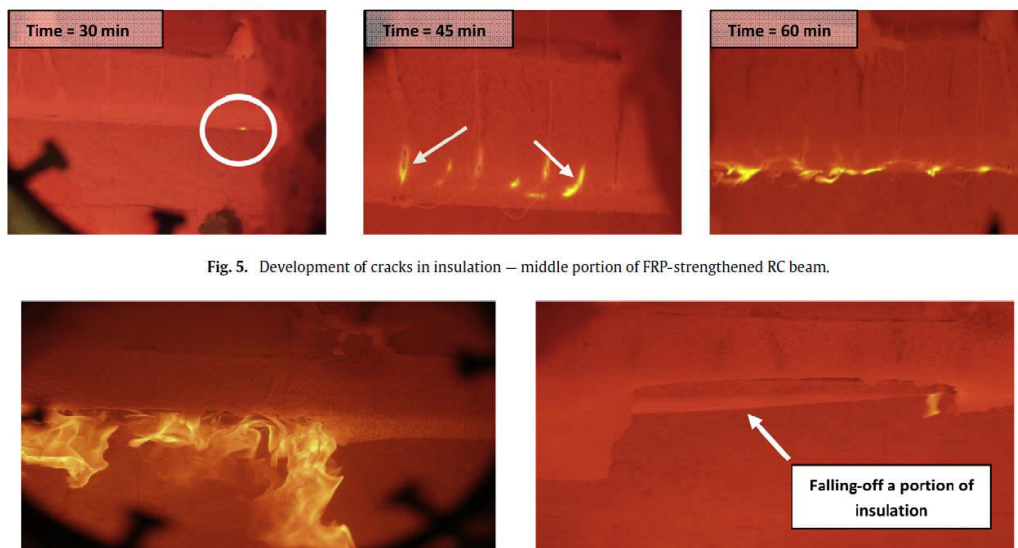
Fig. 5. Development of cracks in insulation — middle portion of FRP-strengthened RC beam.

Figure 2.4: Fire damage to insulation on left quarter span of beam (Ahmed and Kodur, 2011)

Figure 2.5: Unbonded continuous carbon fibers resulting from insulation loss (Ahmed and Kodur,

2011)

To avoid the use of thick insulation coatings and extra steps in the installation process, some

engineers choose to modify an existing organic matrix so it becomes more resistant to fire.

Modification of a matrix in such a way generally involves the addition of a fire resistant

compound into the polymer resin that helps reduce bond degradation in the high temperature

environment. In 2013, Ji et al. performed a study on the use of nanoclay infused epoxies as a

way of creating an organic FRP matrix that could withstand higher temperature ranges. Before

blending the resin and curing agent, nanoclay platelets approximately 1 nm thick and 70-150 nm

wide were added to the resin. Using a variety of mixers including ultrasound, the nano particles

were blended for a period of near three hours. Hardener was then added prior to FRP sample

preparation (Ji, et al., 2013).

An additional three hour mixing process, however, can be costly depending on the stage at

which mixing occurs. An Intumescent coating was still required for the exterior of the FRP as the

inclusion of nanoclay did not completely shield the matrix from fire, just toughen it up a bit.

But modifying the matrix doesn't necessarily mean adding something to an organic resin or epoxy. By modifying the type of matrix that we use from organic to inorganic we can switch out a material that responds poorly to the presence of fire or increased temperature for one that can withstand incredible heat with little side effects.

2.7 Inorganic Matrix Composites

While traditional Portland cement matrix has been used in a variety of applications for over a century and inorganic polymers have been employed for decades in various protective applications they haven't received attention as potential composite matrices until relatively recently. Both compounds have been tested in conjunction with reinforcing fibers in an attempt to create new types of FRP systems that provide benefits in repair and retrofit that aren't possible with organic matrices.

2.7.1 Carbon Fiber and Inorganic Matrix

In the past two decades, several studies have been conducted on carbon fiber reinforced polymer composites to see just how successful the CFRP performs with an inorganic matrix. Results were mixed depending upon the inorganic matrix selected. In the case of Portland cement grouts the average particle size of the grout materials makes it incredibly difficult to properly wet the carbon fibers and penetrate into the tows. This causes a poor development of the bond between fiber and the member being reinforced. Similar issues arose in a study by Hashemi and Al-Mahaidi, whose results showed that while their cement based mortar matrices we able to generate increases in flexural capacity of 10-15% above their control, the increases came nowhere close the 35% increase shown with similar reinforcement bonded with an organic matrix (Hashemi and Al-Mahaidi, 2012). Similar issues occurred in more extensive testing by Menna et al. where a variety of samples were tested using various fiber types and

both organic epoxy and inorganic sodium-silicate/metakaolin based polymer. The only

combination of fiber and matrix that proved ineffective in increasing the standard beam's

moment capacity was the inorganic compound combined with carbon fiber reinforcement.

Specific results are provided in the table below. After flexural testing these beams were

analyzed with scanning electron microscopy (SEM) and it was determined that full penetration

of the carbon fibers was not achieved by the inorganic matrix (Menna et al., 2013).

Specimen	External reinf.	Impregnated matrix	No. of plies	Axial stiffness ratio S (–)	Mechanical reinf. ratio μ (%)	Increase of mechanical reinf. ratio $\Delta\mu$ (%)	Experimental M_u (kN m)	Increase of experimental M_u ΔM_u (%)
Beam U	–	–	–	–	10.39	–	25.5	–
Beam S (1)	Zinc coated steel	Geopolymer	1	0.181	22.31	114.63	53.9	111.26
Beam S (2)	Zinc coated steel	Geopolymer	1	0.181	22.31	114.63	53.6	109.79
Beam C (1)	Carbon	Geopolymer	1	0.053	15.83	52.31	27.4	7.25
Beam C (2)	Carbon	Geopolymer	1	0.053	15.83	52.31	30.2	18.07
D-Unreinf.	–	–	–	–	*9.62*	–	*29.6*	–
A-1	*Zinc coated steel*	*Epoxy*	*1*	*0.16*	*20.42*	*112.12*	*51.8*	*75.05*
A-2	*Zinc coated steel*	*Epoxy*	*1*	*0.32*	*31.21*	*224.24*	*72.7*	*145.64*
A-3	*Zinc coated steel*	*Epoxy*	*2*	*0.32*	*31.21*	*224.24*	*60.2*	*103.65*
B-1	*Brass coated steel*	*Epoxy*	*1*	*0.14*	*19.07*	*98.11*	*53.1*	*79.72*
B-2	*Brass coated steel*	*Cementitious*	*1*	*0.14*	*19.07*	*98.11*	*43.6*	*47.46*
B-3[a]	*Brass coated steel*	*Cementitious*	*1*	*0.14*	*19.07*	*98.11*	*42.9*	*45.03*
B-4[a]	*Brass coated steel*	*Cementitious*	*2*	*0.28*	*28.51*	*196.21*	*52.0*	*75.86*
C-1	*Carbon*	*Epoxy*	*2*	*0.21*	*22.36*	*132.30*	*57.9*	*95.74*
C-2	*Carbon*	*Epoxy*	*3*	*0.42*	*35.09*	*264.60*	*80.9*	*173.43*

Table 2.5: Flexural testing results, italicized results from Prota et al. (Menna et al., 2013)

Ongoing research into aluminosilicate based geopolymers at Rutgers University has shown

better results. In testing similar carbon fiber reinforced beams, some with organic matrix and

some inorganic matrix, increase in flexural capacity was found to be similar. The main difference

in the matrices came in the type of failure. The organic matrix lead to a more sudden debonding

while the inorganic geopolymer acted like an extension of the concrete of the beam and

creating a smoother strain distribution and more gentle failure (Krutz and Balaguru, 2001). A

joint study performed at the University of Alabama five years later confirmed the results and

demonstrated that inorganic geopolymer can be successful with carbon fiber reinforcement

(Toutanji et al., 2006)

This mention of more sudden and brittle failure does bring about a point of concern for CFRP designed with inorganic adhesive. Though geopolymers exist that can provide a more continuous bond with a concrete surface and less brittle failure, carbon fiber itself is incredibly stiff and doesn't allow for much deflection or warning if in fact a carbon fiber composite is about to fail. This notion has been just one motivator for creating a working composite system with high strength steel.

2.7.2 Steel Reinforced Inorganic Polymer Composites

Now that high strength steel cords have become more readily available the viability of steel in composite reinforcement has grown significantly. Cement or geopolymer based matrices that behave like concrete can bond just as efficiently with steel as concrete itself.

Cement based matrices such as grouts while still relatively recent have been tested more extensively than their geopolymer counterparts. This is due to the more common knowledge of grout or mortar design, the chemical steps for geopolymer for example are far more complex and far less utilized in civil engineering. Though particle size can be an issue when applying a matrix to a carbon fiber tow, steel wires are substantially thicker and can bond with grouts with relative ease. Grout, however can be bulky when applied and can require a more manually intensive mixing and finishing process. In a study in 2006 Prota et al. were able to create a steel reinforced grout that was capable of holding loads comparable to an organic epoxy counterpart, however, anchoring nails were needed to hold stabilize the steel cord reinforcement as the grout set. This required extra labor to drill holes and attach the anchors (Prota et al., 2006). For all the successes that have been achieved with steel reinforced grout there are many practical draw backs to its continued use. This led to the material that will be the focus of this dissertation, Steel Reinforced Inorganic Polymer or SRiP.

SRiP combines the strong mechanical bond, flexural support, and improved ductility of high

strength steel cords with a matrix that can be applied similarly to paint and require little extra

protection effort from fire. One of the earliest instances of SRiP research was published as

recently as 2009 when Papakonstantinou and Katakalos introduced what they referred to as a

"novel strengthening system," that combined high strength steel cords with an inorganic, fire

resistant matrix known as a geopolymer. This regime only involved a few reinforced concrete

beams, some with SRiP reinforcement, and demonstrated that SRiP was a viable option in repair

and retro fit of beams. The use of the aluminosilicate polymer resulted in improved stiffness

over organic matrices and resulted in no observed delamination between the matrix and the

concrete substrate. Yielding of steel reinforcement was the primary failure mechanic followed

by a slippage of the steel in the SRiP. Curing time was determined to have a significant impact on

the flexural capacity of repaired beams and allowing the matrix to cure for a standard 28 day

cycle improves polymer performance (Papakonstantinou and Katakalos, 2009). In fatigue testing

of SRiP, Papakonstantinou and Katakalos were able to create SRiP reinforcements that resulted

in improvement of flexural strength of upwards of 40%.

Beam	Testing frequency	Ultimate applied load max (N)	Applied load max (N)	Applied load min (N)	P_{max}/P_{ult}	Number of cycles to failure, N	Strain on steel experimental (analytical) (μ strain)	Stress on SRiP (MPa)	Steel reinforcement stress range max–min (MPa)	SRiP stress range max–min (MPa)
						(a) Nonstrengthened RC beams				
C-1	Monotonic	23,480	n/a[c]	n/a[c]	n/a[c]	n/a[c]	n/a[c]	n/a[c]	n/a[c]	n/a[c]
C-2	Monotonic	24,035	n/a[c]	n/a[c]	n/a[c]	n/a[c]	n/a[c]	n/a[c]	n/a[c]	n/a[c]
C-3	2 Hz	—[a]	10,500	750	0.44	2,000,000	729 (979)	n/a[c]	217.67–21.95	n/a[c]
C-4	2 Hz	—[a]	15,000	750	0.62	2,000,000	n/a[c] (1,641)	n/a[c]	350.19–21.95	n/a[c]
C-5	2 Hz	—[a]	15,500	750	0.65	1,700,000	n/a[c] (1,714)	n/a[c]	364.78–21.95	n/a[c]
C-6	2 Hz	—[a]	16,500	750	0.69	325,000	1,503 (1,865)	n/a[c]	394.87–21.95	n/a[c]
C-7	2 Hz	—[a]	20,000	750	0.83	60,000	2,543 (2,452)	n/a[c]	512.43–21.95	n/a[c]
						(b) RC beams strengthened with one layer of SRP with inorganic matrix				
R-1	Monotonic	34,034	n/a[c]	n/a[c]	n/a[c]	n/a[c]	n/a[c]	n/a[c]	n/a[c]	n/a[c]
R-2	Monotonic	32,397	n/a[c]	n/a[c]	n/a[c]	n/a[c]	n/a[c]	918	n/a[c]	n/a[c]
R-3	2 Hz	—[b]	16,000	750	0.47	2,000,000	n/a[c] (1,269)	n/a[c]	271.16–17.32	275.85–19.07
R-4	2 Hz	—[b]	17,000	750	0.50	1,575,000	1,220 (1,434)	326	304.04–17.32	307.72–19.07
R-5	2 Hz	—[b]	18,000	750	0.53	870,000	1,879 (1,673)	472	351.91–17.32	424.51–19.07
R-6	2 Hz	—[b]	20,000	750	0.59	192,000	n/a[c] (1,939)	n/a[c]	405.15–17.32	578.69–19.07
R-7	2 Hz	—[b]	22,000	750	0.65	104,000	2,330 (2,093)	548	435.85–17.32	587.34–19.07
R-8	2 Hz	—[b]	24,000	750	0.71	65,000	2,478 (2,277)	593	472.67–17.32	548.13–19.07
R-9	2 Hz	—[b]	28,000	750	0.83	5,000	2,978 (3,224)	681	567.32–17.32	778.21–19.07

[a]Assumed to be same as C-1 and C-2.
[b]Assumed to be same as R-1 and R-2.
[c]n/a=not available.

Table 2.6: Summary of Monotonic and Fatigue Loading Testing Details and Test Results

While testing of aluminosilicate geopolymer exposed to fire or high temperatures there has yet to be any testing of SRiP composite in a simulated fire situation. This dissertation looks to identify the effects of fire on a steel cord and aluminosilicate composite and determine if SRiP is an effective method of improving flexural capacity without worry of severe fire damage.

2.8 Summary

History of FRP Materials

- The invention of two part epoxy resins and fiberglass helped revolutionize engineering in the mid-1900s.

- WWII and the need for materials drove an increased use in FRP systems, which also boasted lighter weight for aircraft or seacraft.

- FRP was first used in Civil Engineering to make "The House of the Future," but gained

  popularity as a repair material when it was discovered resins could bond to concrete

  and steel effectively.

Matrices

- An organic based matrix can have a variety of uses but it tougher to use in structural

  applications when deterioration is an issue.

- Inorganic matrices are growing in popularity in certain areas. The most common

  inorganic matrices initially were grouts and similar compounds but more intensively

  design geopolymer compounds have been presented in recent years.

- Aluminosilicate geopolymers can exhibit similar properties to concrete but don't hold

  the same bonding draw backs.

Fibers

- Traditionally, fibers used in FRP are extruded from glass or carbon.

- Carbon fiber is currently the most popular due to its lightweight and incredibly high

  strength.

- Steel wire was generally not used as the strength to weight ratios were quite low. New

  advances have brought about high strength steel wires that make steel a feasible

  support in FRP.

Fiber Reinforced Polymers

- Using an FRP system can require a great deal of surface preparation

- Temperature plays an important role in FRP systems. Curing temperatures can be fairly specific for various organic or inorganic coatings.

The Dangers of Fire

- Organic matrices are especially susceptible to fire and high temperature events.

- Due to increase transportation of flammable materials, roadway fires are more common.

- Tanker spills such as in Bridgeport, CT in 2003 can result in massive fires that greatly damage bridge or overpass structures.

- New solutions for FRP systems are needed in order to reduce the chance of full loss of structure in fires and other high temperature events.

- The newest of these composites is the Steel Reinforced Inorganic Polymer.

CHAPTER 3 MATERIAL SELECTION AND MECHANICAL PROPERTIES OF THE COMPOSITE

3.1 Introduction

While the materials selected for use in this research take into account a large body of work in

inorganic polysialate matrices performed at Rutgers University, careful modifications were made

to fit the requirements of a thicker steel cord as opposed to the more commonly tested carbon

fiber tow. As for the steel cords themselves, much of the selection process stemmed from

commercial availability and recommendations from existing publications, however, testing to

verify both standard properties of the steel as well as the steel's compatibility with the specific

aluminosilicate system selected were required to ensure the effectiveness of proposed repairs.

This chapter will discuss both practical and standardized testing performed on early samples of

inorganic matrix and steel wire to validate the selected materials and confirm key properties as

well as address mechanical testing performed in early works that reflects on the performance of

the modified matrices in this thesis.

3.2 Preliminary Testing

Initial tests performed on the materials used in this thesis fell under one of two categories,

standard testing which followed ASTM guidelines for things like flexure and slant shear, and

practical evaluations that focused on areas such as the application of materials. The goals of

preliminary testing were two-fold. First, it was sought to develop an inorganic aluminosilicate

matrix that can sufficiently bond steel wires to a concrete surface with a simple application

process. The matrix would need to flow efficiently between pieces of steel and into small

surface voids on the concrete but be thick enough that it could successfully encase the steel

cords. Secondly, the steel cords required a high strength design to give comparable flexural

results to more common types of fiber reinforcement. Steel needed to also maintain a relatively

low profile when applied to the exterior of the tested beams. Additional criteria such as enhanced mechanical bonding and ease of procurement were looked into during the selection process.

3.2.1 Steel Cord Selection

It was determined that an initial steel selection could be made first, as many of the requirements for the steel to be used could be found documented either by the manufacturers or in previous studies involving SRiP. With this in mind, SRiP investigations were explored to identify a steel wire with the following properties:

- A strong tensile strength to properly support a flexural load similarly to carbon fiber reinforcement.

- Enhanced ductility over standard FRP systems to allow for better visual identification of damage due to exposure to fire.

- Improved methods of mechanical bonding in a similar fashion to deformations on rebar.

- Commercial availability for easier procurement and adaptation of the system to field use.

- Convenient installation to allow for easier transition to field application in the future.

In terms of ultimate strength, a high strength steel will be able to compete with the incredible reinforcing capabilities of carbon fiber. SRiP investigations all must be able to replicate these strength conditions so this does little to narrow down the results. Most steels allow for more ductility than carbon or glass fiber so the second criteria is not difficult to achieve with documented materials either. The easiest differentiator for steel cord selection falls to the availability of materials.   The main type of steel cord used by a large amount of studies of steel

reinforced polymer, steel reinforced grout, and steel reinforced inorganic polymer was 3x2 brass coated steel cord from Hardwire LLC located in Pocomoke City, Maryland (Barton et al., 2005; Huang et al., 2004; Prota et al. 2006).

Hardwire LLC has two main types of steel cord available, a collection of 12 brass coated high strength wires wrapped with a single additional steel wire called "12x" and a set of three straight steel wire filaments wrapped in two additional filaments at a very high angle, known as the "3x2" cord. 3x2 cord is the primary cord used in the Hardwire LLC reinforcing systems.

To create their cords, Hardwire draws steel into thin wires approximately 0.0138 inches in diameter. In drawing out the cords to such a small diameter, the single crystals that make up the steel are pulled into a strong pearlite microstructure and are oriented in the drawing direction. This also orients them in the direction of primary loading in reinforcement applications, further enhancing tensile properties. Wires are then coated in a thin brass layer to help protect the steel from oxidizing. As mentioned above, 5 of these filaments are twisted together to form the 3x2 cords of total diameter of 0.035 inches. Each cord has a breaking load of 346.2 lbs and a 2.1% strain to failure. The high twist angle of the wires also creates a stronger mechanical bond with a matrix similar to the deformations on rebar used in reinforced concrete. 3x2 cords are priced comparably to glass fibers but strength properties similar to carbon fibers.

Figure 3.1: 3x2 Braided steel cord (Hardwirellc.com)

In addition to selling individual cords, Hardwire also provides unidirectional cord arrays attached

to a polyester scrim, referred to as tapes. They provide three densities of tapes, low density

provides 4 cords per inch width of tape, medium density provides 12 cords per inch width of

tape, and high density provides between 10 to 20 cords per inch width of tape. Tapes are sold in

rolls of 50, 500, and 2000 feet each 12 inches wide. Tapes provide an evenly spaced set of cords

that can be attached simply to concrete, steel, or wood surfaces. When attached they can

provide up to 8kips per inch of tape.

Figure 3.2: Hardwire LLC High density roll of "tape" (hardwirellc.com)

Given its availability, cost, and mechanical properties, Hardwire's tape system is an ideal reinforcement for composites and a well proven choice to test for this research regime.

3.2.2 Material Investigation Using Bricks

At the start of the material selection process it was determined that a series of simple but efficient tests would be needed in order to narrow down the exact mix design for the inorganic matrix. Even though several base versions of the aluminosilicate material were documented in previous experiments and in depth testing of the effects of various constituent materials' quantities was performed in previous research, these experiments dealt solely with the coating or an application of the coating and a glass or carbon fiber. Given the differing geometry between steel wires and thin fibers tows it was important to make sure that the steel and the geopolymer will develop a proper bond. This testing thus looks into the ability of the coating at various proportions to penetrate the between the fibers as well as into the desired concrete or masonry surface and effectively combine the two into a solid structural unit.

3.2.2.1 Practical Application Tests

The application of an aluminosilicate geopolymer to a concrete surface would closely resemble to some the application of paint onto drywall, wood, or any number of other surfaces. In painting, thin, even coats result in a more desirable appearance to the surface and guarantee a greater control over the quantity of materials used. Similar concerns arise with the application of an inorganic polysialate matrix, with the added caveat of the matrix, whether applied as a bonding agent or as a protective coating, behaving in some respects similarly to concrete. Shrinkage in particular is a much greater issue with this specific type of geopolymer and must be factored into composite design more so than in organic matrices. As the aluminosilicate geopolymer begins to set, the particles will tighten up and shrink together, which in thin amounts of material leads to predictable micro-cracking but nothing that can impact the aesthetics of the coating or its bond with the surface. In larger layers of matrix, however, these micro-cracks are magnified by the shrinkage of the additional material and can result in cracking that is not only macroscopically visible but also detrimental to the bond and strength of the system.

For inorganic polymer FRP systems utilizing thin tows of carbon or glass it can be quite simple to work the material into a very thin layer while still completely encasing the small diameter strands, individual fibers are between 7 and 13 nanometers on average, thoroughly in the polymer. When creating a steel reinforced inorganic polymer composite system, the engineer is no longer dealing in strands on the scale of a few nanometers but metal filaments closer to the order of millimeters. Naturally, these greater cord diameters will require more polymer material surrounding them to hold everything in place. The increased thickness, then, of the polysialate coating will result in an increased risk in major shrinkage cracking and decrease the bond

between the steel, polymer, and concrete surface. To create an acceptable SRiP composite system a balance would need to be struck in the workability of the polymer, something not too thick that is wouldn't evenly apply to the surface and crack, but not too thin that it could not thoroughly coat the steel wires.

From these parameters a testing regime was developed to see the effects of polymer shrinkage on the SRiP and to select an optimal polysialate composition to use in the larger scale SRiP testing. Using base designs generated from prior aluminosilicate research, a general mix proportion was selected that was known to work well with more common fiber types. Two samples were created for each matrix composition; the testing of these samples will be described in the next sections of this chapter. Mortar based bricks were used to create the samples as they provided a surface comparable to that of concrete. The bricks measured 7 ¾ inches long by 3 ¾ inches wide by 2 ¼ inches deep.

Samples of Steel wire tape were cut to fit on the brick specimens. A cutting tool was purchased based on recommendations by the manufacturer (hardwirellc.com), though the project budget did not allow for the purchasing of the highest capacity electric cutting tool. As such, a less powerful electric cutting tool was acquired and used in conjunction with an existing angle grinder. A mark was made 6 inches up the length of the steel cords with a metal etching tool. The material was then raised near the area of the cut to prevent any damage from grinding or cutting to the table underneath. Using the angle grinder, a line was made across all the strands along the marks. This removed some of the cord material to allow the lower power electric cutting tool to cut an even line through the cords. The same tool was then used lengthwise between the cords to cut the steel tape's backing material every 3 inches. The final result was approximately twenty 3 inch wide by 6 inch sections of Hardwire steel tape, each section

containing approximately 36 steel cords. For each set of mix proportions, one brick was coated to test the response of the coating to heating and a second brick had one of the prepared samples of steel tape bonded to its surface.

Prior to application the surfaces were cleaned with water and a wire brush to remove any sediment present. A similar cleaning process will be used with the full scale testing as most matrix systems require a surface free of debris to create a proper bond. The brick surfaces were allowed to then dry slightly to allow for a proper bond. In field applications, water use is generally associated with cleaning via pressure washer, which uses a high pressure stream to remove particles from a surface. Commonly, grinders and brushes are used to prepare and clean a concrete surface.

Preparing the coating for application takes between three and five minutes depending on the specific proportions and materials being used. The polysialate geopolymer consists of two parts, a potassium based liquid component and a blend of compounds and fillers that make up the solid component. The solid component is generally pre-batched to mix with 100g increments of the liquid component and sealed in a water tight plastic bag. The Liquid component is stored in sealed canisters and is weighed out at the time of mixing. It is possible to add small amounts of water, in the area of 10-15g, to 100g of liquid component should a thinner matrix be desired. For this testing, solid components were batched for use with 100g of liquid component.

Proportions within the solid component were based on those used to create an inorganic carbon fiber polymer (CFRP) in earlier research at Rutgers University. This mix design also included 10g of water to thin the mix for easier wetting of carbon fibers. It was hypothesized that the thicker diameter steel cords would not need the matrix to be thinned in such a way and that subsequent mixes would not include this added water. To prepare the aluminosilicate matrix,

the liquid component is first massed out and poured into a high speed blender. It should be noted, this process will be detailed again in Chapter 4, including step by step images of how the coating was mixed and applied to the full size beams. For the initial matrix tested, 10g of water was also measured and added into the blender at this time. After the liquids were obtained, the pre-batched bag of solids was opened and added into the liquid in the blender. Care was taken to make sure that no solid material was spilled outside of the blender and that as much material was moved from the bag as possible. When all materials had been added the lid was placed on the blender to prevent loss during mixing. The blender is turned on and placed on its lowest setting and moved up in order to its highest setting. The components of the matrix are then blended for approximately 90 seconds. The mixer is stopped and the sides are scrapped with a plastic spatula to make sure all solids are consistently blended. The polysialate is allowed to rest for 60 seconds to make sure that both the materials and equipment do not over heat. A second round of blending then occurs for 60 seconds. The matrix was worked through with the spatula to makes sure all solids have been mixed in and may then be applied directly from the blender or poured into a separate container or directly onto the surface that it will be applied on.

For the non-reinforced bricks, some material was poured onto the prepared surface of the brick and spread around with a plastic spatula. This allowed for a thin, even coating that penetrated into the rough surface of the brick. The brick reinforced with steel cords received a similar initial coating. After this base was put down on the bricks to be reinforced, a small amount of additional matrix was poured onto the surface. One of the precut hardwire tape pieces was then pressed down into the matrix with the cords facing the surface and backing facing outward. A small amount of matrix was poured on top of the steel and worked around the cords with the spatula. At this point, the excess aluminosilicate was transferred into a cup or other small container and placed inside a refrigerator. The cold temperatures delay the set time of the

aluminosilicate and allow for a workable material up to three hours after mixing. It should also be noted that while the drop in temperature does delay the exothermic reaction that causes the polysialate matrix to set, the decrease in temperature will still result in a slight thickening of the material. The initial coatings were allowed to set up for approximately one hour. The excess coating was then removed from refrigeration and mixed through to make sure it had not set in any way. A second coating was applied to both the reinforced and non-reinforced bricks in order to create a smoother finish and in the case of the reinforced brick make sure that the steel tape was completely and evenly coated. This was again done by pouring coating on the surface and spreading it out with a plastic spatula.

In a small number of cases during sample production, it was noted that parts of the tape would naturally bend up from the surface of the brick. The majority of these cases occurred near the end of the length of steel tape where it had been trimmed. In the event that a reinforced brick demonstrated this small amount of separation a small acrylic plate was placed on the top surface of the Hardwire tape and a weigh of some kind, normally a concrete cylinder was placed on the plate. This method ensured that the tape properly bond with the bricks and was only needed while the first layer of coating cured. The acrylic does not bond with the aluminosilicate coating as efficiently as concrete so the plate was easily removed after the coating had sufficient time to set, approximately 24 hours. The plastic did have an impact on the finish of the coating, as it was much smoother than areas of coating directly exposed to air. In some cases, additional cracking was noticed near these smoother, glassier looking areas. This was tied to existing cracking in some of the composite samples, which will be discussed within this section of the chapter. All samples were cured at room temperature in open air conditions for a period of 7 days before additional testing was performed.

Figure 3.3: Reinforced Concrete Brick Sample

Two major observations were made from the initial testing of a coating that worked for CFRP:

- The increased diameter of the steel did in fact require a thicker amount of material to properly coat and, therefore, a more viscous version of the inorganic matrix is required.

- The thicker amount of matrix also leads to an increased number of shrinkage cracks which have should have a negative impact on both bond strength and aesthetics.

A zinc oxide filler was used to thicken the inorganic polymer. This compound is already present inside the polymer and an increase in its quantity results in a greater viscosity without interfering in the necessary reactions to form the polysialate. While it would initially make sense to just keep adding the filler agent, referred to in batching as "Part D," to a single mix until a desired matrix consistency is reached, several different sets of mixes were made where the amount of Part D for each was incrementally increased by 10g from 0g to 100g of additional part

D. As the bricks still had to receive heat and flexural testing, this method would allow a balance to be struck between the thickness or geopolymer, resistance to heat, and ability to form a functioning composite. Through application, approximately 50g of additional Part D proved to create a thickness of material that would apply evenly and efficiently coat the steel tape.

There was still an issue, however, of cracking in the matrix after it had set. This would occur in areas where the matrix had to be applied in a thicker layer and thus showed greater shrinkage cracking. These cracks would generally follow the steel cords as the cords would restrain the geopolymer directly around them. Figure 3.1 shows a steel tape reinforced brick with shrinkage cracking in the matrix. Some of the cracking is highlighted by a red circle.
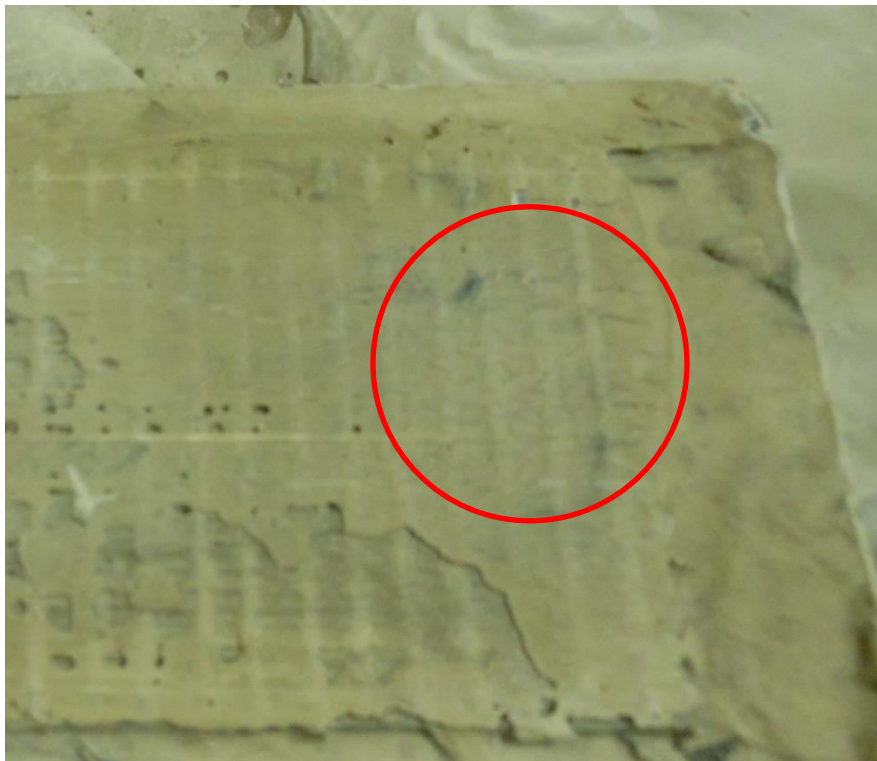
Figure 3.4: Shrinkage cracking in the Aluminosilicate geopolymer near the steel tape backing

The standard solution to reduce the shrinkage cracking would be to add in some reinforcement to take some of the strain that shrinkage causes. The larger diameter reinforcement, while

necessary to support flexural loads, leads to the aforementioned thicker layers of geopolymer coating and enhances the shrinkage cracking. To combat the cracking, a smaller reinforcement will have to be introduced throughout the matrix. While this research sought to use a more ductile flexural reinforcement, in steel, carbon fiber provides an easy solution to the shrinkage problem. The fibers can be cut to small lengths and dispersed into the matrix to prevent cracking in many directions. Carbon is also the most temperature resistant of the small diameter fibers mentioned in Chapter 2 of this dissertation and should function in heating with the insulation of the Polysialate matrix.

The fibers used to prevent cracking were pitch based carbon fiber made by Mitsubishi Chemicals. The fibers themselves came prechopped in 6mm lengths with a fiber diameter of about 11 microns and a recommended fiber dosage of about 3-6% of the volume of our material. For a 100g liquid component batch of geopolymer matrix this came out to be approximately 6g of chopped carbon fiber. Fiber was added into the mixes in two ways, by hand mixing after blending of the matrix and prior to blending of the matrix components. In the first case fibers were kept at longer lengths and would seemingly provide a greater coverage per fiber. In the second method fibers would be distributed mechanically, but also would potentially be chopped finer by the blades of the blending device. For both cases the carbon fiber matrix was applied in two ways. In the first method, the initial coat of geopolymer would not contain any carbon fiber while the second coat going over the top of the steel tape would have the 12g of chopped fiber present. In the second method, both the initial coat and secondary top coat would contain the 12g of chopped carbon fiber. These two methods were selected to identify if material costs could be reduced by lessening the amount of carbon fiber present in the composite and would also test if there was any impact on bond having the carbon fiber pieces in the areas of the geopolymer between the steel tape and the brick surface.

While the level of cracking could not be determined until curing, it was almost immediately that

hand mixing proved to be a less than ideal method of introducing the chopped fibers into the

matrix. Adding the fibers in after mixing generated another mixing step into the procedure, one

that could vary in quality wildly depending on the individual doing the mixing. Carbon fibers in

the hand mixed matrix also proved to clump more readily which not only causes issues for fiber

distribution for mechanical needs but creates a less visually appealing finish. Even when mixed

well, the hand mixed fibers were visible in the matrix and caused the surface to appear patchy.

The mix also became much thicker and was a great deal harder to apply, especially on the

reinforced bricks.

Figure 3.5: Hand Mixed Carbon Fiber Sample

Several immediate improvements were noticed for the coatings with carbon fiber added to the

solid components before everything was mixed. Firstly, no additional steps or time were added

to the process as fibers were now blended as part of the normal procedure. Secondly, the

mixing itself was more consistent as it was now performed by the equipment and not an individual. Thirdly, the additional chopping and mechanical distribution of the fibers altered the thickness of the matrix only slightly so early Part D filler modifications could be easily carried over. Lastly, the additional chopping and mechanical dispersion of the fibers prevented clumping, spread fibers evenly, and even lead to the black fibers modifying the color of geopolymer from a light tan to a more concrete-like grey.

Figure 3.6: Blender Mixed Carbon Fiber Sample

After setting, the blended carbon fiber geopolymer samples displayed little to no shrinkage cracking visible to the naked eye. Further testing of carbon fiber preparation and content will be addressed later in this dissertation.

Two more admixtures, isopropyl alcohol and iron oxide pigment, were also considered for early testing. Isopropyl alcohol was included in some early samples of brick tests as a way to reduce bubbles in the composite due to the release of gases as a byproduct of chemical reactions. For these samples, 10g of isopropyl alcohol was added to the matrix after the first stage of blended has occurred. This process was done to help ensure the alcohol was present for the correct stage of the chemical reaction. The specific effects of the alcohol will be addressed in the discussion of the flexural samples. Iron oxide pigment was considered as a proposed method of improving bond strength, much in the way that a slight layer of rust on rebar improves the bond with concrete. It was determined, however, that these tests would be better suited for comparison with a more final aluminosilicate matrix design so any improvements in performance would represent the enhancing of an already successful material. Flexural beam repairs and slant shear repairs were conducted with a more limited selection of matrix proportions later in testing and it will be in those tests that some iron oxide enhanced samples would be investigated.

3.2.2.2 Heating of Bricks

Heating tests were performed on the non-reinforced bricks in order to verify that the specific proportions of polysialate geopolymer will withstand temperatures comparable to those experienced in a fire. An electronically controlled oven was set to 500°C (932°F) and allowed to get fully up to temperature. One at a time, cured, non-reinforced specimens were placed inside of the oven and heated for 30 minutes. After 30 minutes, the brick was removed and allowed to cool to a temperature it could be safely handled. The next brick would then be placed in the oven for 30 minutes as well. Once properly cooled the coating on the bricks was observed to see if any damage occurred due to the heating. This was performed with both naked eye

observations and the use of an USB powered microscope. In all cases of this general

aluminosilicate geopolymer design, no cracking or damage appeared to occur as the result of

the heating. This is especially important for the samples with carbon fiber blended in as the

carbon fibers should be well protected in the composite and not generate another potential

failure point

The effect of heating on the full composite of the geopolymer and the steel tape will be

investigated in the full scale testing.

3.2.2.3 Flexure of Bricks

To get an idea of the ability of the coating to bond the Hardwire tape to the concrete brick, the

brick samples were broken in flexure and a visual inspection would be made of the failures that

occur. As the brick dimensions are not large their maximum load they will support in their

compressive zone in flexural will not be very high, compared to the incredible high potential of

the steel tape in the tension zone. The bricks are also very deep relative to the testing span

which, when cracking, would results in the edges of the crack opening up wide as it propagates

and putting additional stress on the bond between the brick and composite as these sharp

edges press into the steel and polymer layer. These factors should lead to the reinforced bricks

generally failing from a cracking in the brick leading to a debonding of the composite. Shear

failure would be relatively unlikely due to the high ratio of depth of the brick to testing span but

should a sample fail in shear, it will then be determined if the failure resulted from a strong

bond in the composite or defect in the brick.

As all bricks and steel tape were identical materials any differences in the load/deflection

performance of the reinforced bricks could be attributed to the specific polysialate matrix

holding the steel to the brick.

The testing was performed on a Sintech 10/GL MTS testing apparatus set up for flexure in three

point bending. A span of 7 inches was used and loading was done at the midpoint of the brick.

Data was monitored and recorded in Testworks, the program associated with the equipment.

Data was produced by an extensometer tied to the machine's moveable crosshead and a 10 kip

load cell affixed to the cross head. A point load attachment was screwed into the load cell to

apply the midspan load across the width of the beam evenly. The load point was moved into

position lightly contacting the top surface of the brick's compression zone and both the load cell

and extensometer were zeroed. Figure 3.7 shows the typical set up for a reinforced brick

flexural test. A load rate of 0.01 inches of deflection per minute was monitored by the Testworks

software. Data was recorded by the program along with a real time graph of load versus

deflection and saved as a text file. These files were later converted into Microsoft Excel

spreadsheets for easier analysis and data management. Testing was automatically stopped by

the system when a major failure was detected. A sample test screen for the Testworks 4

software used in the testing is shown below.

Figure 3.7: Testing Setup for Flexure of Reinforced Brick Specimens
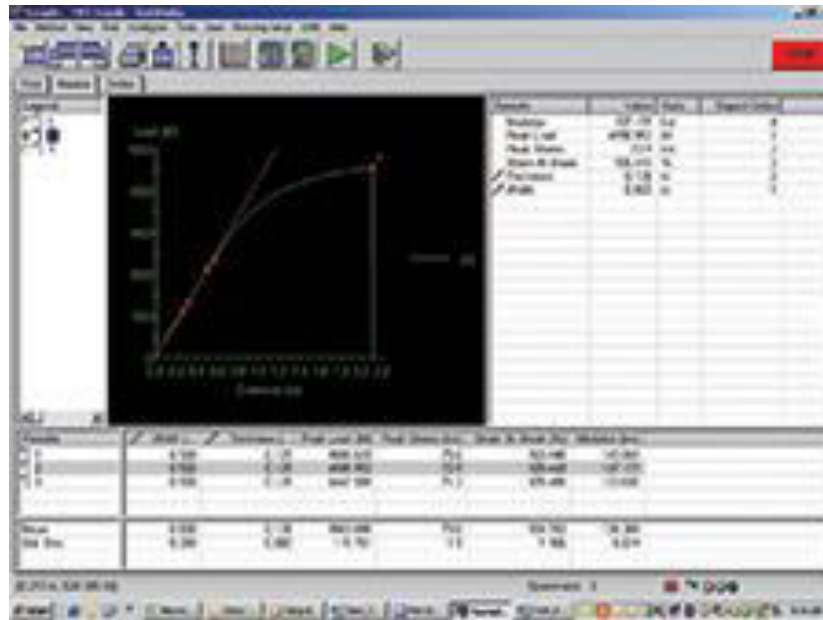
Figure 3.9: Sample screen of Testworks 4 software

As predicted, the majority of all specimens failed due to the increased stress at the composite caused by the crack widening at the center of the brick. This led to a delamination of the composite to varying degrees depending on the mix. In the case of one brick, shear failure resulted from the flexural loading; however, further investigation proved that this brick had a flaw present from manufacturing that lead to this failure. This was reinforced by the data which showed the reinforced brick only withstanding about 5% of the load that bricks with similar matrices held.

For those bricks that did fail as expected, valuable data on not only successful proportions but on matrix preparation were obtained. Figure 3.10 shows some selected load versus deflection curves for different mix proportions and methods. Figure 3.11 shows results for three bricks all with an additional 50g of "Part D" filler and 12g of chopped carbon fibers that were mechanically blended into the matrix.
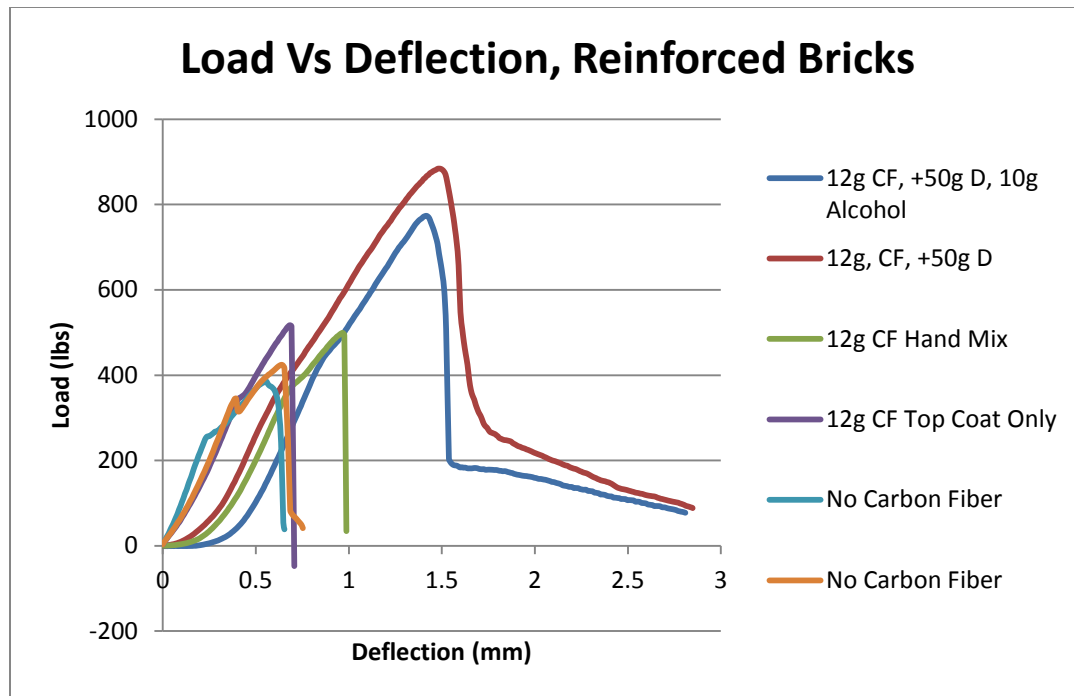
Figure 3.10: Load vs Deflection for Selected Reinforced Bricks
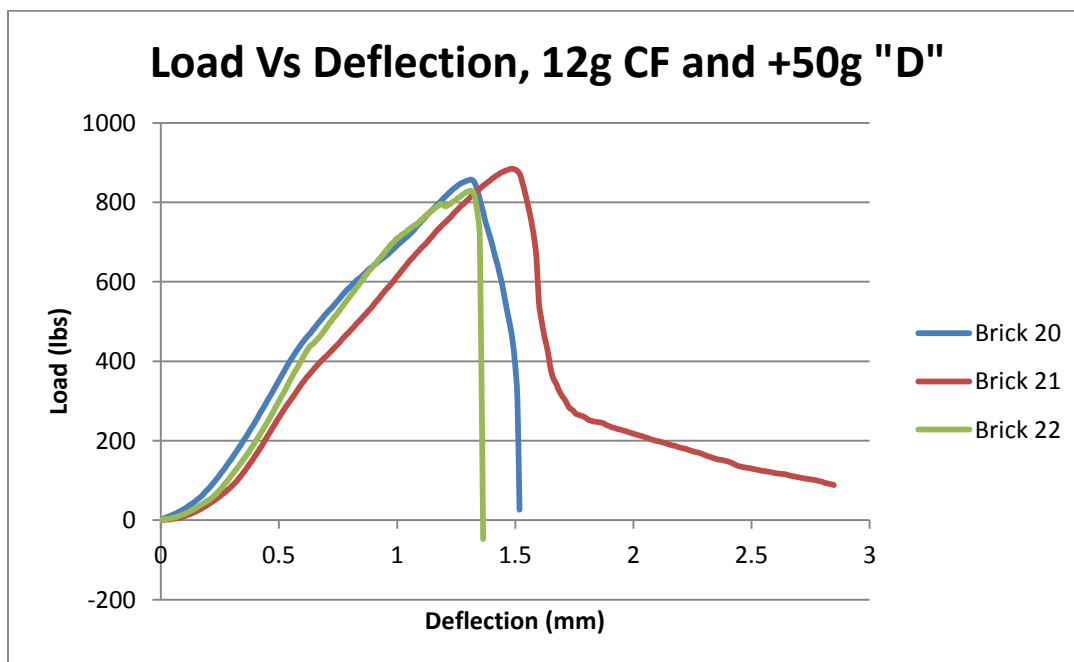
Figure 3.11: Load Versus Deflection for bricks with 12g Carbon Fiber Mechanically Blended and

an extra 50g of the "Part D" Filler

The best performance of any of the bricks occurred in samples with a geopolymer thickened with an additional 50g of part D filler and with 12g of chopped carbon fiber blended into the mix. The maximum flexural load of these mixes exceeded 800 lbs occurring at deflections greater than 1.25 mm. Without any chopped carbon fibers included in the geopolymer matrix, we see that the bricks only deflected approximately two thirds to three quarters of a millimeter before failing at loads near 400 lbs. The presence of chopped carbon fibers does in fact alleviate much of the visible shrinkage cracking in the base composite and reinforce the matrix enough to significantly improve bond. This 100% increase was not solely due to just the presence of carbon fiber in the matrix. The methods of mixing and application played important parts in the strength increase. As we see in the samples with carbon fiber only present in the top coat of the matrix and carbon fiber that was manually mixed into the geopolymer, strength increases were only about 25% of the controls and deflection did not have a consistent increase over the control samples. There are a few reasons for this:

- Hand mixing does not additionally chop the fibers and thoroughly distribute them leading to more even coverage.

- Hand mixing can lead to clumping which further hinders distribution and, more importantly, can result in areas around the steel cords without proper matrix penetration.

- Only applying fibers in the exterior coating of geopolymer doesn't prevent any shrinkage cracking within the first coat, it just prevents the more visible cracks.

- Extra part D filler helps thicken the polysialate matrix which allows for a more complete coverage of the steel tape, especially when combined with the carbon fiber.

Another important detail seen in the testing was the effects of the isopropyl alcohol on bond strength. As previously stated, the isopropyl alcohol added into the mix helps to eliminate bubbles that could develop in the mix due to gases released in the aluminosilicate geopolymer's reactions. The main idea here being that these bubbles will lower the area of the matrix and could lead to gaps near the reinforcement. The data suggests, however, that any benefit from eliminating the bubbles seems to be lost most likely due to the alcohol interfering in some other chemical reaction. The sample including alcohol still held near 750lbs in flexure but this represented an approximately 10% drop off in strength from the samples without alcohol.

From these preliminary tests it is apparent that the original base mix, which again was designed for use with carbon or glass fiber tows, needs some modifications to properly work with steel wire tape. By adding in 50g of a zinc oxide filler and 12g of chopped carbon fiber into the solid matrix components before mixing the matrix is made more suitable for use with thicker steel cords. One more phase of initial testing will be conducted on the geopolymer, this time to verify that the selected quantity of carbon fiber is optimum for use in SRiP applications. This testing will also focus on determining if there is any benefit to further chopping the carbon fibers before mixing the geopolymer and if there is any noticeable benefit to adding in iron oxide pigment as mentioned in section 3.2.2.1.

3.2.3 Repaired Flexural beams

Additional verification of the geopolymer matrix was conducted in the form of flexural repair testing. This testing was used to confirm that the selected matrix could create a consistent bond with concrete surfaces and also allowed for slight variations in carbon fiber content to be explored. A small investigation was also conducted at this point into the effectiveness of iron oxide pigment in positively impacting the bond performance with concrete.

For this round of tests, six geopolymer mix designs were created based on the 12g carbon fiber

and 50g additional zinc oxide mix from the brick testing. As this mix was already proven to be an

effective choice for the SRiP applications in this dissertation, only minor modifications were

made that had not been tested in the brick samples. The first change tested was in preparation

of the carbon fibers. From the brick testing, a clear benefit exists to allowing the chopped

carbon fibers to be additionally chopped and mechanically distributed by the blending

equipment. The question that arises from this fact is could further chopping and distribution

result in a stronger bond performance as fibers have the chance to be spread more evenly

throughout the coating. As the reactions in the matrix are exothermic, and the mixing process

can generate additional heat from the equipment, the extra stage of chopping of the fibers will

be performed as a part of the batching of the solid components. Referred to in this dissertation

as "preblending," this stage consists of placing the solid components of the geopolymer matrix

in the same blending apparatus as the matrix itself will be mixed in. The solid ingredients are

blended for approximately 60 seconds to achieve the aforementioned additional distribution of

carbon fibers without increasing the heat during the chemical reaction. In the original testing,

the 12g batch amount of chopped carbon fiber was selected based on the manufacturer

recommendation of a fiber volume of 3-5%. This amount represented the low end of

manufacturer recommended fiber volume. A mix representing the higher end of the

manufacturer recommendations will also be considered at this stage. This mix will contain 50%

more chopped carbon fiber, a total of 18g. To make sure this larger quantity of fiber is properly

distributed the 18g carbon fiber mixes will all be subjected to preblending as described above.

Finally, a variant of each of these mixes will be tested with 10g of iron oxide included in the solid

components. Iron oxide is generally used as an inorganic pigment to provide a paint or coating

with a reddish hue. The theory behind its inclusion in the coating is that for reinforced concrete,

the concrete itself tends to form a better mechanical and chemical bond with slightly rusted

rebar (rebar with a layer of iron oxide on it). By including some iron oxide in the matrix it is

hoped that the bond will improve with the concrete surface.

The six mixes used in the flexural repair testing were:

- The base geopolymer plus 50g of extra Part D and 12g of Carbon Fiber

- The base geopolymer plus 50g of extra Part D, 12g of Carbon Fiber, and 10g Iron Oxide

- The base geopolymer plus 50g of extra Part D and 12g of Preblended Carbon Fiber

- The base geopolymer plus 50g of extra Part D, 12g of Preblended Carbon Fiber, and 10g
  Iron Oxide

- The base geopolymer plus 50g of extra Part D and 18g of Preblended Carbon Fiber

- The base geopolymer plus 50g of extra Part D, 18g of Preblended Carbon Fiber, and 10g
  Iron Oxide

Flexural Repair testing involved four primary steps: First, non-reinforced concrete prisms

specimens had to be created to facilitate flexural testing. Second, the beams had to be broken in

flexural so a repair could be made. Third, samples of the geopolymer would be mixed and used

to reassemble the broken concrete prisms. Fourth, after proper curing of the repair material,

the prisms will be retested to determine the relative effectiveness of each mix proportion.

Creation and testing of samples were performed under the guidelines of ASTM C31 and ASTM

C78 Standard Test Method for Flexural Strength of Concrete (Using Simple Beam with Third-

Point Loading). Concrete prisms were 11 inches long with a 3 inch by 3 inch cross section to

confine to the ASTM required minimum span length of three times the beam depth. The beams

used in this dissertation were originally cast as part of previous research regime investigating

concrete crack repair. An excess of flexural beams were cast and enough additional samples were available to accommodate three beams for each of the six matrix proportions.

A self-compacting concrete was utilized for the casting of the concrete prisms so no vibration would be required for the specimens. The concrete was mixed and samples prepared in the structural engineering lab at Rutgers University Busch Campus. The design was as follows:

- 802 lbs/yd3 of Type I Portland cement provided by Lafarge North America's Whitehall, PA manufacturing plant
- 1408 lbs/yd3 of concrete sand provided by Weldon Material's quarry in Watchung, NJ
- 1312 lbs/yd3 of 3/8" stone also provided by Weldon Material's quarry in Watchung, NJ
- 318 lbs/yd3 of water

Custom formwork was created for the research in order to cast 60 concrete prisms simultaneously. Materials for the custom gang mold formwork were obtained from Tulnoy Lumber in Carteret, New Jersey. Samples were left in the mold for 24 hours before being demolded and moved to a standard laboratory curing fog room. Compression strength of the concrete was 6,660psi after 28 days of curing.

Flexural testing was performed with the same MTS Sintech 10/GL computer controlled testing apparatus as the brick experiments. Once again this equipment included a 10kip load cell and crosshead for deflection measurement. Samples were labeled 1 to 18 and tested in third-point bending with a span length of 11 inches and 3 inches between custom welded loads and supports. The location of the loads and supports were also marked, as well as the top surface that the load contacted. The loading rate for samples was 0.02 inches of deflection per minute. Initial breaks of concrete prisms had an average modulus of rupture of 184.19 psi.

To prepare broken prisms for the repair process, any small particles were cleaned from the

surface of each break. The appropriate coating was then mixed as described earlier in this

chapter. Iron Oxide was added to the planned mixes during the batching of solids. Preblending

occurred immediately after the batching of the solids. Half of each beam was placed vertically

on a flat surface so its break was visible. The broken surface was then lightly coated with the

appropriate design of geopolymer using a 2 inch sponge brush as seen in Figure 3.12.

Figure 3.12: Application of geopolymer matrix for Flexural Repair testing

The same was done for the second half of each beam, at which point one half was inverted and

the breaks were matched up and then pressed together. The self-weight of the prisms were

used to hold the halves together during air curing which is depicted in Figure 3.12.

Figure 3.13: Repaired Flexural Samples

Samples were left undisturbed for 28 days before they were again tested in third point bending using the exact testing equipment and rig from the initial breaking. Load versus deflection data was recorded for each test and the breaking loads for all samples are presented in the table below. From the data, the initial mix with 12g of carbon fiber and no preblending performed the best, holding an impressive average of 95.23% of the initial load as well as showing cracking through concrete and matrix (Figure 3.13); however, no clear effect was visible from the change in fiber percent, preparation, or the presence of iron oxide. This lack of a pattern could be due to issues with the initial breaks where portions of the beam at the main break site chipped away. This leads to a smaller effective area of the repair and the sustainable load would be smaller. Based on these results, the standard mix used for full scale SRiP testing will be the base aluminosilicate geopolymer with an additional 50g of zinc oxide filler and 12g of carbon fiber.

Summary of Flexural Repair Testing						
Mix Design	Sample Number	Initial Breaking Load (lbs)	Repaired Breaking Load (lbs)	Average Initial Breaking Load (lbs)	Average Repaired Breaking Load (lbs)	Percent of Initial Load held
Base Mix, +50g Part D, 12g Carbon Fiber	Beam 16	442.033	533.143	507.357	483.154	95.23
	Beam 17	533.669	448.025			
	Beam 18	546.368	468.295			
Base Mix, +50g Part D, 12g Carbon Fiber, 10g Iron Oxide	Beam 11	409.16	394.904	572.150	361.833	63.24
	Beam 12	670.464	272.798			
	Beam 13	636.827	417.796			
Base Mix, +50g Part D, 12g Carbon Fiber Preblended	Beam 1	604.507	246.131	574.462	214.278	37.30
	Beam 2	408.827	148.717			
	Beam 3	710.052	247.985			
Base Mix, +50g Part D, 12g Carbon Fiber Preblended, 10g Iron Oxide	Beam 4	639.064	307.125	581.687	294.581	50.64
	Beam 5	477.455	319.251			
	Beam 6	628.541	257.368			
Base Mix, +50g Part D, 18g Carbon Fiber Preblended	Beam 7	581.999	419.536	603.706	367.151	60.82
	Beam 8	577.499	424.548			
	Beam 9	651.619	257.368			
Base Mix, +50g Part D, 18g Carbon Fiber Preblended, 10g Iron Oxide	Beam 10	586.383	319.414	667.931	347.359	52.01
	Beam 14	691.911	318.44			
	Beam 15	725.499	404.223			

Table 3.1: Breaking Results of Flexural Repair Testing
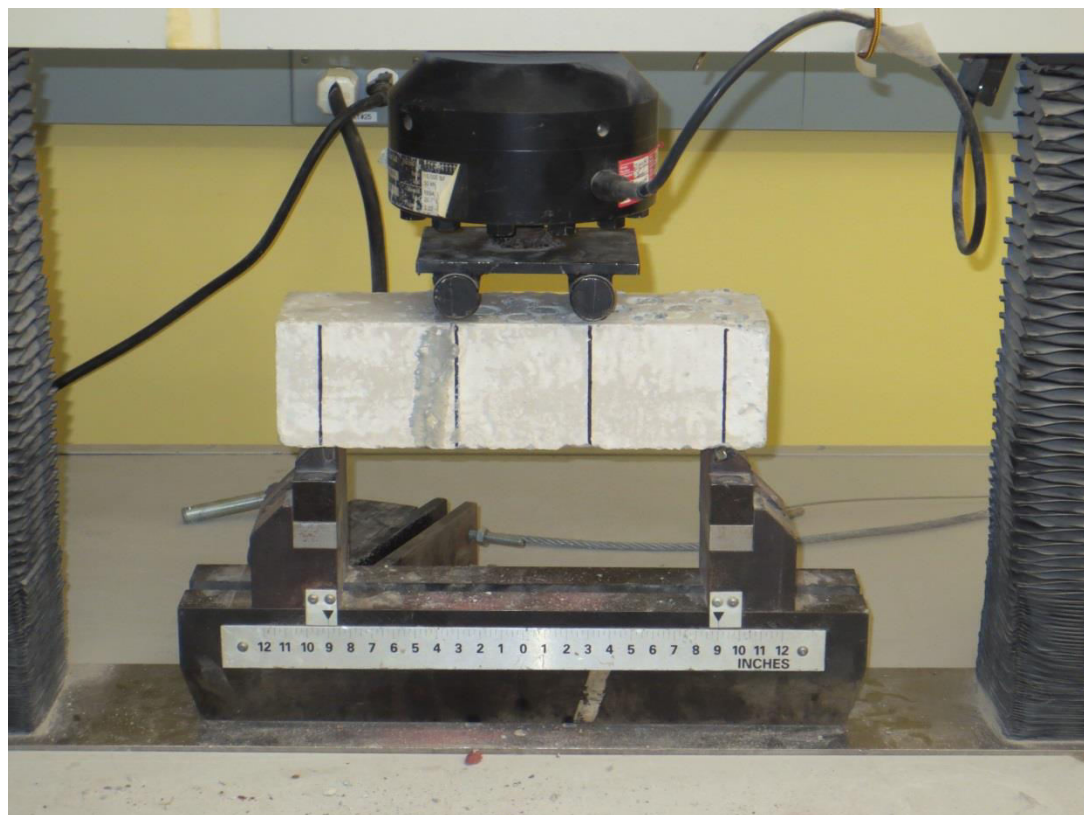
Figure 3.14: Flexural Testing set up of repaired concrete prism

Figure 3.15: Flexural failure through both repair matrix and concrete
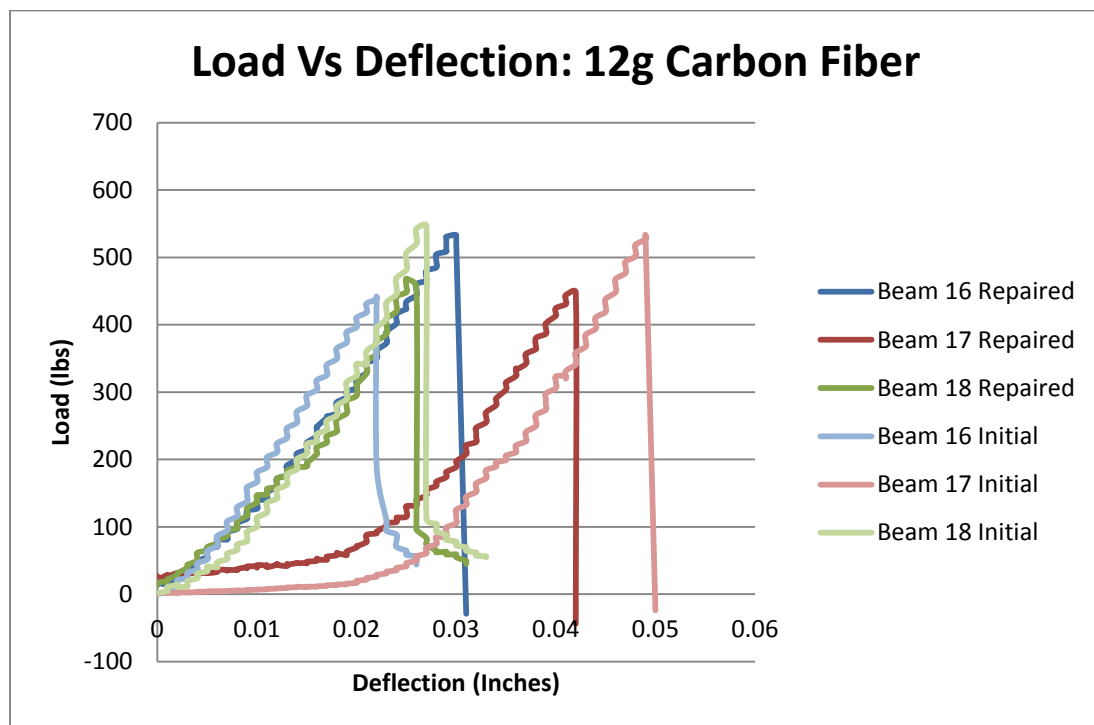
Figure 3.16: Load versus deflection for 12g Carbon Fiber Matrix Samples
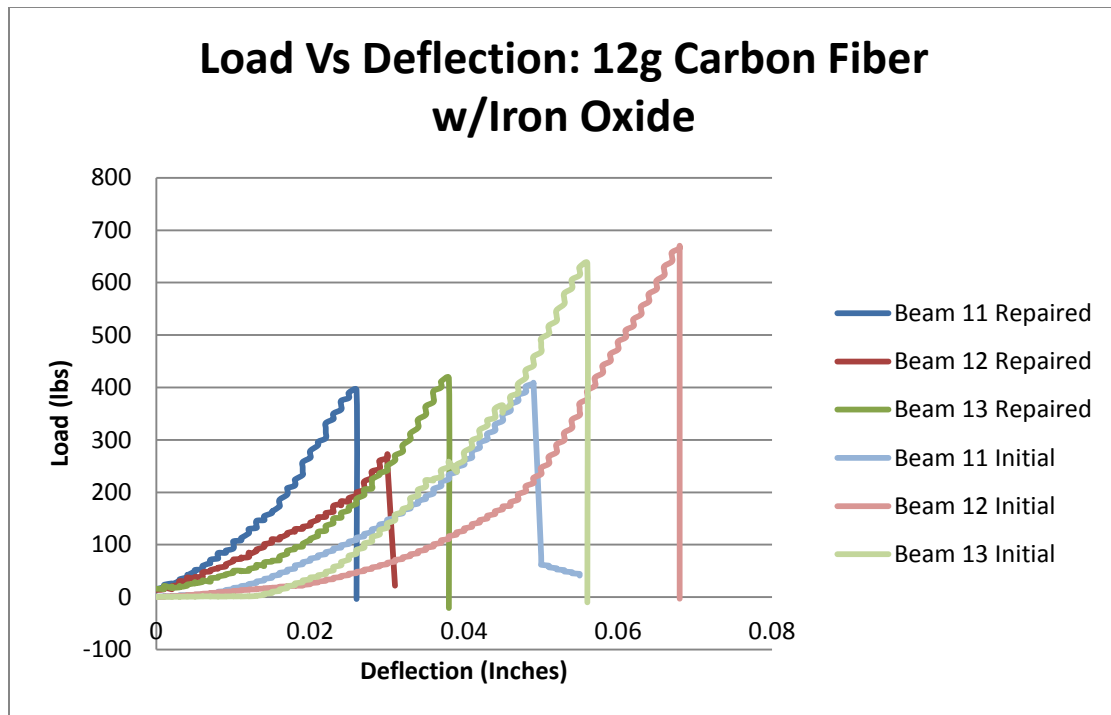
Figure 3.17: Load versus deflection for 12g Carbon Fiber with 10g Iron Oxide Matrix Samples
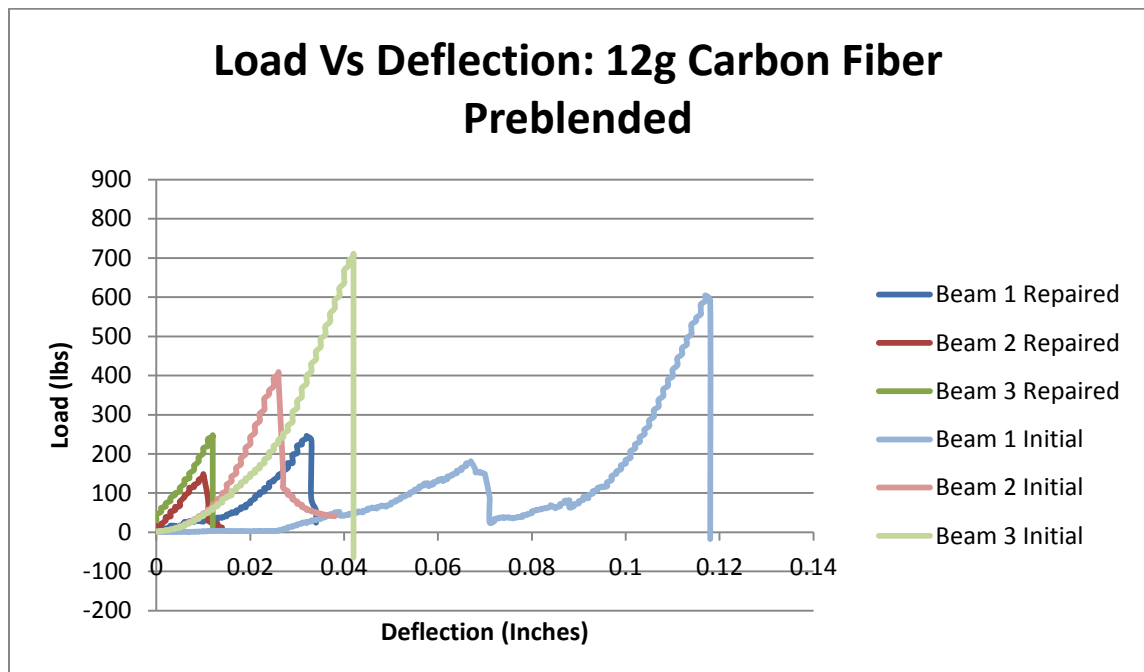
Figure 3.18: Load versus deflection for 12g Preblended Carbon Fiber Matrix Samples
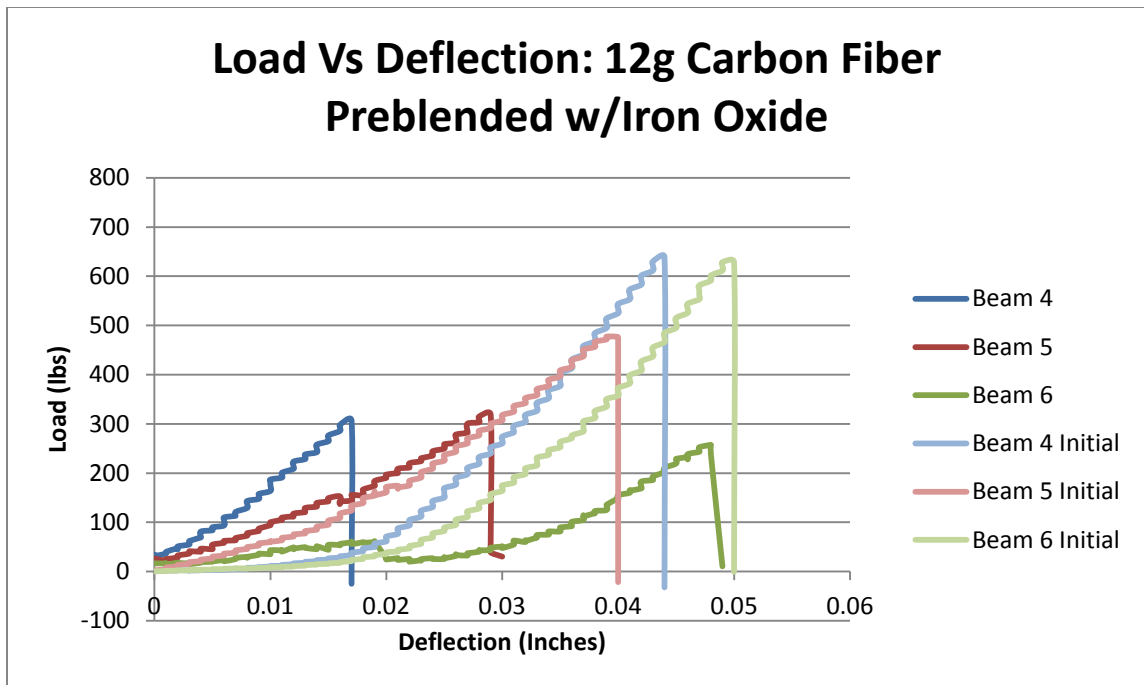
Figure 3.19: Load versus deflection for 12g Preblended Carbon Fiber with 10g Iron Oxide Matrix
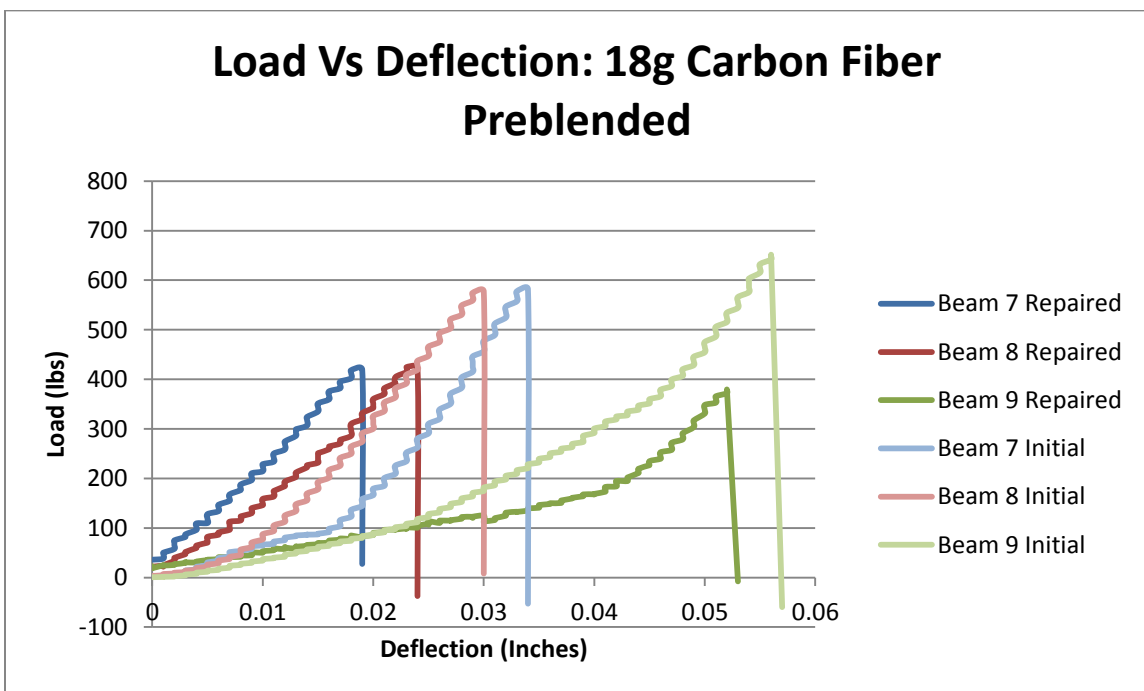
Samples

Figure 3.20: Load versus deflection for 18g Preblended Carbon Fiber Matrix Samples
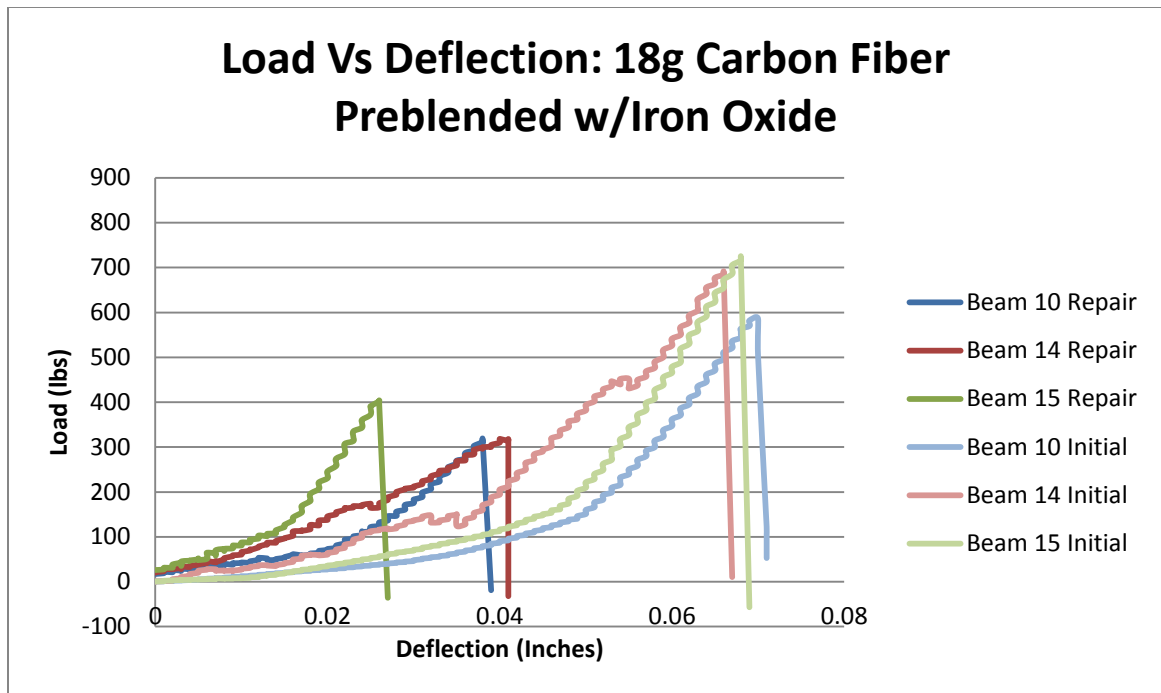
Figure 3.21: Load versus deflection for 18g Preblended Carbon Fiber with 10g Iron Oxide Matrix

Samples

3.2.4 Slant Shear Testing

A common way to study the bond strength of an adhesive material with concrete is to use a

slant shear test (ASTM C882, 2012). Slant shear testing is controlled by ASTM C882, and uses a 3

inch diameter, 6 inch tall cylinder of concrete that has been cut at a 30 degree angle and bonded

back together. Cylinder halves were coated in geopolymer matrix and placed back into a

standard 3 inch by 6 inch cylinder mold to maintain proper shape while setting. Repaired

specimens were air cured for a minimum of 28 days. After curing, each repaired cylinder was

tested in compression with a 250 kip press. Results for all samples hovered near 3,500 psi and

no mix was observably, significantly stronger than any other in this capacity. As such, further

testing with a greater sample size would be beneficial to determine the effects of the slight

differences of each mix on slant shear. It was also noted that a relatively thick layer of

geopolymer was present in the samples that had been placed back into their mold to set. This could lead to some cracking do to shrinkage but also a large joint in the middle of the sample to fail at. Most cylinders seemed to fail smoothly at the repaired surface, signifying a proper bond was not developed in the samples. Figure 3.22 shows one slant shear sample that did fail somewhat through the concrete at its top, however, a smooth geopolymer surface with what appears to be shrinkage cracking is in fact present on the rest of the cut cylinder face, supporting the claim that the layers may have been too thick.

Figure 3.22: Initial slant shear testing with smooth failure at repair site

Additional samples were manufactured, this time using a thinner layer of geopolymer and a

wooden jig to let the cylinders set with the cut surface lying horizontally. These cylinders did still

fail along the repaired surface; however, they also showed cracking through the concrete, such

as in Figure 3.23.

Figure 3.23: Failure through concrete in secondary slant shear testing

3.3 Summary

Steel Cords

- Required something commercially available with convenient means of installation.

- Hardwire LLC provides readily available steel wire produces in individual braided strands

  or "tapes" that attach the strands parallel on a mesh.

- Individual cords can hold 346.2 lbs with a 2.1% strain to failure.

Initial Testing

- Reinforced cement bricks with steel wire and geopolymer to test the ease of application. Bricks were heated in an oven as well to try and detect any issues with the selected materials. After coating bricks were broken in flexure to gage how well the SRiP composite bonded to the cement brick.

- Additional of small amounts of carbon fiber into the matrix helped prevent shrinkage cracking and secure the bond between the steel wire and geopolymer.

- Additional additives considered in testing. Isopropyl alcohol can reduce bubbling from gases formed in chemical reactions. Iron oxide was hypothesized to improve bond strength as surface rusted rebar can bond more effectively with concrete.

- After consistent flexure results were achieved with bricks coated with a selected geopolymer recipe small concrete beams were tested to further assess their effectiveness.

- Plain concrete beams were broken in flexure and repaired with a selection of geopolymer recipes. After proper curing time they were retested to assess the strength of the geopolymer itself.

- Iron oxide did in fact prove to have a positive impact on the strength in these tests, albeit a very small impact.

- Slant shear testing was also performed to check bond strength. Results were not overly positive as it appeared the coating was applied far too thick and shrinkage cracking was present in many samples.

CHAPTER 4 – EXPERIMENTAL INVESTIGATION: LOAD DEFLECTION RESPONSE

4.1 Introduction

To properly investigate the performance of SRiP reinforced RC beams in high temperature

scenarios, a baseline must be determined for the performance of concrete beams with varying

levels and types of external reinforcement. In this dissertation, a series of shallow reinforced

concrete beams were created to facilitate testing of the external composites in question.

Shallow reinforced concrete beams were selected to maximize the surface area of the beams'

tension zones and allow for sufficient quantities of steel reinforcement to be bonded. Shallow

beams have been used to test both SRiP and steel reinforced grout systems to determine the

effectiveness of these materials in increasing flexural capacity of reinforced concrete members

(Prota et al., 2006; Menna et al., 2013). In the previous experiments combining inorganic matrix

composites and shallow concrete beams, cross sections of beam used measured 200 mm deep

and 400 mm wide (8 inches deep and 16 inches wide). For this dissertation the depth and width

were half of these earlier studies, 4 inches and 8 inches respectively. This smaller cross section

was selected to account for maximum capacity of the load cells to be used in testing and to

utilize laboratory space more efficiently while other research projects also required casting of

beams.

In Chapter 4, the process by which all full scale shallow beams were manufactured shall be

detailed. Any additional material testing, such as on concrete or steel rebar, will be addressed in

this chapter as well. A thorough mix procedure for the geopolymer as well as installation

procedure for the composite will be fully detailed to demonstrate the required level of work.

This will lead to the first series of full scale flexural tests on the shallow reinforced concrete

beams. These samples will be controls that will be compared to samples that are heated to high

temperatures to identify the loss of load capacity and damage to the SRiP.   These heated

samples will be addressed in Chapter 5 of this dissertation. The full flexural testing procedure

will be reviewed in this chapter as well.

4.2 Manufacture of Shallow RC Beams

Construction of the beams progressed in three phases. First, the beams' dimensions were set,

the basic concrete properties were selected, and the necessary reinforcing steel quantities were

calculated. After all of the details have been compiled, the reinforcement cages needed to be

constructed to the desired specifications. Beams were finally cast in wooden molds and cured to

the specifications needed for this testing regime. The beams were created in what were

effectively two different batches. For the second batch, a different assembly method was used

for the rebar cages to allow for a simpler construction and beams were cast in sets of two to

improve quality control. Specifics on each of these phases are provided in the next 3 subsections

of this chapter.

4.2.1 Design of Shallow RC Beams

As stated in the introduction, using a shallow beam design for external reinforcement testing

allows for a more significant surface area to apply the composites being tested. The dimensions

of the beam were selected to match well with existing laboratory equipment and have

comparable size to reinforced concrete beams regularly tested in Rutgers University's Civil

Engineering Laboratory. A width to depth ratio of 2:1 will be used just as in testing by Prota et al.

and Menna et al. Beams were designed to be 8 inches wide by 4 inches deep by 96 inches long.

Flexural strength was initially calculated using an average compressive strength of the concrete

of 5000 psi. Each beam contained 2 #2 rebar in compression, 2 #2 and 2 #3 rebar in tension and

#2 double leg stirrups spaced 4 inches center to center. Using a 120 kip Forney Tension machine

samples of the rebar were tested in tension to verify their ultimate strength for more accurate

flexural calculations. From this verification testing it was determined the average yielding strength of the rebar used was approximately 70,000 psi. Figure 4.1 shows the planned typical cross section of each shallow reinforced concrete beam.
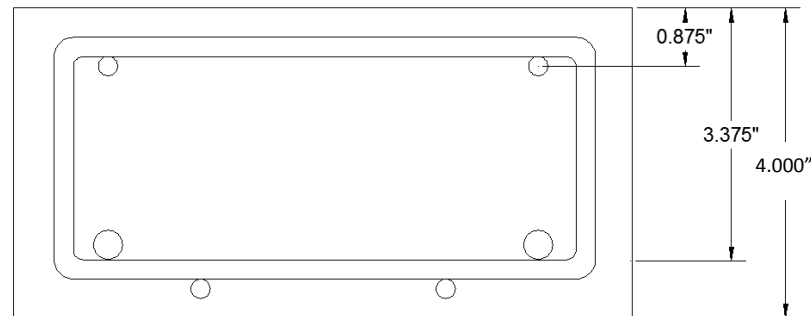
Figure 4.1: Typical planned cross section of shallow reinforced concrete beams

After the beam design was finalized, work began on assembling the internal reinforcement.

4.2.2 Rebar Cages

To begin the sample preparation, sixteen reinforcement cages needed to be hand assembled to provide basic support to the concrete beam samples. These sixteen beams would make up the first round of full scale samples, with more beams being created to fill in other necessary testing areas later on. For this first set of beams, #3 deformed bar and several 4 feet by 8 feet sheets of #2 welded wire mesh with a 4 inch spacing were purchased from Samson Metals in Cranbury, New Jersey. The welded wire mesh was initially purchased to reduce the construction time from tying on stirrups every four inches of the beam. The mesh would also account for the #2 compression and tension bars so only the #3 bars would need to be tied on. Using standard bolt cutters the #2 sized bars are snipped relatively easily and the mesh could be cut to an

appropriate size for the beams. Number 3 bars were cut to length using a chop saw with a steel cutting blade. Before attaching the #3 bars the cut section of mesh had to be bent to have the compression bars and legs of the stirrups in the appropriate place. The bending process proved more difficult than originally anticipated. No bending equipment existed in the laboratory that could handle an 8 foot length. A special rig had to be created to properly restrain the mesh so it could be bent. The mesh was placed along an I beam with the location of the bend being placed along the edge of the beam's top flange. An 8 foot piece of square tubing was placed on top of the mesh and clamped tightly to the I beam. When clamps were secured in at least three places the top of a sledgehammer was used to hammer and bend the mesh to the correct location. At this point the #3 compression bars could be tied to the mesh cage.

Bending wire mesh to create the rebar cage took a great deal more time and physical effort than originally anticipated so it was determined that producing individual stirrups and tying them in place would in fact be the more efficient method of construction. For the second set of beams #2 rebar was purchased and cut with bolt cutters and then bent with a metal bending apparatus into the correct stirrup dimensions. Compression and tension pieces were also cut and tied into place. Overall, the traditional method of cutting and bending individual stirrups proved must faster and had better quality control. Had the length of mesh to bend been smaller the original process may have been the more desirable option.

4.2.3 Casting and Curing

Upon completion of the steel mesh cages, preparations began for the pouring of the first set of sixteen shallow concrete beams. Four wooden gang molds each holding 4 beams were created to accommodate the casting of the beams. Pine boards were ripped to a width of four inches and affixed to a half inch plywood base to form the walls of the mold. The boards were spaced

started at one edge of the plywood and were spaced apart the desired width of the beams. This spacing left an unused area of the base to allow for excess concrete from screening and troweling the beams. Silicon caulking material was applied at the bottom edge where the walls and base meet. This helped to avoid seepage of concrete below the mold walls and prevent any uplift of the walls that would compromise the dimensions of the beam. The base itself was first wrapped in polyester sheeting to prevent warping due to moisture in the concrete.

Cages were laid in the molds so the top surface of concrete in the mold would match with the top of the concrete beam, tension steel to the bottom of the mold/beam. Once the rebar cages were placed a two foot long piece of #4 rebar was bent into a triangular shape and attached to the top of each cage as a picking point for transporting the beam. After setting the pick hooks, thin boards were affixed to the top of the walls at four locations going across the molds. These thinner boards helped maintain the beam width at the top of the beams in the presence of lateral pressure from the concrete. A total of 48 four inch by eight inch cylinder molds were laid out and coated in a release agent. These would serve as compressive strength samples to check the adequacy of the mix as well as verify the concrete strength close to beam testing.

It was determined that to cast so many beams and cylinders in one sitting with such a high volume of concrete required, close to 1.3 cubic yards with a 20% waste factor, the best course of action would be to order a truck of concrete from a local plant, Clayton Concrete in Edison, NJ. As plans were being made, another researcher was working on making calibration slabs for a separate research project. This project also required over one cubic yard of a normal concrete mix. To conserve some funds the other project agreed to use the same concrete design requirements and approximately three cubic yards of concrete were ordered. The concrete

requested used 3/8" coarse aggregate with a target slump of four inches and desired 28 day compressive strength of 5000 psi.

The four gang molds were spaced out evenly on the strong floor of the Rutgers University structures laboratory on plastic sheeting to prevent any damage to the floor underneath. A total of 3 additional researchers were gathered to assist in the pouring of the beams and cylinders required for this investigation and slabs for the aforementioned calibration project. It was determined that the slabs would be cast first, as there were less samples, however, issues with the internal rebar led to delays in the pour of the beams. During this delay, the truck operator wet the concrete additionally to keep it workable; however, this was done without researcher consultation and, as will be discussed later in this chapter, contributed to a severe decrease in the planned strength of the concrete.

Beams and cylinder samples were produced in accordance with ACI C31 Making and Curing Concrete Samples. An edged pine 2x4 was used to screen off the majority of the excess concrete in the large molds. Either end of the wood board was held flush with the top surface of the mold and pulled across the beams while being moved back and forth in a sawing motion. The beam surfaces were then finished with trowels to insure as smooth a surface as possible for the application of loads during testing. Finishing of the concrete beams was performed by multiple researchers and therefore there were some differences in quality of finish between beams. Cylinders were capped and placed next to beam molds and all samples were covered with polyester sheeting. After 24 hours, beams and cylinders were demolded and kept together in polyester sheeting. Burlap was placed on top of the samples and wet daily to cure them.

While the initial plan called for a casting of another 16 beams in a similar fashion to the first set, there were deemed to be a number of drawbacks with the larger pour. Firstly, the number of

individuals available to assist was rather low; this could again lead to delays and issues with the concrete consistency. With so few people and so many samples, it can also be difficult to maintain quality control in a small period of time. While the finishing was a minor issue in the first pour another factor that was discovered later in testing, and will be addressed in subsequent chapters, was the position of the rebar cages. For a few samples, the rebar cages experienced a bit of uplift when the concrete was poured into the molds. This uplift changed the position of the tension and compression steel which impacted the performance of the beams in flexure. Luckily, these beams were used in some speculative samples that were not as key to the main points this research intended to investigate.

For the next set of beams, several changes were made to increase the casting efficiency and further improve sample quality. Beams would not be cast in the original gang molds but instead in preexisting, individual molds. This allowed for smaller pours to be done in house and greater focus to be placed on each sample. In these existing molds the shallow beams would be cast on their sides as opposed to how they will sit in the testing rig. Casting on the side negated the impact of any small amount of uplift on the vertical position of the tension and compression steel. Horizontal shifting could have impact on torsion but not enough to drastically effect the failure pattern of these shallow beams. Casting beams on their sides also moved the position of the pick hook to allow for better instrumentation and less risk of interference with the flexural loading mechanism.

In this round, two beams were produced at a time with a minimum of 6 cylinders. Beams cast at the same time were planned to be tested at the same time, with 3 cylinders checking 28 day strength and 3 extra cylinders to verify strength on the day of flexural testing. Beam molds were labeled to keep track of the tension and compression sides of the beam. Sample creation and

protection were carried out following ACI C31 and the other preparations above. The concrete

mix was designed using ACI 211 Design of Normal Weight Concrete. The desired slump was 4

inches and aggregate size was 3/8 inches just like the original mix, however, the desired 28 day

strength was reduced from 5000 psi to 3000 psi to match closely with the actual strength of the

first concrete pour. The testing of both designs of concrete will be discussed further in

subsequent sections of this research. A total of 12 additional beams were cast in this manner.

The initial set of 16 beams would be used in heat testing to better allow for more time in the

testing schedule if there are any issues. The second set of 12 were used as controls for each type

of external reinforcement with a handful of extra beams produced in case of any issue with

other samples or additional validation of certain materials needed. Information on the

application process for SRiP composite will be addressed in the next section.

4.3 Application of SRiP Composite

The application process for the Hardwire/Geopolymer SRiP consists of five steps that insure a

proper bond between the concrete and the composite. These steps are: material preparation,

surface preparation, mixing of matrix, physical application of SRiP components, and curing of

composite. The following sections will detail out each step and provide some insight on how

best to adapt some laboratory techniques to field application.

4.3.1 Material Preparation

The preparation of the steel reinforcing wires as well as the geopolymer matrix components are

rather simple and can be performed well in advance of the actual application process.

4.3.1.1 Steel Wire Preparation

Hardwire 3x2 strands come in large spools of either individual strands or "tapes" that feature

strands connected on a composite mesh backing. The tape width is approximately twelve

inches. For this investigation, the density of wires selected was 12 strands per inch. Hardwire

pieces used would be 6 inch wide and 72 inch long. To produce pieces of this size, 6 foot lengths

were cut from the spool and then the mesh backing was split down the middle. To cut through

the steel wires Hardwire LLC recommended the use of electric power shears (Figure 4.2). A

120V, 50/60Hz electric shear was purchased from McMaster-Carr to cut the strands.

Figure 4.2 Power Shears (mcmaster.com)

While the shears cleanly cut the wires initially, after a few passes the blades dulled enough that

the thickness of the steel strands was too large for the shears. To resolve this issue, an angle

grinder with a steel grinding disc was used to remove a line of material across the planned cut

line. The wires were ground down to about two thirds of the thickness along this line which

allowed the power shears to cut through the wires without issue. The grinder could not be used

to fully cut through as that would prove too difficult to completely cut each wire safely and efficiently. For instances where Hardwire was to be used without any mesh backing the cut strands were pulled from the backing and any adhesive was cleaned from the strands. This process is not necessary for field application as spools of individual strands are sold by Hardwire LLC.

4.3.1.2 Matrix Material Preparation

Initial batching of the matrix materials is a quick process. As discussed previously, the aluminosilicate matrix is made of two primary components, a solid component and a liquid component. The individual compounds that make up the solid component must be weighed and combined in a water proof container such as a sealable plastic bag; this includes any pigments, fibers, or other filler agents. Additionally, special steps may need to be taken after batching but those will be discussed in greater detail in later chapters. Materials are batched with respect to 50g intervals of liquid component so if a batch is prepared that would require 100g of the liquid component that should be included on the label with the name of the mix. The liquid component itself should be stored in a cool if possible area in a sealed container for transportation. The liquid component is not batched until mixing is about to commence.

4.3.2 Surface Preparation

Before applying SRiP to the beams, their tension faces had to be properly cleaned to make sure that the composite would bond effectively. Failure to do so can result in unpredicted debonding and sudden failure in the repaired material. Beams were removed from their curing location and placed on saw horses with their tension sides facing up. For standard fiber reinforced polymers the surface of the concrete is ground down to remove the outer layer of cement paste and expose the aggregate.

Without exposed aggregate most epoxies used with FRP will not bond and lead to early failure; however, the similarity of geopolymer to concrete matrix allows it to form a bond without fully exposing coarse aggregate. To further verify this, the beams used in this investigation were not mechanically ground down but were cleaned with a wire brushes. A first pass was made with a wire brush attachment on an electric drill. This allowed for the smoothing out of any rougher portions of the tension face of the beams without significant labor hours spent.

Figure 4.3 Cleaning with a handheld wire brush before application

After wire brushing, beams were quickly gone over with a standard hand brush and any fine dust was removed with the use of bursts of air from an air compressor. It should be noted that for field application beams will be in situ and dust will not easily collect on the tension faces during cleaning. Using a permanent marker, the edges of the proposed repaired section was outlined for each beam. The six inch by six foot sections of reinforcement would each be centered on the beams so lines were made one foot from either end of a given beam and one inch from either side to better guide placement.
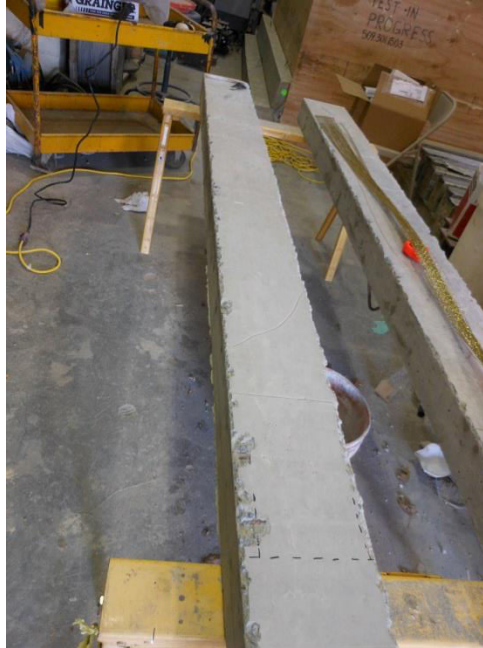
Figure 4.4 Guidelines Marked on Beam

4.3.3 Mixing of the Matrix

Once the application area was marked off the geopolymer could be mixed and installation could begin. A high RPM blender is required to properly blend the particles and the liquid component of the matrix smoothly. For this investigation, a Ninja brand, 1500 watt blender was used for mixing. The main mixing pitcher was placed on a gram scale and zeroed. Solid components were batched for use with 200 grams of liquid component, so 200 grams of liquid component was measured in the pitcher. The pre-batched solid components were then added into the pitcher on top of the liquid component.

The blender was powered on and the speed was increased from setting one to setting four over a period of about ten seconds. Blending at continued for 90 seconds before the setting was lowered back down to one and then stopped. The mix was allowed to rest for about 30 seconds in order to prevent any overheating of the equipment and matrix. Using a silicon spatula, the

sides of the pitcher are scrapped thoroughly to make sure all the solid component blends

properly into a homogeneous mixture. Blending resumes for another 90 seconds and the matrix

was transferred to plastic containers for application.
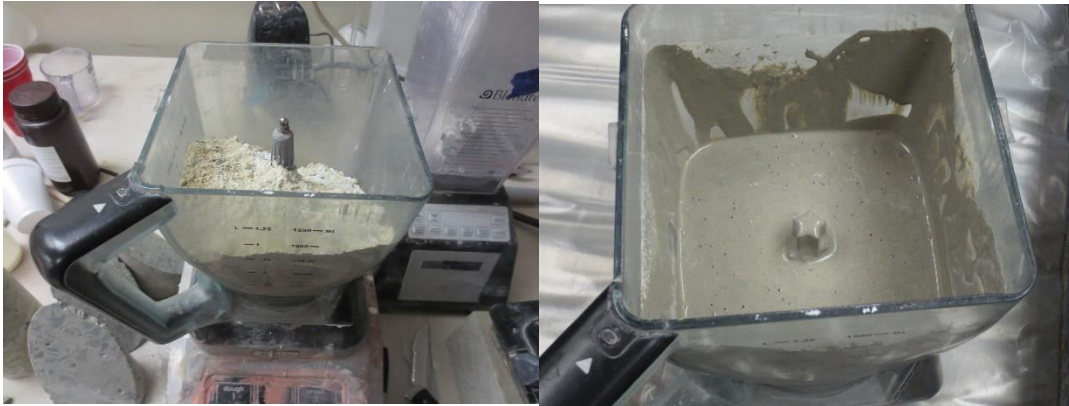
Figure 4.5 Geopolymer Matrix Before and After Mixing

4.3.4 Application of SRiP Components

The prepared, wet geopolymer matrix can now be applied to the marked surface of the

concrete. A small portion of the aluminosilicate mix is poured onto the beam and spread within

the marked boundary using a plastic spatula commonly used for repairing drywall. The precut

Hardwire reinforcement is then lined up with the markings and carefully laid into the matrix.

After lightly pressing the steel into the geopolymer by hand, the spatula is run down the length

of the cords to press them further. This process starts at the middle of the beam and move

outward towards each end. Using this method ensures that any air pockets or voids near the

middle of the beam, the section most critical for flexure, will either be completely

removed/filled or pressed closer to an area where less flexural strength is needed. Additional

amounts of the aluminosilicate are poured on top of the reinforcing wires and the additional

material is spread in a similar fashion until completely covering the Hardwire.

While the steel fibers remain stationary on their own due to the beams being turned upside down during the SRiP application process, additional precautions are taken to prevent any shifting of the composite during initial setting. During some initial practice applications, it was discovered that once the Hardwire was sufficiently pressed into the geopolymer the only areas that would curl or lift were the ends. To combat this effect, pieces of quarter inch plexiglass, cut to be three inches wide and six inches long is placed at either end of the beam laying across the reinforcement. Spare concrete cylinders were then placed atop the plexiglass to hold the ends firmly in place as the composite set.

The beam and composite were left undisturbed for approximately 24 hours so they could set. For samples that required two layers of external reinforcement the above process was then repeated, making sure to align the new layer of wires with the first and is again let to rest for 24 hours. Once all layers of wires had been applied and the exterior layer has set, an additional amount of geopolymer was mixed and a final topcoat was placed over the fibers. This topcoat will smooth out the appearance of composite and fill any small voids after the initial covering. The topcoat must be applied within two days of the previous layer or the layers may not properly bond together.

Fully set beams were moved aside to cure in the open lab conditions for 28 days before they would be tested. The beams themselves were rested compression side up on bricks at either end to prevent the composite from contacting the ground before testing. In all 6 main variants of reinforcement were used in this testing: Standard reinforced concrete, a single layer of SRiP reinforcement with the mesh backing facing the beam, a single layer of SRiP with no backing, a single layer of SRiP with the mesh backing facing away from the beam, two layers of SRiP reinforcement with the mesh backing facing away from the beam, two layers of C-Grid carbon

fiber mesh (for comparison with steel and further information on the bounding potential of the inorganic polymer.

4.4 Flexural Testing of Unheated, Control Samples

Before flexural testing was performed, 4"x8" concrete cylinders were crushed to obtain the exact strength of the concrete. Due to the additional water added in initial casting, the day of concrete strength was only 3340psi, compared to the desired 5000psi. Because of this massive difference in strength calculations were redone on flexural and shear strength of the beams to find the expected maximum flexural load of the controls and guarantee failures in shear would not occur. Shear capacity totaled 10,096lbs while the strongest beam was predicted only to hold 9,316lbs. The testing continued as planned once it was determined that the beams would fail in shear as planned. Future beams were designed with an f'c of 3,000psi to better match the weaker concrete of the initial samples.

In order to determine the effectiveness of the proposed SRiP composite post fire exposure, baseline strength must be determined for each SRiP set up created. Samples were placed with a gantry crane into a large flexural press capable of testing beams of upwards of 12 feet in standard third point bending. The press was set up with a series of load cells and linear variable differential transformers (LVDTs) to record both the increase and load and increase in deflection at several locations in the beam in real-time. The instrumentation rig was created using equipment from early deflection testing performed by Matthew J. Klein and P.N. Balaguru of Rutgers University. Details on the instrumentation and modifications made are included in the next section of this research. A total span length of 92 inches was used for each beam, allowing for a 2 inch overhang of each support. Beams were tested in third point bending, with loads applied 30 2/3 inches from each support, until failure of the beam occurred.

4.4.1 Instrumentation

The data collection system utilized a total of 2 load cells, 3 LVDTs, as well as a camera and calibrated scale set up to map further deflections beyond the LVDTs limits. Load cells were placed at the location of each load point at the third spans and LVDTs were placed at each load point as well as at the midpoint of the beam (see Figure 4.6). This allowed for the recording of the loads and deflections at these key regions throughout the testing of the beam and would also verify that loading was performed in as close to even and consistent of a manner as possible.
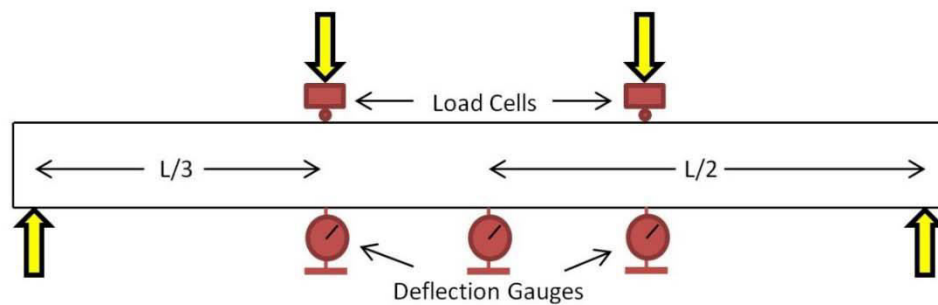
Figure 4.6 Instrumentation Set-Up (Klein 2013)

For this research, two RSB1 resistive load cells calibrated to 10 kip of compression and three DISP displacement sensors with a 1.5 inch range were used. The data from each load cell and LVDT was transferred to a laptop via individual conversion boxes (DI-1000U) and USB 2.0 connections fed into the computer through an externally powered 7 port USB hub (see Figure 4. 7). The data from each was simultaneously collected by a program called SensorVue, a proprietary software package from LoadStar Sensors. The software was modified to the

specifications need for this and previous research. For this series of testing, data was set to be

recorded every 5 seconds and maximum load was monitored by the software incase breaking

fell outside of a 5 second interval. All data saved to a .csv file that could be easily processed in

Microsoft Excel or another similar spreadsheet program.

Figure 4.7 Sensors and Connections
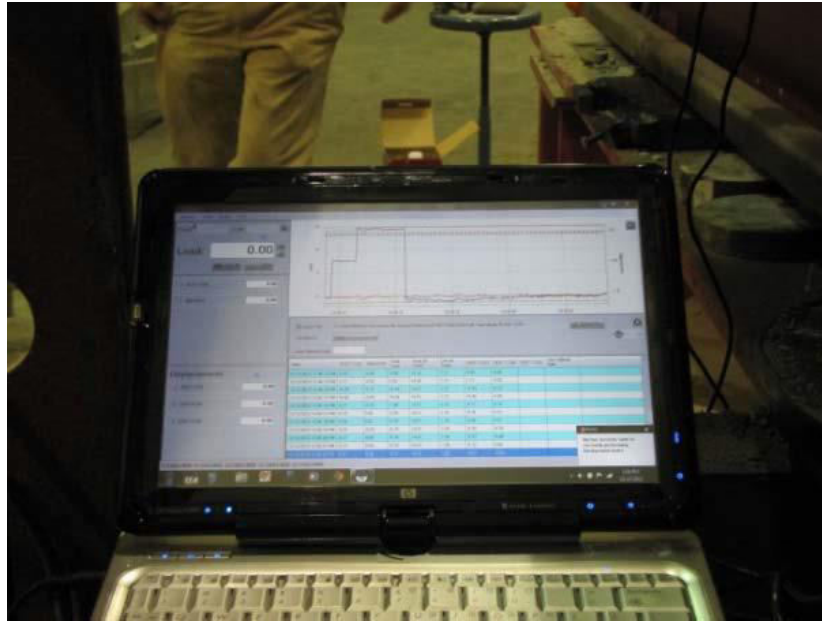
Figure 4.8 SensorVue Interface (Klein 2013)

An initial problem was presented with the LVDTs as the existing units only measured a

deflection to a maximum of 1.5 inches and for these shallow beams the deflection at failure

would be potentially a great deal higher. Higher range LVDTs that worked with the already

existing software proved to be prohibitively expensive and another method had to be

developed. A vertically mounted scale was magnetically affixed to the flexural press and aligned

with markings at the center of a beam. A video recording device was then set up to capture the

movement of these markers along the scale as load was applied to the beam (see Figure 4.8).

After completion of testing the video can be transferred to a computer and used to determine

the deflections after the LVDTs are no longer useable. Before full testing, this procedure was

calibrated using the LVDTs themselves. The angle of the recording was adjusted so that the

deflections viewed matched up with the LVDT readings over one inch of movement. Camera and

tripod positions were then marked off to allow for repeatability. After testing was completed for

a beam, the video could be matched up with the LVDT readings near a deflection of

approximately one inch. Then, as all readings were set to record ever ten seconds, the video could be moved ahead and matched with the remaining load values. While this process proved to be rather intensive, it ensured that accurate readings could be obtained within the budgetary and equipment constraints.

Figure 4.9 Additional Deflection Recording

4.4.2 Results of Non-Heated Controls

In an ideal, tension controlled failure of a composite reinforced RC beam the steel wires attached would all rip apart in tension and there will be evidence of the internal tension steel also rupturing as well. In addition to this rupturing, it is desired that if any area of the composite pulls off from the beam, there should be evidence of concrete pulling off as well. The pulled off concrete shows evidence of a strong bond forming between the matrix used and the concrete itself. In this research, observations about the tests and breaks will be detailed, followed by an

initial presentation of the numerical data obtained from the controls. Greater detail on testing

data will be presented in Chapters 5 and 6 as this will include the heated samples as well.

4.4.2.1 Observations from Flexural Specimens

There were several important observations to come from the testing of the control beams.

Some of these pertained to general failure in FRP reinforced concrete beams. Others were more

specific to the materials used. From this control testing, it was noted that:

- Almost all beams showed a failure in the outermost internal steel reinforcement (Figure

    4.10). This indicates that upon failure of the composite, the loading transferred fully to

    the tension steel and caused it to rupture, as hoped. As the beams were shallow, it was

    easier for the concrete to crush in the middle so not all the tension steel did fail by the

    time the compression zone of the concrete failed. Further testing later in this research

    will verify if a deeper beam will exhibit a complete failure in the tension steel or not.

Figure 4.10 Ruptured Tension Bar in SRiP Control Beam

- The majority of the steel wires in the composites did not break through completely, though some did. Instead most exhibited an area that pulled off from the concrete. These did include a varying amount of concrete pulling off as well (Figure 4.11) and in all cases, save the control with no composite, there was exposed aggregate after failure. This shows that the bond between the geopolymer and cement paste of the concrete was formed. While further grinding and surface preparation can lead to a more effective bond, the validity of the bond that did form with little grinding will show if the composite was still close to calculations.

Figure 4.11 Levels of Concrete Pull Off in Beams

- The orientation or presence of the backing material on the Hardwire did not have a major impact on the bonding strength of the composite. These results back up claims by the manufacturer that orientation of the Hardwire tape's backing will not affect the standard flexural strength of the reinforced member.

- Due to the nature of the original beam casting, there was a slight bit of uplift in some of reinforcement for a few of the beams. Given the shallow beam geometry this had an impact on the depth of the steel and an impact on the predicted load calculations. While most of these samples were used to perform extra testing with standard wire meshes or carbon fiber, a couple were needed for the SRiP testing. As such, additional calculations

and controls were needed to correct for the change in maximum load those beams could theoretically hold. Again, more detailed numbers and analysis will be discussed in subsequent chapters.

- When the beams were broken and the Hardwire was again exposed, it was noted that the brass coating that originally gave the Hardwire a golden color appeared to have come off the wires. It is believed this is due to some reaction with the geopolymer or the presence of an incredibly strong bond between the brass and geopolymer. The bonding capabilities of aluminosilicate to brass has not been tested so additional investigation would be needed to fully explore this relationship. No noticeable issues arose in the samples due to this phenomenon but further studying could aid in the refinement of the materials.

Figure 4.12 Brass Coating No Longer on Steel Strands

4.4.2.2 Results of Flexural Testing

Initial results for the control beams showed that most beams performed slightly better than

calculations anticipated. Table 4.1 Shows that all but the beam with two layers of hardwire

outperformed the predicted loads. Most of these differences could be explained by slight

variations in the steel positioning or that many values given about material strength tend to fall

on the lower side for safety. For the two layers of Hardwire, however, the experimental load

was 10.8% lower than expected. The simple explanation for the lower maximum load relates to

the diminished returns in adding more layers of composite. Each additional layer should

theoretically add the same amount of moment but adding more layers can also impact bonding

and other properties of the composites that limit the strength gain in each subsequent layer.

Flexural Load Capacity, Control Beams			
Steel Used	Designation	Predicted Load (lbs)	Experimental Load (lbs)
No Hardwire	No HW	4776.16	5250
1 Layer Backing on Concrete	HWI-1	7198.58	7655.76
1 Layer Backing Away	HWO-1	7198.58	7267.84
1 Layer No Backing	HWN-1	7198.58	7580.64
2 Layers Backing on Concrete	HWT-1	9316.03	8305.8

Table 4.1: Maximum Flexural Load Held by 'Control' Beams

A load versus deflection graph for a reinforced concrete beam with external composite should present several identifiable characteristics. As load increases two major changes in the slope of the curve should been seen: the first when early in loading when the concrete reaches its cracking moment and the second later on when the steel starts yielding in the concrete. There also should be a steep drop off upon ultimate failure of the composite that then plateaus out as the tension steel tries its best to maintain load on the beam. Figure 4.13 shows a typical load/deflection response for an SRiP reinforced beam as seen in one of the samples of this research.
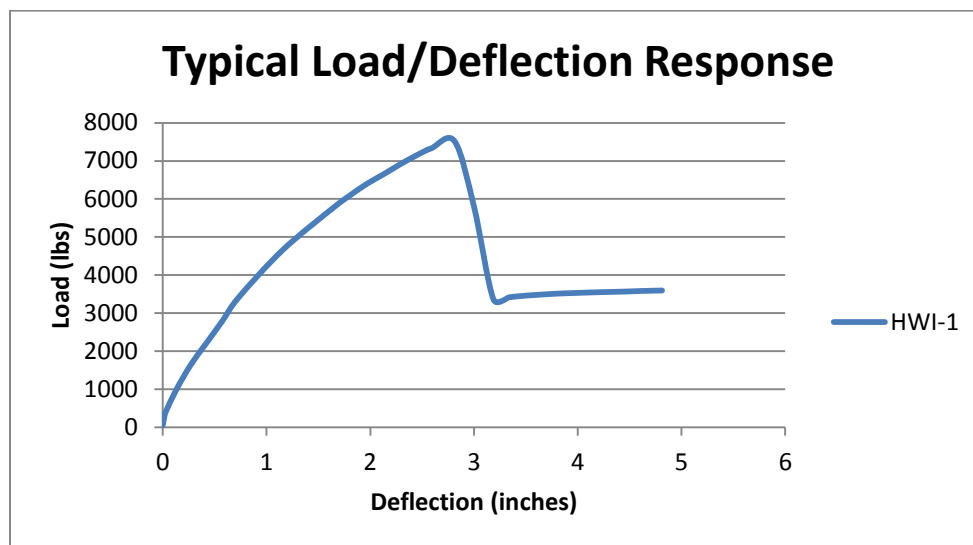
Figure 4.13 Typical Load/Deflection Response of an SRiP Reinforced Beam

Figure 4.14 below shows the load versus deflection graphs for the main control SRiP beams. Several details about these beams are apparent from the comparative graph:

- The slopes of the control beam and beams with only one layer of SRiP reinforcement showed followed similar patterns. This means the stiffness of the beams with one layer were not greatly affected by the presence of the composite. This differs from composites that use glass or carbon fiber as they will stiffen up drastically. The more

ability a beam has to bend, the easier it is to identify a potential failure, which is a
downside of glass and carbon fiber that appears less prominently in SRiP composites.

- Adding a second layer of composite does cause a significant increase in stiffness for the
beam, as evidenced by the steeper slopes of the load deflection curve of HWT-1. It
should also be noted that while the double layer composite failed at approximately half
of the deflection of the single layers of SRiP (1.5 inches compared to 3 inches) the
ultimate load the two layer beam took still deflected a slightly greater distance than the
control specimen and would provide a similar warning of failure as regular reinforced
concrete.

- The sample that differed the greatest from the typical load/deflection curve the greatest
was the sample without the backing. This could be due in part to the hand laying of
individual lengths of wire or from the lack of the grid shaped backing that would have an
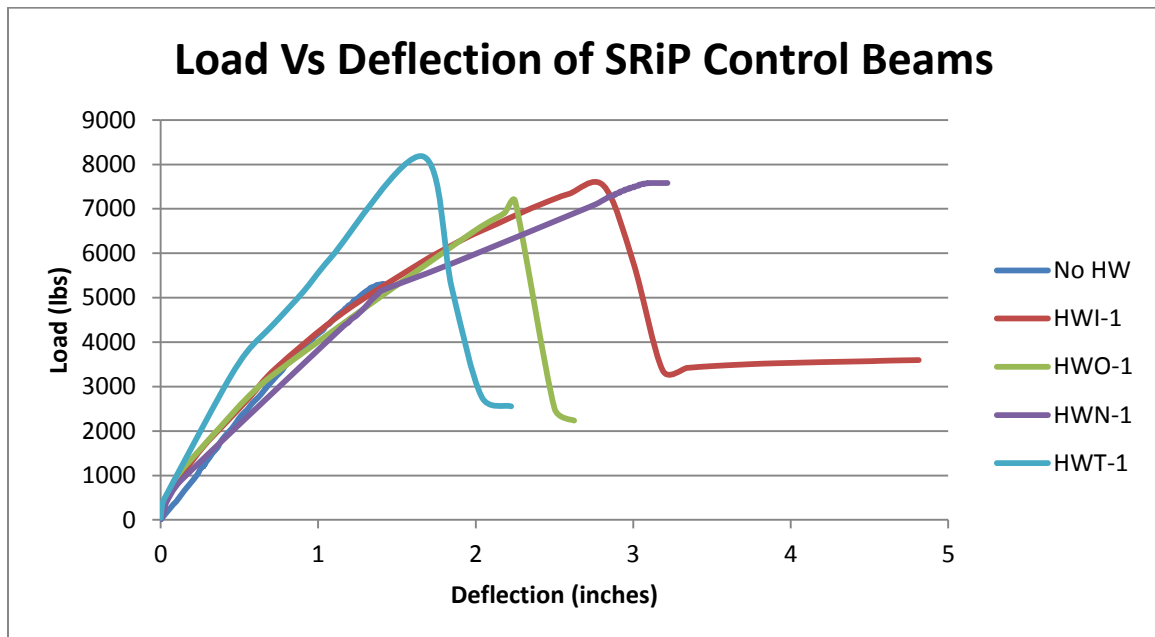impact on wire spacing and possibly on the stiffness.

Figure 4.14: Load/Deflection curves of the SRiP control samples

4.5 Summary

SRiP Load Deflection Response

- To maximize area on beams for SRiP composite a scaled down version of shallow beam by Prota, et al. were designed. These beams would be 8 inches wide and 4 inches deep.

- Beams were cast in wooden molds in two main sets. The first set was poured with concrete ordered on a mixing truck. The quality of this concrete was poor, and the scale of the casting was too large for the amount of researchers so the second set of beams was cast a few at a time and concrete was mixed in house.

- Beams were cast along with 4 inch by 8 inch cylinders to spot check the strength of the concrete. All concrete items were demolded after 24 hours and kept in similar curing conditions.

- Hardwire strands were cut and sized well in advance of any application of composite. Geopolymer ingredients were all prebatched ahead of time to maximize the amount of focus that could go into application.

- Minimal surface preparation was done compared to traditional FRP composites. One major benefi to aluminosilicate is a reduced amount of labor for surface cleaning.

- Thicker "fiber" such as with this steel require care to make sure the matrix penetrates through/around them. Steel has larger gaps so it is good to work the matrix through with a firm edged laboratory spatula.

- Beams were tested in third point bending with load data taken at the loading points and deflection data taken simultaneously near the center. Additional deflection data was recorded with a grid system and scale that was filmed during testing.

- Most samples had breaks through tension steel showing load transferred properly after the SRiP failed.

- Presence of some concrete pull off when the composite failed shows bonding occurred between the geopolymer and concrete without elaborate surface preparation.

- Different orientations of the steel wire backing material were used. The "tapes" of Hardwire are designed to function with the backing side up or down but this does not account for fires, which is what this research sought to simulate.

- All samples showed significant flexural improvement in both strength and ductility over the plain RC beam at this stage.

CHAPTER 5 – EXPERIMENTAL INVESTIGATION: EFFECT OF HEATING

5.1 Introduction

As addressed earlier in this dissertation, several research programs have been created

worldwide to investigate different combinations of steel and inorganic matrix to form

composites. While these show the effectiveness of SRiP for enhancing the flexural, shear, and

torsional strength of reinforced concrete members, none of these programs focus on the

performance of SRiP composites in the presence of high heat events, such as fires. Neglecting

this line of testing ignores possibly one of the strongest benefits of inorganic matrices versus the

more traditional composite epoxies, the ability to withstand high temperatures.

Figure 5.1: Wood Avenue Overpass Fire (nj.com)

One recent example of the dangers of fire for beams occurred on August 4th of 2015 near exit 13

of the New Jersey Turnpike near Linden, New Jersey. A dump truck rear ended a towed vehicle

before crashing into the Wood Avenue overpass abutment, overturning, and catching fire. The

fire quickly spread to the overpass structure, exposing the steel beams to the flames for an

extended period of time. A more dangerous situation arose on July 28 of 2008 on the Bill

Williams River Bridge connecting Lake Havasu City and Parker, Arizona. In this incident, a tanker truck transporting approximately 7,600 gallons of diesel fuel overturned on the bridge and in the process burst into flames. A study of the prestressed girders of the Bill Williams River Bridge showed that the operating ratings of the girders were reduced by over 20% of the initial design (Davis, Tremel, and Pedrego, 2008). Had these structures been dependent upon a traditional external composite for additional strength, the composites could have delaminated and additional repairs would be required to return the structures to a functional level. Concern over the ability of FRP with epoxy based resins has also been expressed by the ACI. The ACI Guide for the Design and Construction of Externally Bonded FRP Systems for Concrete Structures even recommends in fire conditions to use unrepaired load capacity for service loads of FRP treated beams (ACI Committee 440, 2002). This accounts for the epoxies tendency to fail and debond in temperatures in excess of 200°F.

The majority of testing for FRP strength in fire either ignore inorganic systems or use an extra inorganic coating on top of the selected matrix to attempt to protect the FRP. Kodur and Ahmed tested a total of four rectangular RC beams strengthened with an organic epoxy FRP and a vermiculite-based Insulation layer. The beams were tested with both a design fire and ASTM E119 standard fire using two point loading to about 50% of normal beam capacity. Figure 5.2 shows the results of their testing, including a debonding of the FRP layer of Beam 3 after approximately 30 minutes of fire exposure. Kodur and Ahmed concluded that an insulation layer was essential to maintain the FRP bond during a fire (Kodur and Ahmed, 2011). Williams et al. performed similar ASTM E119 testing using T-Beams with FRP and a vermiculite-based insulation layer. From their testing they also determined that an inorganic insulation layer is key to securing proper fire rating for FRP (Williams, et al., 2005).
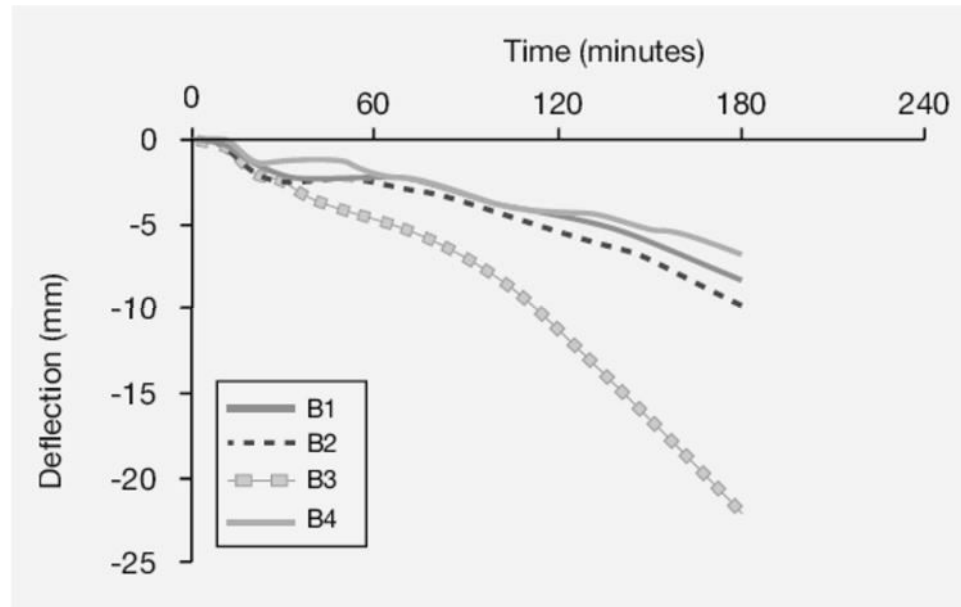
Figure 5.2: Mid-Span Deflecitons (Kodur and Ahmed, 2011)

Hashemi and Al-Mahaidi developed research in Australia that showed the use of an inorganic

matrix with carbon fiber, instead of a standard epoxy, could plausibly maintain bond strength

throughout an event. Matthew Klein of Rutgers University took this concept further and showed

that standard, rectangular, RC beams externally reinforced with an inorganic matrix FRP when

exposed to near 1000°F maintained bond strength and additionally exhibit predictable losses

(Klein, 2013). This research utilizes this existing testing set up while making modifications to

account for the shallow nature of the main beams being tested. In addition, samples from these

2013 tests have been maintained and will be cleaned and repaired to create a direct comparison

with the behavior of a geopolymer/carbon composite and a geopolymer/steel composite.

With the increased use of commercial trucks to ship highly flammable chemicals has come an

increased risk of high temperature and longer burning vehicle fires. In instances where accidents

with these vehicles occur under bridges or overpasses, the support beams are exposed to a

great deal of fire. Any traditional composites cannot last much longer than a half an hour in

temperatures exceeding a few hundred degrees Celsius and can be drastically damaged even if the fire is contained within 15 to 30 minutes. Because inorganic polymers behave similarly to concrete, they can provide insulation to the fibers they are combined with. While steel too reacts negatively to high temperatures, geopolymer material can provide it some protection and still allow for the more observable and safer ductile failures. The composite itself withstands the fire for longer and should failure occur, it will have an increased chance of warning engineers.

By modifying an existing rig, this research was able to test samples of SRiP reinforced beams, constructed similarly to those controls in the previous chapter, and expose them to a high temperature scenario. The effectiveness of the composite set up in fire events can be determined by studying each beams response to heat while in a loaded condition and maximum flexural capacity after heating. In addition, secondary beams from a previous research regime were cleaned, treated with the new SRiP, and tested to provide additional data that can be directly compared with existing results. This chapter will detail the methods, apparatus, and results involved in the heat and flexural testing of the shallow beams as well as the preparation, repair, and testing of the set of existing reinforced concrete beams. These tests will be compared with previous data to demonstrate the effectiveness of the proposed SRiP in the described fire events.

5.2 Initial Rutgers Testing

The testing jig utilized for this testing regime was first developed by Matthew Klein as part of a doctoral study in geopolymer composite and its repair capabilities. A series of externally reinforced concrete beams were used to verify a secondary hypothesis that aluminosilicate geopolymer would provide a continuous bond through a high temperature event such as fire. The research, however, used carbon fibers with the geopolymer matrix and for some samples,

utilized a cementitious coating mixed with structural glass beads (Klein, 2013). A series of tests were developed by Klein in order to validate the selected equipment and prove the effectiveness of the geopolymer in the proposed application. Initial tests and results verifying the experimental method will be discussed in this section while the rig itself will be discussed in greater detail later in the chapter.

For the testing program, an initial total of six rectangular, reinforced concrete beams were cast. These beams were strengthened with an inorganic epoxy and carbon fibers

5.3 Initial Verification Testing of Heat Rig

Due to the rig already being set up testing was done to verify the effectiveness of the rig for the shallow beams, make any necessary changes, and see how long testing cycles would need to be to see proper results during heating and cooling. For an initial sample test a control beam with no reinforcement was used to identify a baseline performance of the reinforced concrete. At the recommendation of the earlier Rutgers testing, the initial testing window of twelve hours was selected. Over those twelve hours, the sample would be inverted and placed in a testing jig and subjected to a load resulting in approximately 40% of the cracking moment of the beam. The deflection of this load was noted to be approximately one third of an inch. The loading jig, depicted below in Figure 5.3, placed supports on the middle thirds of the compression side of beam, the underside now that the beams were upside down, and the loading points at the beam ends. Load cells at these ends would monitor the loading and could be adjusted with a wrench to deflect the beam further. Deflection gauges placed on the underside of the beam ends and one near the center of the beam would help record the total deflection achieved. Before testing officially began, the loaded beam was left in situ so that any immediate lose in load due to relaxation would not be factored into the load lost due to the repeated heating cycles.

Figure 5.3: Loading apparatus for heat testing rig

Two electric heating elements where clamped down to the middle of the beam on the tension side. The elements reached a heat of over 1000°F when allowed to heat up fully, a heat that would replicate those capable of damaging a beam in the case of a fire. These elements attached to electrical timers capable of cutting their power at the desired intervals. In the initial testing cycles, the beams would be heated for a period of 2 hours and then cooled for a period of 2 hours all while the loading on the beams are monitored via the load cells. As the tension side of the beam heats up a temperature gradient forms in the center of the beam and the outer face of the beam expands. This expansion results in an additional deflection in the beam and a subsequent relaxation in the loading applied at the ends. This relaxation and the accompanying drop in load will level out when the temperature in the beam has reached its peak. While allowing the beams to sit at this position for some time will not have any negative impact on the testing in results, identifying the time it takes to reach this maximum point will allow for the samples to be tested more quickly and within a more reasonable time frame. The initial testing showed that the drop in loading leveled off at about 1 hour of heating and

returned to a stable value after about one hour of cooling (Figure 5.4 below). As such, future

tests of the samples would be tested over a total of 6 hours each with 3 cycles consisting of 1

hour of heating and 1 hour of cooling. More details on this testing will be provided in section 6
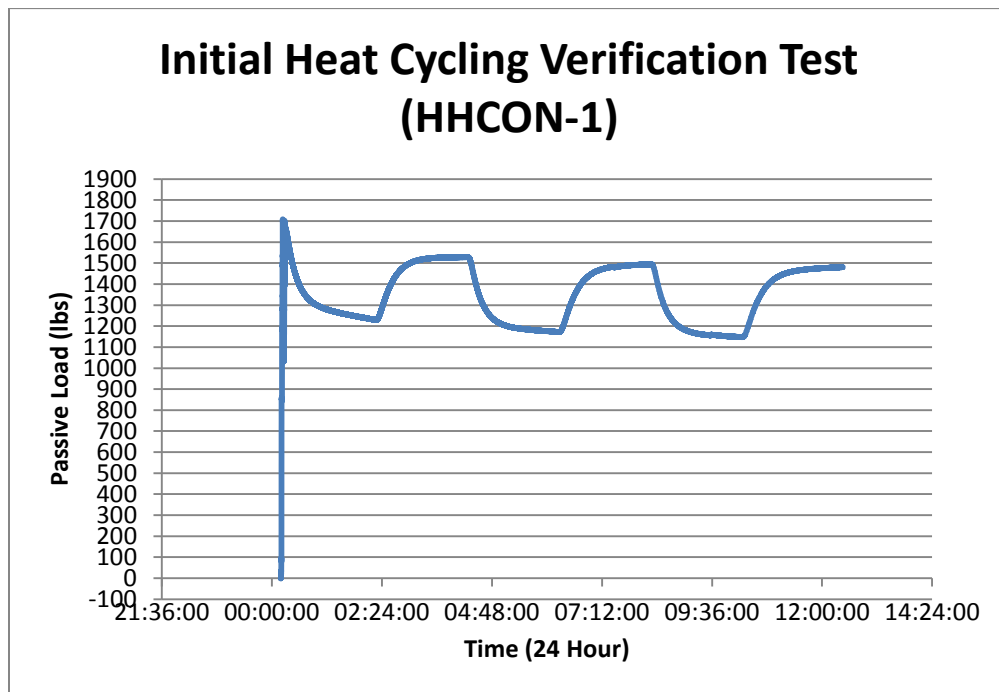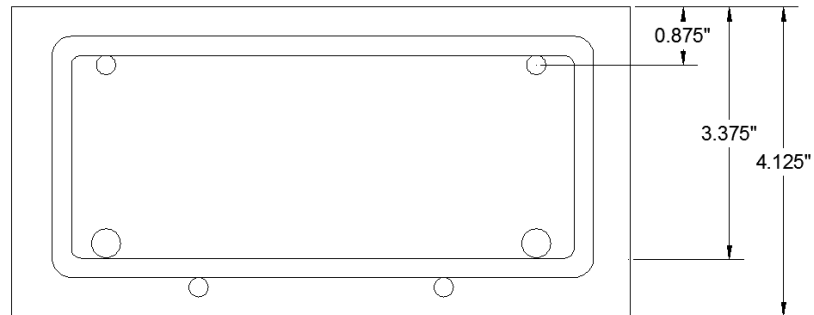
of this chapter.

Figure 5.4: Extended Cycling period for Initial heating test.

5.4 - Test specimens

Specimens for this testing followed the earlier specifications used in the flexural strength testing

of the non-heated samples. Beams were 4 inches deep, 8 inches wide and 8 feet long with

reinforcement matching their non-heated counterparts (Figure 5.5).

Compression: 2 #2
Tension: 2 #2, 2 #3

Figure 5.5: Cross section of heated RC beam samples

In addition to continuing the testing of the shallow beams, an additional testing opportunity

presented itself in the form of the FRP beams originally tested by Matthew Klein in his research

(Klein 2013). The beams had not been tested to failure as part of the original regime and

remained in the lab facilities intact. Two additional questions could be tested with the presence

of these beams. The first question: How well can the inorganic polymer bond to a surface that

once had a similar geopolymer present? Bond is a crucial part of external fiber reinforcement

working and concrete and similar materials often have trouble adhering and bonding to already

set concrete. In the situations proposed at the beginning of this work, the SRiP would allow for

the beams to stay intact or provide at least a safer and more predictable failure. In the latter

case, replacement of the SRiP system could still be necessary and the concrete must still be able

to bond with the SRiP after the old external reinforcement system is removed.

The second question, one posed after all the original samples and geopolymer were established:

What other ways can the chemical bond between the geopolymer and concrete be improved?

The proposed solution in this later stage of the testing revolved around the intentional rusting of

rebar. In some instances where epoxy is not required, rebar can be intentionally rusted on the

outside to provide a better bond with the concrete. As such, this stage of the research also tested the ability of iron oxide to improve the geopolymer's bond with the prepared concrete surface. The iron oxide would be added into the matrix of some of the "repaired" beams to see if there is any impact on the maximum load attainable by the beam or way in which the SRiP ultimately failed.

Additionally, more carbon fiber was added to the matrix of each of these beams to enhance the bond as well. 3 cases of additional chopped carbon fiber in the matrix were considered: 12 grams of fiber added to the dry ingredients and blended before a liquid component was added in, 12 grams of chopped carbon fiber added with the wet components of the matrix, and 18 grams added to the wet components.

To prepare these samples for testing, they first needed to be cleaned of the existing FRP attached to them. This FRP was composed of a similar aluminosilicate to that used for the in this study and Carbon Fiber strands. An angle grinder with a disc made for steel was able to completely remove the FRP and matrix as well as grind down some of the concrete and expose some fresh aggregate. While it was earlier noted for the inorganic matrix used in this testing regime that such thorough grinding was not completely necessary, when reapplying a geopolymer to an area that once had geopolymer it can be beneficial to grind more and remove more area that the original coating could have penetrated into.

Once the surfaces were prepared SRiP was applied to each in a manner dictated previously in this research. In this instance, the orientation/presence of the fiber backing was kept constant based on the results of the initial testing. Some samples maintained the exact matrix used in the SRiP composite for the shallow beams with the additional chopped carbon fiber as noted above while some contained that same matrix infused with powdered iron oxide. The iron oxide

powder was batched along with the other solid components of the geopolymer and mixed in prior to the liquid Part A component being added.

5.5 Testing Equipment/Rig

The testing rig consisted of three main assemblies that worked together to collect all necessary data during each six-hour testing session: a loading jack/support structure, a heating element system, a data collection system.

The loading jack contained two central supports and two adjustable, threaded end points. Beams would be placed tension face up onto the central supports and under the adjustable end points. The end points tightened to apply load on the beam, deflecting each end downward. Beams in this rig mimicked a traditional third point bending test but allowed for the heating element to sit on the tension face.

Two electric strip heaters were clamped to the center of the beam to simulate fire damage on the beam surface. The strip heaters connected into two electric timers that could cycle the power to the heaters at the required intervals.

The data collection system utilized the same deflection gages and load cells from the flexural testing. The load cells were affixed to the structures at each end of the beam so as they were tightened and the beam ends forced downward, the load on each side was recorded. The deflection gages were placed under each end and in the center of the beam to show the full deflection at the center compared to the ends. With the unique positioning of the beam, the setup of deflection gages allowed for a better understanding of changes in position and curvature of the beam. All gages connected into a USB hub device that in turn fed to a laptop computer. The same Loadstar program recorded all values simultaneously. The laptop itself was also positioned in such a manner that the built-in camera faced the testing set up. This allowed

for remote monitoring of the testing after the initial test determined both the optimal testing time frame and safety of the test method.

5.6 Heat Testing Procedure

For both the shallow beams and repaired beams the samples were placed into the testing rig using an overhead gantry crane. The deflection gages were positioned as discussed in the previous section and the heating elements were attached to the center of the tension face of the beam. For the shallow beams, their width was too large to use the previous method of securing. In this case, a series of c-clamps were used to hold the heating elements in place on the beams.

Once the beam and all required components where in place and the data collection devices were connected to the recording software the rig could be loaded. Both sides of the beam would be deflected evenly deflected to three tenths of an inch, as determined from the initial test. Using a pipe wrench, the loading bars on each side of the beam were adjusted alternately 0.05 inches at a time until they reached the required deflection. Once deflected, the beams sat under loading for approximately 30 minutes to allow for some loss of load due to relaxation, minimizing the impact of relaxation during the actual cycling of heat.

After the relaxation period, the electrical timers were set to the exact times they needed to be cycled on and off to match the heating and cooling periods. These types of electrical timers operate off of the hour of the day and not a desired time period so a strict schedule needed to be created for the testing.

Beams were photographed and stored on their sides after testing to note any damage and protect the heated area. Within a few days of heat testing, generally after a few beams have

been gathered up, samples were placed into the flexural testing rig described in Chapter 4 and loaded until failure. More details of this stage of the testing is presented later in this Chapter.

Details on the shallow test samples and repaired test samples will come in the following sections. Results for those tests will also be presented in alternating sections.

5.6.1 Shallow beam tests

Two beams were manufactured of each variety of SRiP beam tested in the initial flexural stage: plain reinforced concrete, SRIP with backing facing out, SRiP with backing facing in, SRiP with no backing, and two layers of SRiP. One of the plain reinforced concrete beams was used for the initial verification of method test so as not to compromise any SRiP samples.

The goal of this stage of testing was to determine the SRiP's resistance to prolonged heating and its ability to maintain load after the intense heating event has subsided. In a practical sense, for this type of geopolymer and steel wire to survive a high temperature fire, the visible physical damage needed to be minimal and the beam had to hold enough load to continue use as normal or prevent a catastrophic failure before repair can occur.

Successful beams showed as little damage as possible and could maintain a significant portion of the applied load. Any decrease in applied load after heating can reveal permanent deflection within the beam, specifically the beam expanding on the tension side due to the heat and the ends deflecting away from the loading bars.

5.6.2 Shallow Beam Heating Test Results

The results of this testing consist of a series of load and deflection graphs as well as observations of the beams after heating. Again, the purpose of this testing was to see the effects of high temperature events on the curvature and in situ load of SRiP reinforced RC beams as well as the

effects on the ultimate strength and deflection of the same beams. The latter will be discussed

in the next section of this Chapter. The table below contains calculated and experimental data

compiled from each beam sample (Table 5.1). This data includes the load, and deflection for the

beam when loaded into the rig as well as the change in load during the increases in

temperature. Experimentally determined values are denoted with a subscript "exp." The in-

depth calculations for the values in this table are shown in Chapter 6. The loads shown are for 1

of the actual point loads (Pn) and the theoretical singular point load representing the loss due to

the temperature increase.

Beam	Pn (lb)	δ (in)	δexp (in)	ΔP (lb)	ΔPexp (lb)
HHWO-1	754.975	0.41	0.31	350	381.4
HHWO-2	845.435	0.41	0.33	350	305.1
HHWI-2	660.29	0.41	0.325	250	324.2
HHWN-1	846.305	0.41	0.31	400	381.4
HHWN-2	925.57	0.41	0.3	250	419.5
HHWT-1	987.545	0.41	0.355	350	258.2
HHWT-2	853.385	0.41	0.33	350	375.6

Table 5.1: Nonlinear Analysis of heated beams, predicted versus actual heat lost for each beam

From the predicted and actual values of load lost due to the development of the temperature

gradient it is apparent that the moment area method proposed by M. Klein does predict the

losses in SRiP reinforced beams as with FRP with inorganic matrix. Similarities between the

external reinforcement designs used in this research resulted in a single prediction for the

deflection from the temperature gradient. Details on these calculations will be listed in Chapter

6.

A set of load and deflection graphs for each beam are also presented. These show the recorded values of load and deflection as the temperature in the beam cycled. The load graphs show a distinct shark tooth pattern. This ties to the loss in load due to curvature as the temperature gradient propagates in the center of the beam and then the increase in temperature as the beam recovers. At the start of the graph is the subtle drop off as the beam was allowed to relax before heating. This removed some of the error for the loss in load due to the increase in beam curvature. Toward the end of the testing we can see the load level off and give an idea of the actual sustained loss for each test.
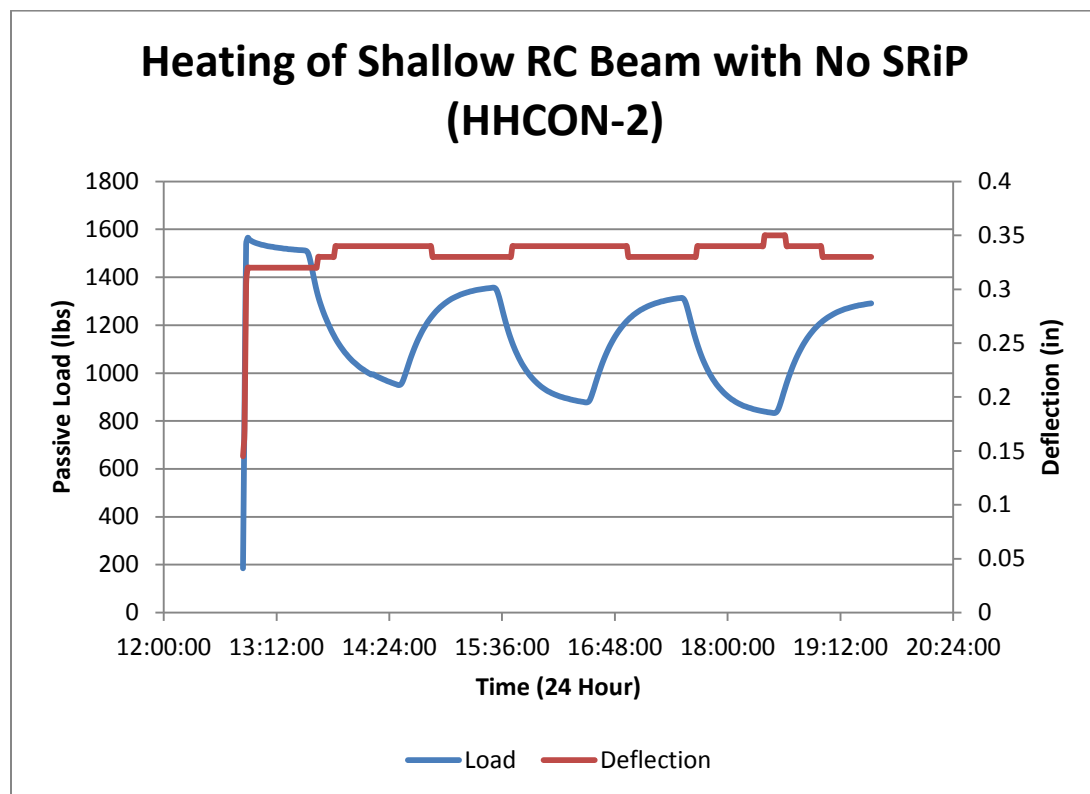

Figure 5.6: Load and deflection of HHCON-2 while undergoing high temperature cycling

The Initial control sample was not depicted as this test was run to confirm the optimal testing period. The control RC beam above demonstrated a decrease in load due to relaxation that

leveled off after approximately 30 minutes in the loaded state. The controls exhibited a steady

decline in load loss and appeared to level out after a third cycle. While load decreased from

1506lbs to 1354lbs over the course of cycle 1 (-10.1%), by the third cycle the load only

decreased by 17lbs (1.1% of the original load). The overall drop in load experienced by the basic

RC beam was 212 lbs or 14.1% of the original load. Minor fluctuations of less than 0.04 inches

were also observed after the start of heating. On these bases, successful SRiP reinforced beams
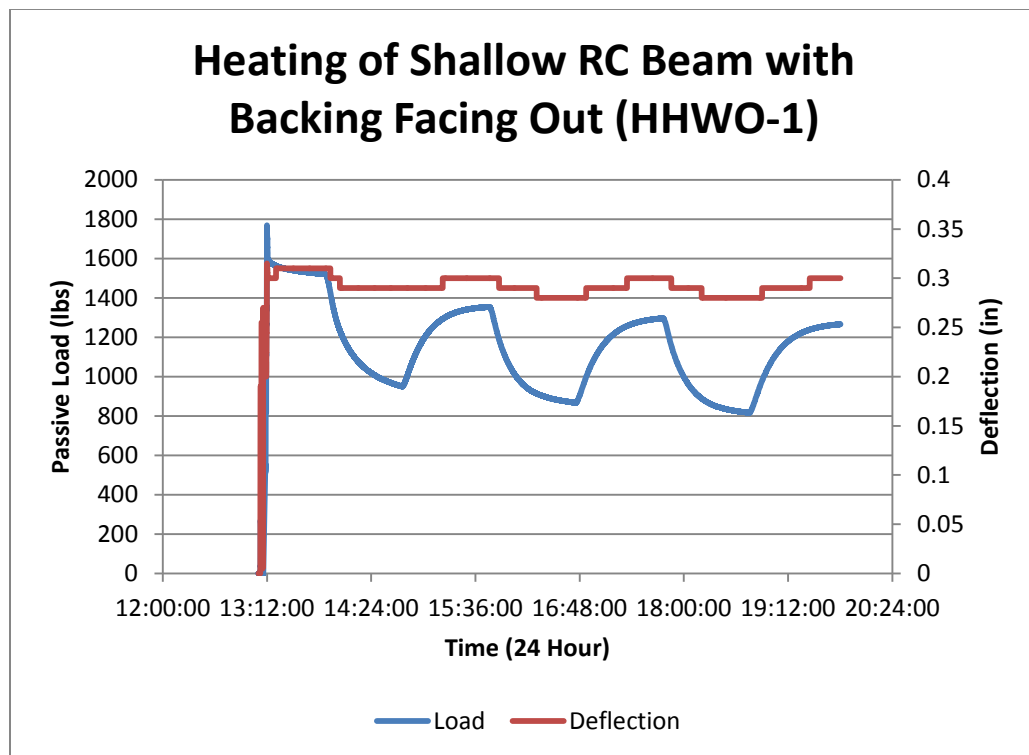
would share similar changes.

Figure 5.7: Load and deflection of HHWO-1 while undergoing high temperature cycling
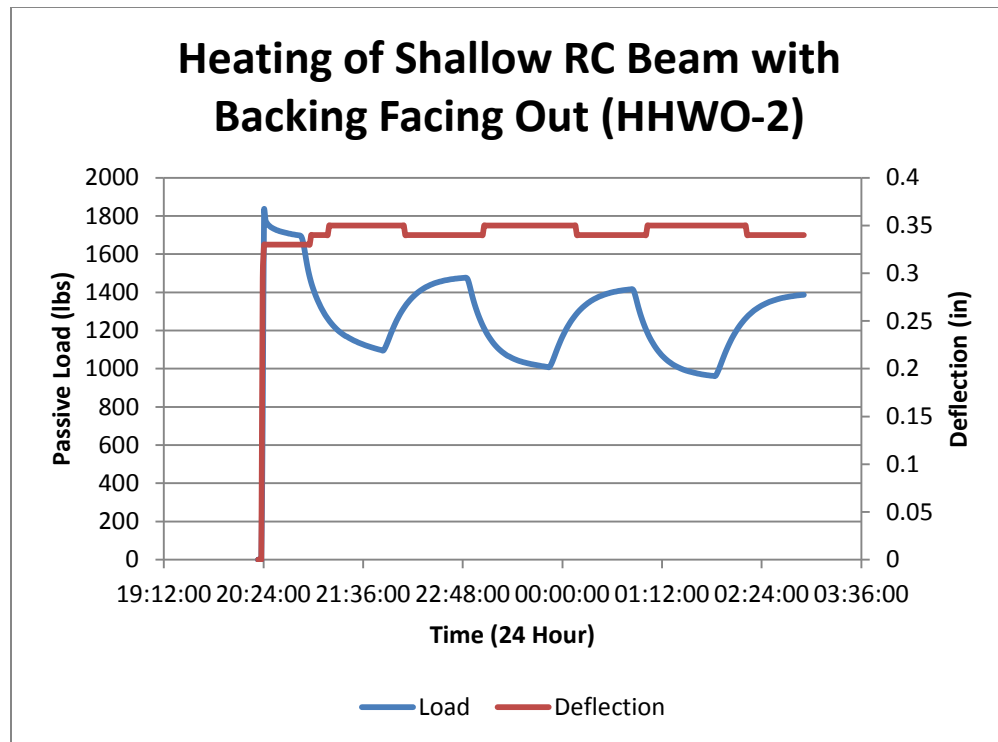
Figure 5.8: Load and deflection of HHWO-2 while undergoing high temperature cycling

As mentioned previously, SRiP reinforced beams with a backing present exhibited at least some black discoloration from the backing burning. HHWO-1 and HHWO-2 were most prominent in terms of burns as the backing was closest to the surface. While HHWO-1 presented a more staggered change in the deflection in the beam, both samples exhibited an overall similar pattern of deflection change to that of the control. The load in HHWO-1 and HHWO-2 decreased by a total of 16.2% and 18.9%, respectively, greater than the 14.1% of the control. It was reasoned that these greater decreases stemmed from the proximity of the steel to the surface contacting the heating strips but also partially because of the compromised outer layer of geopolymer generated from the burning wire backing.
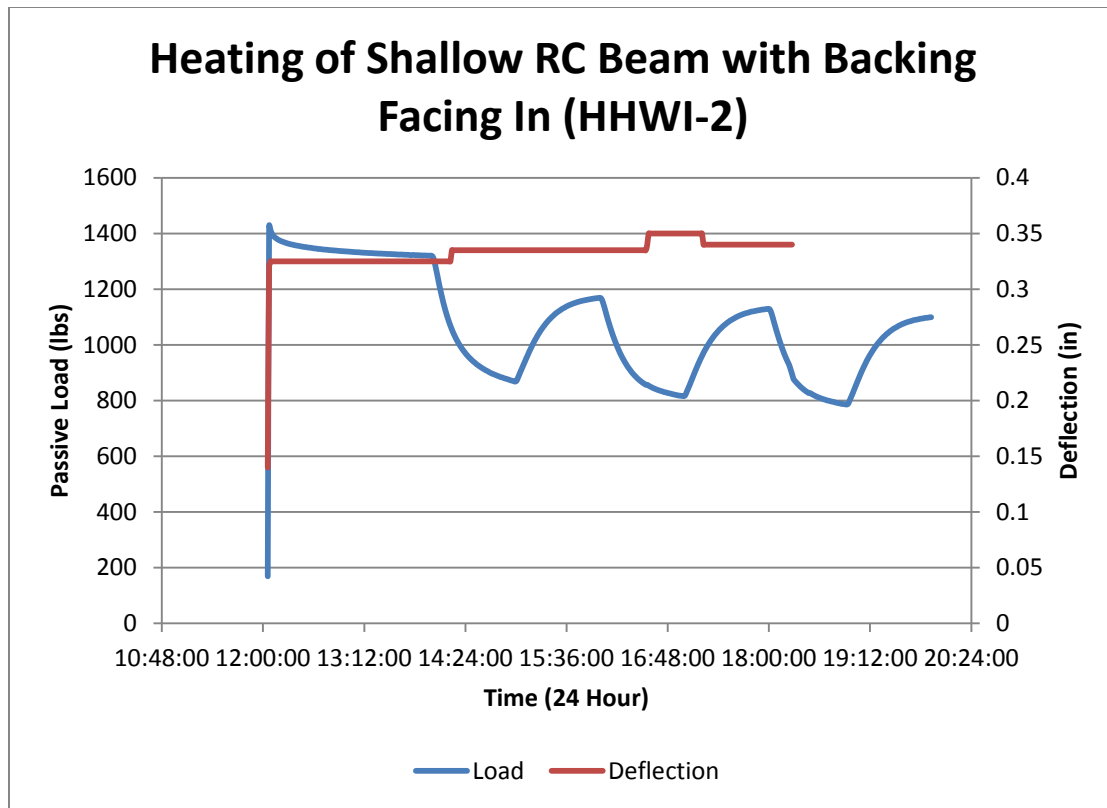
Figure 5.9: Load and deflection of HHWI-2 while undergoing high temperature cycling

An interruption of the deflection gage connection lead to errors in the collection of the data for HHWI-2. This sample showed some stepping in the change in deflection but not spread across the heating cycles as all other samples. The beam itself also reported an unexpectedly lower load than the other beams, even the control. This led researchers to believe that the data collection system had some sort of connection issue. The sample demonstrated a 17.4% reduction in its load, and though the data may be off due to a temporary equipment issue, we can still see an increase in load loss, most likely do to the proximity of steel to the edge of the composite and compromised geopolymer/burnt wire backing.
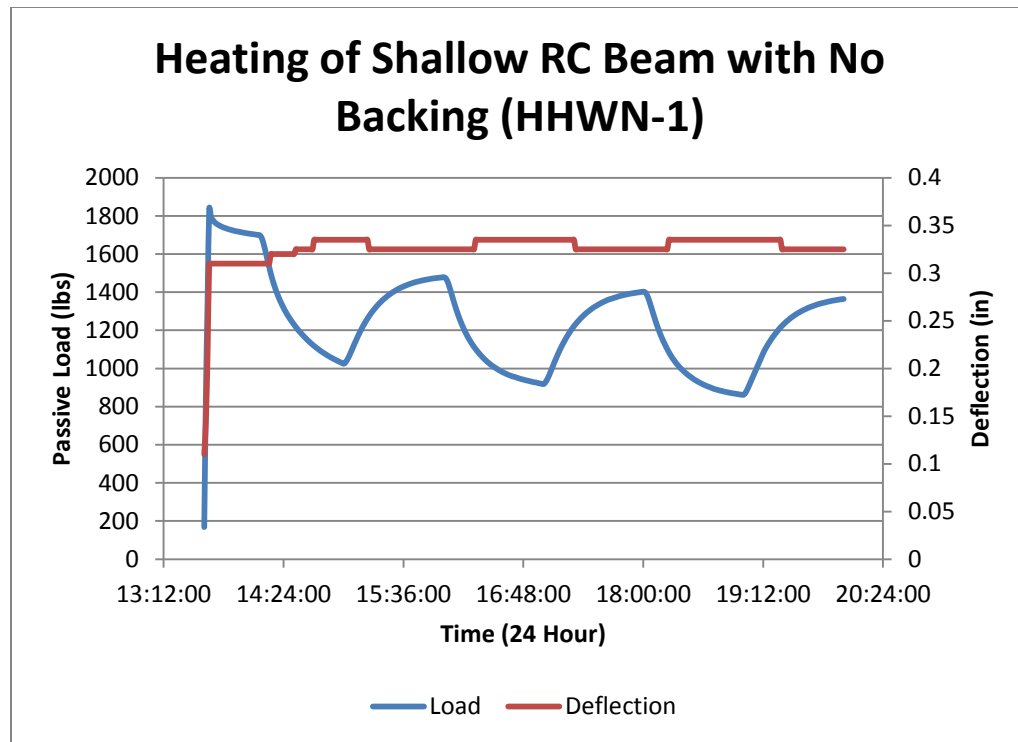
Figure 5.10: Load and deflection of HHWN-1 while undergoing high temperature cycling
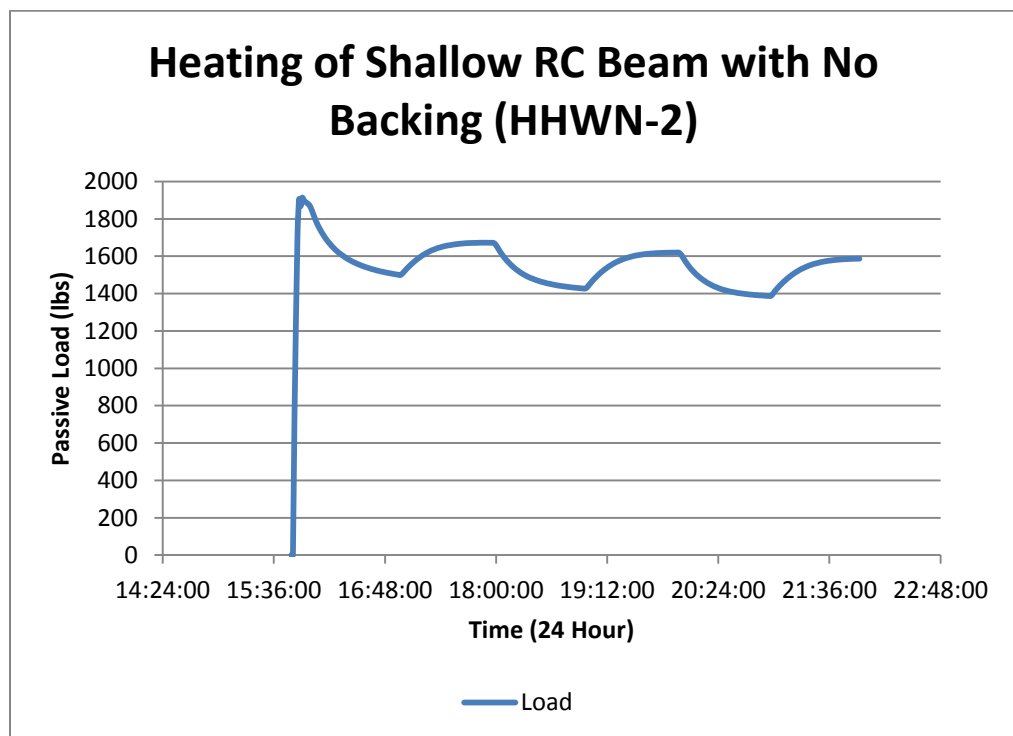
Figure 5.11: Load and deflection of HHWN-2 while undergoing high temperature cycling

The exclusion of the Hardwire backing produced some higher overall loads but still about the same average decrease in load as other SRiP samples. Reductions of 20.6% and 15.2% showed a much greater fluctuation in the possible losses when heating. Deflection data for HHWN-2 was compromised as a gage was stuck in a deflected position and failed to move with the center of the beam. This was corrected for other samples but made these deflection values unusable. The steel wires of these beams were laid individually and not on a backed sheet and some slight shift in directionality of wires could account for differences between the two beams.
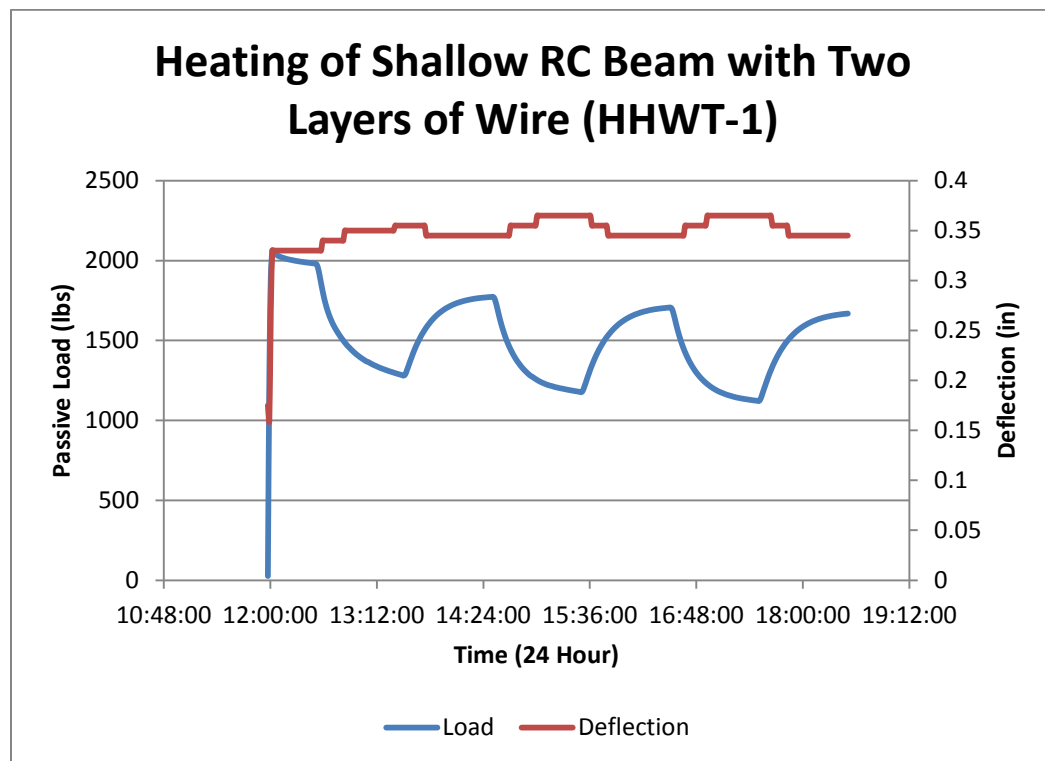
Figure 5.12: Load and deflection of HHWT-1 while undergoing high temperature cycling
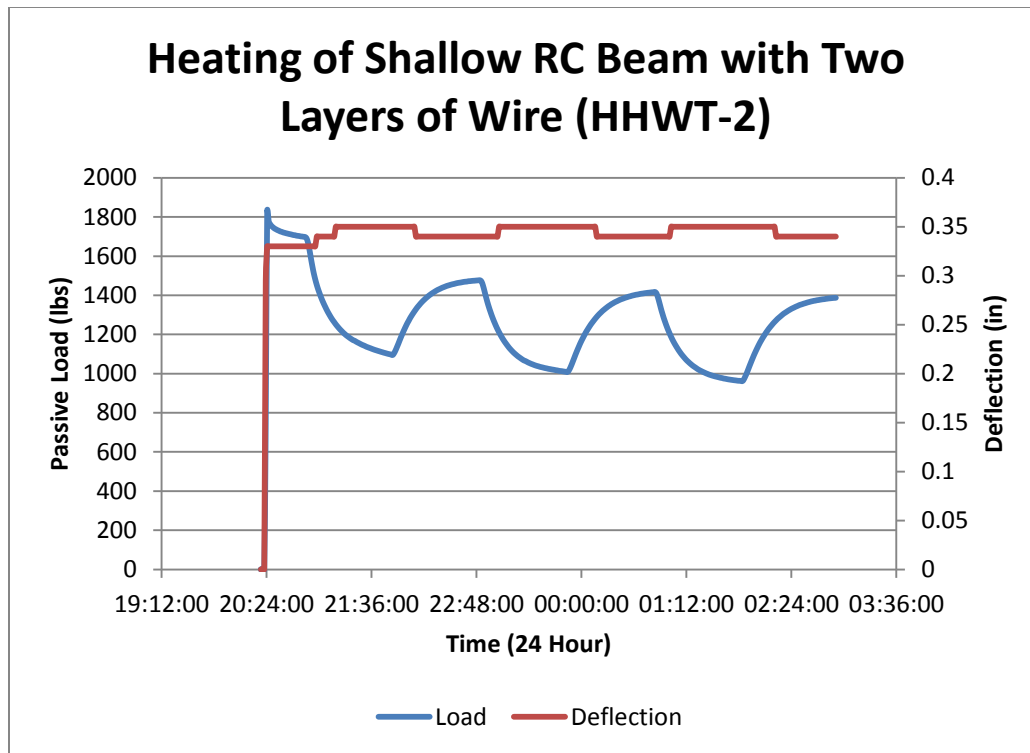
Figure 5.13: Load and deflection of HHWT-2 while undergoing high temperature cycling

Beams with two layers of Hardwire performed very similarly across the board to those with 1 layer of Hardwire but no backing. Load reductions of 19.3% and 16.8% could be due to the presence of more backing material, even though there were more wires and one set was further from the surface.

The losses were slightly larger than the carbon fiber and geopolymer counterparts of earlier Rutgers testing but in the flexural testing presented later in this chapter, an increased ductility can provide for a safer failure scenario and show the true benefit of steel. A more thorough explanation of the mathematics behind these results will be presented in Chapter 6.

5.7 Flexural Testing of Heated/Repaired Specimens

After the heating of shallow RC beam samples and the repair of the normal depth FRP beams were completed, all beams were tested in flexure until failure. Heated samples were compared

to the earlier non-heated controls to assess how the high heat impacted the beam capacity.

Repaired beams were compared to calculated values to see if the presence of a previous coating

significantly affected the SRiP bonding.

5.7.1 Shallow Beam Tests

The graphs of the flexural testing displayed some encouraging results. After heating, all of the

SRiP reinforced beams maintained an ultimate load greater than that of the control RC beam.

The samples with inward facing or no steel wire backing material also maintained a long tail of

deflection still sustaining load after failure; this was not recorded in the two layer samples,

HHWT-1 and HHWT-2 (Figure 5.14).
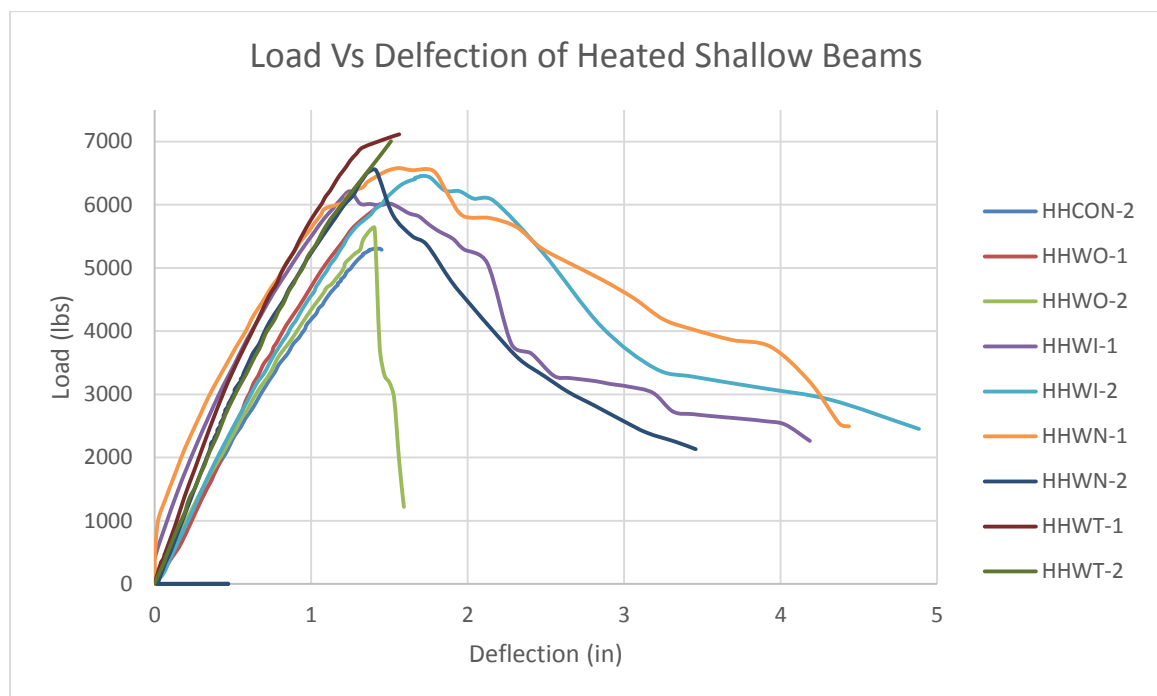
Figure 5.14: Load Vs Deflection Graph for all heated shallow beam samples

In the case of HHWO-1 and HHWO-2, the samples with backing material facing outward, a strength greater than the control beam was just barely achieved. During the heating it was noted that the backing material did melt even under the coating (Figure 5.15).
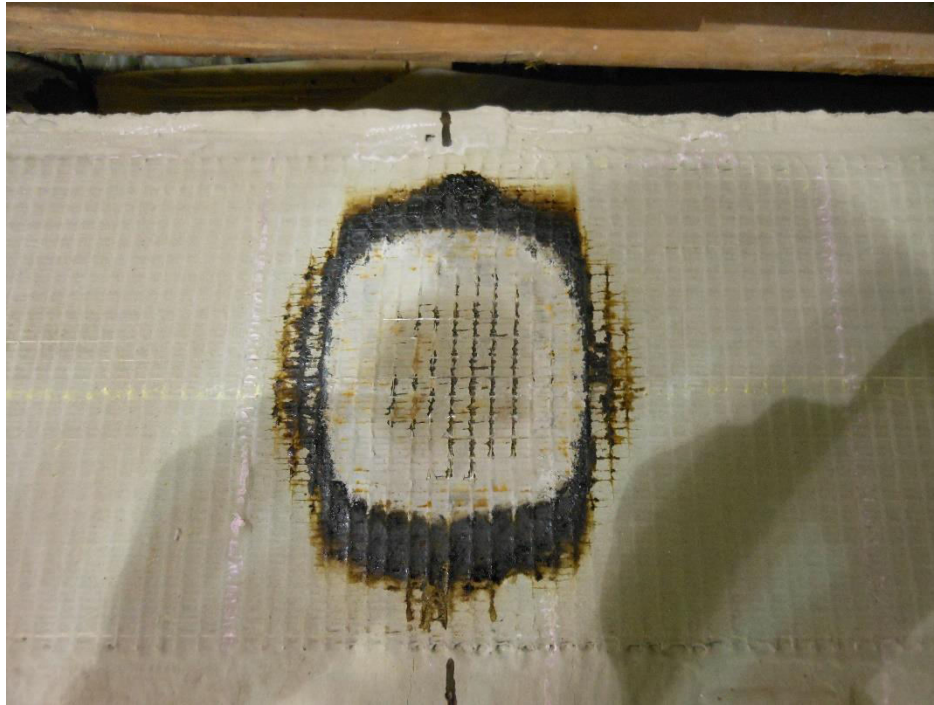
Figure 5.15: Discoloration due to burning backing material

At the time it was theorized that HHWI-1 and HHWI-2 with backing facing inward to the beam would suffer the most as the bond between the beam and SRIP could be compromised; however, it appears that having the backing facing away from the beam impacted the outer layers of geopolymer and allowed more heat to directly influence the steel wires. This greatly reduced the wires' strength and lead to them breaking more quickly than other samples (Figure 5.16). These wires broke through quickly and the backing material appeared in some spots to be a fiber no longer coated with the backing's matrix.

Figure 5.16: Damaged Hardwire Backing

Utilizing just the wires themselves with no backing material or two layers of backed Hardwire

eliminated or mitigated the impact of the backing in the high temperature environment. The

ability to maintain additional strength after the fire damage can be crucial to either allow for

small amounts of traffic to resume or keeping the base structure intact so simpler repairs can be

made to the SRiP and not the overall structure. Flexural result comparisons between heated and

non-heated beams have been made in the next section to give a better idea of high temperature

damage in the beams.

5.7.2 Comparison to Non-Heated Samples

To truly assess the damage done by fire, the heated samples must be directly compared with

non-heated counterparts. As stated in the previous section, maintaining load beyond the base

RC beam is a great achievement, but it must be determined if that load is enough to support any

use. For safety purposes, it would be recommended to make repairs no matter how effective

the SRiP is in reducing the fire damage, but the extent of those repairs is where SRiP of this design can show its true strength.

Below are load-deflection graphs comparing the heated shallow beams compared to their non-heated counterparts. One difference to note between the load-deflection graphs of heated samples and non-heated samples is the initial slope of the graphs. Non-heated samples have a small, steeper slope until they reach their cracking moment and then the slope of the curves decrease. The Heated samples were loaded past their cracking moments during the heating process so their initial slope shows no evidence of this cracking. Comments will be made on each set of beams after the graphs are shown. Each graph also included a control RC beam sample for measure. Heated samples are denoted 'HHW' for 'heated hardwire' while non-heated samples simply have 'HW' for their use of hardwire. In earlier testing, other forms of fiber were considered but data on some either showed no substantial improvement or proved inconclusive in initial testing.
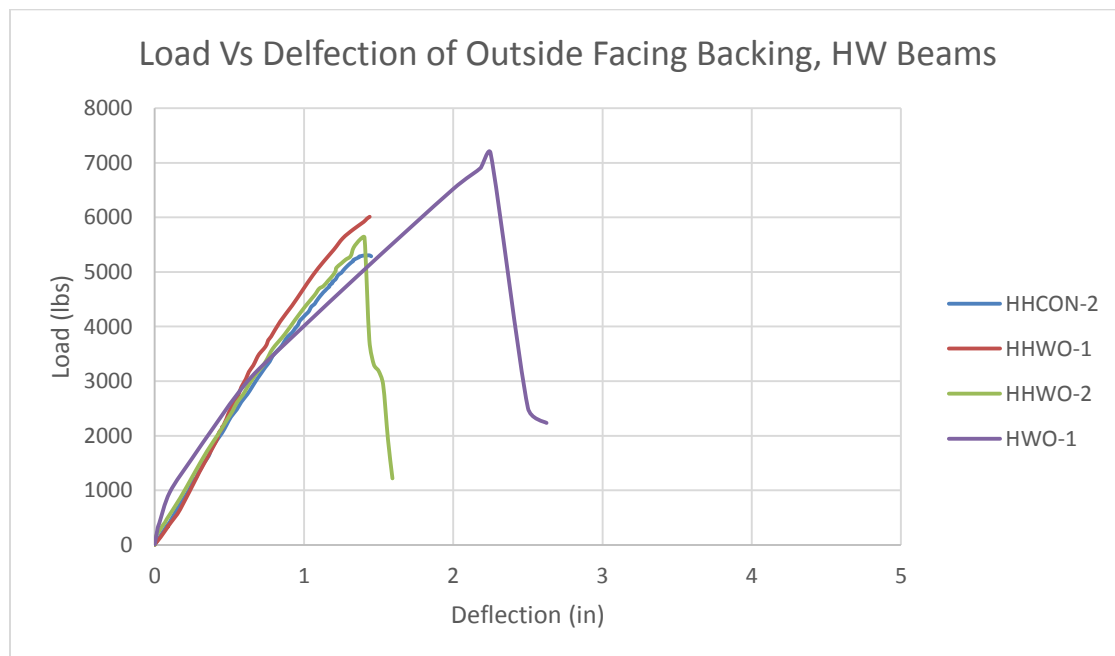
Figure 5.17: Load Vs Deflection of beams with Hardwire backing facing outside

The heated samples with Hardwire backing facing outward experienced a great deal of melting of the backing's own matrix. This, in turn, seeped up to the surface of the SRiP's aluminosilicate matrix and compromised its structure. The heated beams only held on average about 5800lbs of load compared to 7200lbs in the non-heated sample and 5300lbs in the control. While it is worth noting an actual fire event would not necessarily apply heat as up close as was the case in this research, this setup of steel wire with backing does not appear to be sufficient to provide a safe, post high temperature event scenario.
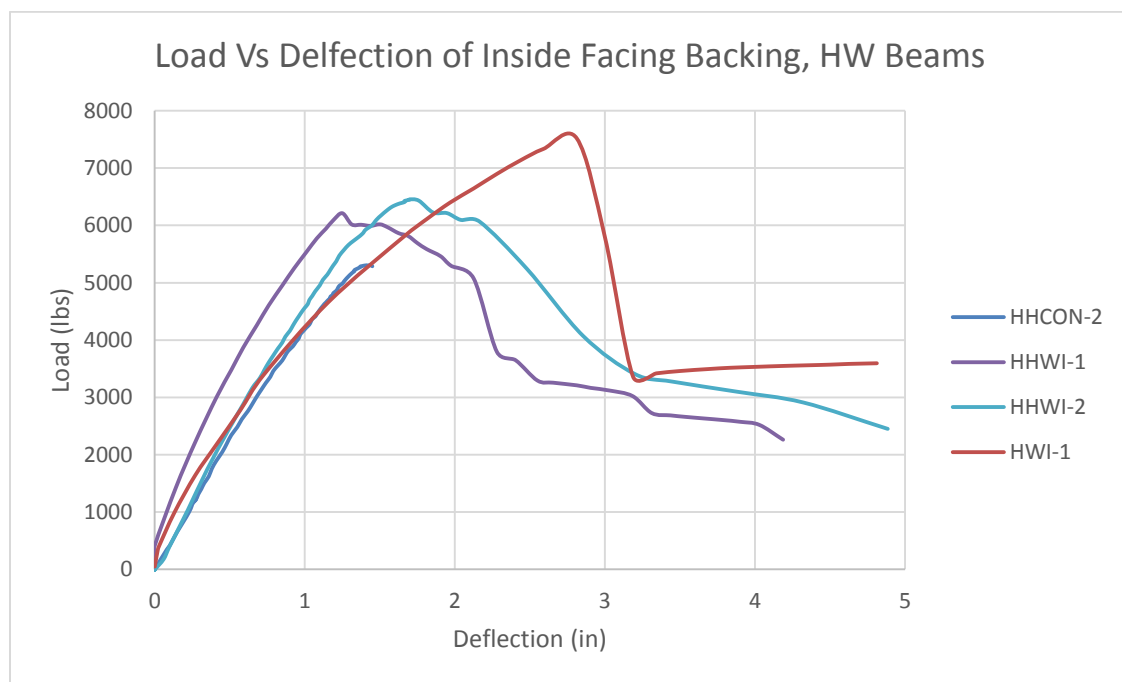
Figure 5.18: Load Vs Deflection of beams with Hardwire backing facing inside

Turning the Hardwire tape so the backing faced inward resulted in a an average heated ultimate load of approximately 6300lbs. When compared with the non-heated beam, heated samples provided 45% of the increase of a non-heated SRiP beam.
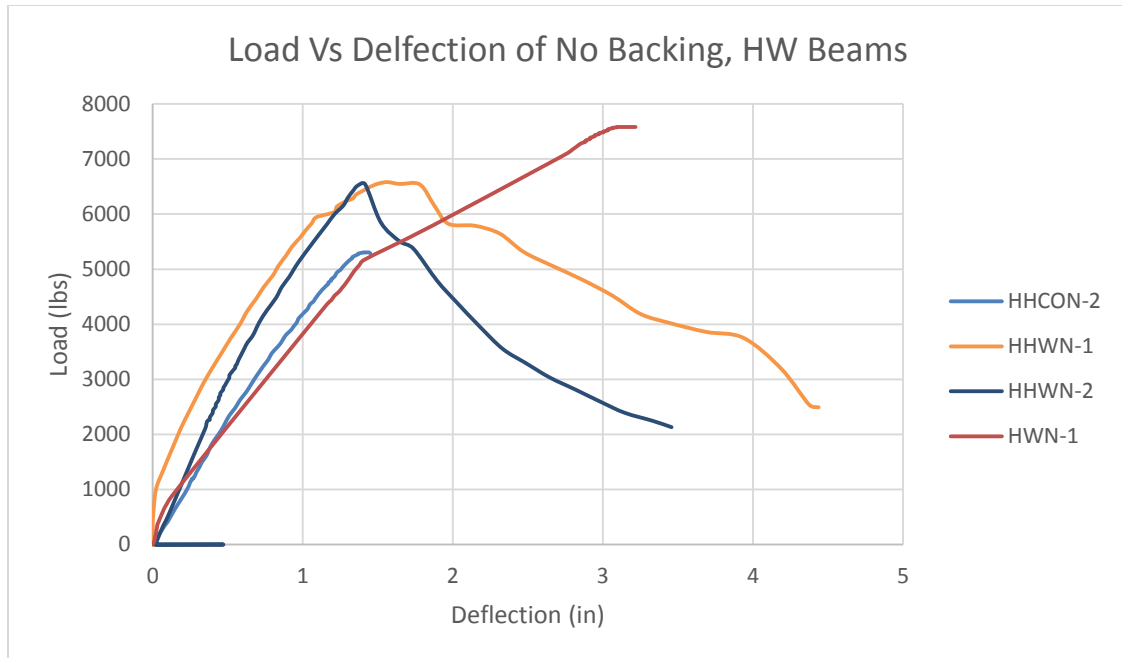
Figure 5.19: Load Vs Deflection of beams with Hardwire and no backing

The performance of the beams with no steel wire backing was very similar to those of the samples with backing facing inward. One would expect these beams to all behave similarly given the same amount of reinforcement and dimensions and these setups of SRiP showed much more predictable behavior. Performance of the non-backed beams here was slightly better than the previously discussed beams, around 55% of the load increase of the non-heated beam. The damage done to the steel wire backing mesh in prior samples is a clear explanation for this slight improvement in beam performance.
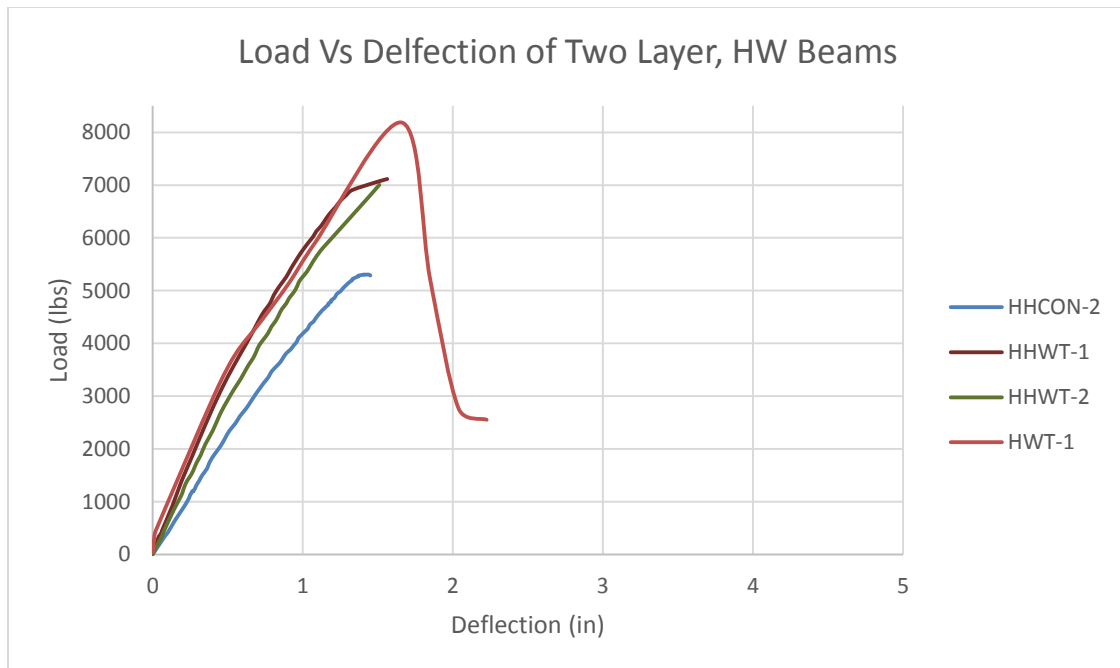
Figure 5.20: Load Vs Deflection of beams with two layers of Hardwire

Not only did an extra layer of Hardwire provide more strength to the SRiP beams, but it appears

to provide an extra bit of insurance against fire damage. The second layer of steel allows one

layer to sit further from the surface of the geopolymer matrix and helps reduce the heat it

experiences in a high temperature event. While there was still a drop off in load, the heated

beams still maintained 62% of the added SRiP strength compared to the non-heated beam.

Utilizing two layers of reinforcement instead of one wider layer can have a significant impact on

the effects of fire damage on SRiP beams. Future testing could investigate additional coating of

geopolymer and see if that too could have a significant impact. Insulation is another common

answer to protecting beams but insulation can too suffer damage from fire and requires an

additional step in the application process.

While the decrease in ultimate load of these heated beams is not ideal, benefits can still be

seen. Standard FRP systems are completely destroyed in temperatures as high as in this testing

and any maintained strength from SRiP is a positive. Ductility provides much safer failures and, combined with the residual SRiP strength, can allow for more orderly repairs and less catastrophic failures. Not all fires will last as long as the hour long cycles presented in this research and may not reach as high of temperatures as tested here. In those cases it could be theorized that less damage would be sustained due to the inorganic matrix.

5.7.3 Repaired Flexural Tests

Repaired beams were compared to expected, calculated values as the major question with these samples was that of bonding. As these beams received more surface preparation to remove existing coating than the shallow beams, issues in early debonding could be potentially attributed to reapplication of a geopolymer over an area previously impregnated by a similar matrix. Again, the aluminosilicate behaves similarly to concrete, which has trouble bonding to a similar material that has already been set.

The repaired beams had three variations in the matrix and one in the steel wires. Each sample was manufactured still using the Hardwire backing material and having that backing face inward to the beam. This directionality proved to be superior in earlier testing to facing away from the beam. Three geopolymers were used in this test: the base mix from earlier testing with 12g of chopped carbon fiber added before mixing, the base mix with 12g of carbon fiber blended in with the dry ingredients before mixing, and 18g of carbon fiber blended in before mixing. A beam with one layer of steel wire and a beam with two layers of steel wire were made with each matrix. The additional carbon fiber can help with the bonding of the geopolymer but can potentially make it too tacky or cause uneven setting. These conditions will be monitored for when mixing the samples.

The predicted flexural strength of the beams with one layer of steel and two layers of steel were calculated to be 14,431lbs and 21,293.73lbs, respectively. These values were calculated using equations listed in Chapter 6 for determining the ultimate load of strengthened, rectangular RC beams in bending. Table 5.2 below shows the ultimate loads of each beam.

Beam Designation	Experimental Ultimate Load (lbs)	Calculated Ultimate Load (lbs)	Percent Difference (%)
1 Layer, 12g	12602.87	14431	12.67
1 Layer, 12g Blended	14380.5	14431	0.35
1 Layer, 18g Blended	14003.96	14431	2.96
2 Layer, 12g	16035.85	21293.73	24.69
2 Layer, 12g Blended	14636.45	21293.73	31.26
2 Layer, 18g Blended	15248.78	21293.73	28.39

Table 5.2: Ultimate Loads of Rectangular RC Beams Repaired with SRiP

The single layer of Hardwire beams all performed incredibly close to expected, while the two layer beams underperformed by a significant percentage. The addition of a second layer increases the potential strength but clearly does not develop as strong a bond as the first layer. There is a possibility that these beams were also over reinforced to the extent that they would not physically be able to handle such a load at their current scale, despite the calculated potential. Focusing on the single layer samples, it is clear that a significant portion of the predicted strength was achieved in each and no noticeable problems arose from their grinding and recoating with geopolymer. The additions of extra chopped carbon fibers show no set pattern, however, and further study would be needed to come up with a more conclusive result.

5.8 Summary

- There is a gap in SRiP research in the area of high-temperate performance. FRP studies that involve high-temperatures often do not include any data on high strength steel. Most inorganic matrixes seen in heat studies are cement or grout based.

- Heating Regime based on previous heat cycle testing by M. Klein. To expand on that regime, the heated samples would also be tested to failure in flexure and compared to the non-heated samples addressed in chapter 4. Cycling the heat can show the reaction of the beams to higher temperatures while they happen. Testing the heated samples in flexure afterward will give a better understanding of the damage they sustained.

- Beams were subject to three Heating and cool cycles totaling six hours per beam. The time frame was determined by running a single test for 12 hours and identifying when drops or increases in loads leveled off. Data on deflection and load were both recorded using identical load and deflection gauges to the flexural testing.

- Two beams were tested of each reinforcement type. Beams were analyzed to identify how much load would be predicted to be lost due to the temperature gradient forming in the middle of each beam. This value was compared to actual load lost to gain insight on the change in curvature in the beam because of the high-temperature event.

- Most beams showed a 15-20% loss in load compared to a 14% loss in load with the plain RC beam. Slightly more than the control so some damage must have been sustained to the wires.

- The backing material on the Hardwire was convenient for installation but had a negative impact on the ability of beams to withstand the high temperatures. The backing melted, seeped out of the geopolymer and burned, causing both aesthetic and structural concerns.

- All heated beams maintained a higher ultimate load than the control but some were negligible. Having the backing material closer to the surface compromised the geopolymer and led to more heat damage.

- The best performers post heating were the beams with two layers of Hardwire. The second layer protected the first from the heat enough that the heated beams only showed a 38% drop off in additional strength provided compared to a similar non-heated sample.

- While not as much information was gleaned from the repaired beams as originally hoped there were still some positives from the testing. There was no clear front runner in terms of an amount of additional carbon fiber to add to the mix for improving bond. The one layer of Hardwire samples all preformed extremely close to predicted values, showing that the previous geopolymer coating had no impact on the bond of the new coating.

CHAPTER 6 – ANALYTICAL INVESTIGATION AND GUIDE FOR PRACTICAL APPLICATIONS

6.1 Introduction

A variety of calculations were utilized in predicting or analyzing the results of the numerous

tests run as part of this research. This chapter will look to go into more detail on these equations

as well as provide some practical suggestions for either further research or field use of SRiP

composites.

6.2 Analysis of SRiP Beams

As two major types of tests were effectively performed this section will detail out each

separately. Methods for analyzing the flexural performance of shallow beams or flexural

performance of the repaired beams, and the performance of shallow beams during the high-

temperature testing will all be addressed.

6.2.1 Analysis of Flexural Tested Beams

The addition of an external reinforcement system completely changes the focus of nominal

moment calculations from the tension steel in the beam to the external reinforcement applied

to the structure. While tension steel will still have an impact in balancing the forces of tension

and compression inside the beam, the composite plays a bigger role in understanding the strain

limits on the tension face of the beam. To calculate the ultimate load each beam could take the

nominal moment capacity was first determined using equations presented by Balaguru, Nanni,

and Giancaspro.

Firstly, β_1 must be calculated for the strength of concrete selected.

$$\beta_1 = 0.65 \text{ if f'c} \leq 4000\text{psi} \tag{6.1}$$

$$\beta_1 = 0.85 - 0.05*(\text{f'c} - 4000)/1000 \text{ if } 4000\text{psi} \leq \text{f'c} \leq 8000\text{psi} \tag{6.2}$$

$$\beta_1 = 0.85 \text{ if f'c} \geq 8000\text{psi} \tag{6.3}$$

Where f'c is the 28-day compressive strength of the concrete used

The minimum values of the reinforcement ratio, ρ, then need to be checked. These values

compare the area of concrete that could act in the beam with the area of reinforcement in the

beam.

$$\rho_{min} = the\ larger\ of\ ...\frac{200}{f_y}\ or\ \frac{3\sqrt{f'_c}}{f_y} \tag{6.4}$$

Where f_y is the yield stress of steel

As debonding and other factors contribute to the strength of a composite reinforced RC beam, a

scaling factor for the strain in the fibers of the composite, K_m, will be calculated.

$$K_M = 1 - \frac{nE_f t_f}{2,400,000}\ if\ nE_f t_f \leq 1,200,000 \tag{6.5}$$

$$K_M = 1 - \frac{600,000}{nE_f t_f}\ if\ nE_f t_f > 1,200,000 \tag{6.6}$$

Where n is the number of layers of composite

E_f is the Young's Modulus of the fiber (29,000,000 psi)

t_f is the thickness of the fibers (0.047in)

Once K_m has been determined the location of the neutral axis, c, is found, the strain in the

composite fiber, ε_f, is calculated, and the strain is compared to a factored strain value, ε_{fe}. The

result will determine the equations for the depth of the stress block, a, and the moment

capacity, M_n.

$$Solve\ for\ c\ using\ 0.85 f'_c b\beta_1 c = A_s f_y + A_f E_f 0.003(\frac{h-c}{c}) \tag{6.7}$$

Where b is the width of the beam

A_s is the area of tension steel

A_f is the area of the composite fibers

h is the depth of the beam

$$\varepsilon_f = 0.003(\tfrac{h-c}{c}) \tag{6.8}$$

$$\varepsilon_{fe} = K_m \varepsilon_{fu} \tag{6.9}$$

Where ε_{fu} is the ultimate strain of the fibers

$$\text{If } \varepsilon_{fe} > \varepsilon_f \tag{6.10}$$

$$\text{Solve for a using } 0.85f'_c b = A_s f_y + A_f E_f \varepsilon_{fe} \tag{6.11}$$

$$M_n = 0.85f'_c ba\left(c - \tfrac{a}{2}\right) + A_s f_y (d - c) + 0.85 A_f E_f \varepsilon_f (h - c) \tag{6.12}$$

$$\text{If } \varepsilon_{fe} \leq \varepsilon_f \tag{6.10}$$

$$a = \beta_1 c \tag{6.13}$$

$$M_n = A_s f_y \left(d - \tfrac{a}{2}\right) + A_f E_f \varepsilon_f (h - \tfrac{a}{2}) \tag{6.14}$$

From here the load on the beam can be calculated and compared to the actual loads each beam broke at. It should be noted one unique property of FRP systems is the danger of debonding that can occur. Should the composite debond, the predicted strength will not be achieved.

With this chord, an ultimate strain of 0.006 in/in seemed feasible for calculations of SRiP beam strength. This is higher than that traditionally depicted in ACI code. Further testing can verify this for SRiP reinforced beams and it could be possible to adapt the code to better match these strains.

6.2.2 Nonlinear Analysis of Heated Shallow Beams

In the case of a beam being heated uniformly across the entire structure, the method of virtual work can be used to help calculate the deflection in the beam due to a temperature gradient. As mentioned in Klein 2013, the method of virtual work does not apply perfectly to the setup of this heat cycling does not have a temperature gradient throughout the entire beam, and

reinforced concrete often does not have a neutral axis located in the center of its cross-section.

Klein utilized this method in earlier testing but switched to using the design guidelines

presented in the American Concrete Institute Committee 318 Code Provisions and elastic-beam

theory.

To begin, the flexural rigidity of each beam, elastic modulus multiplied by the area moment of

inertia of the beam cross section (EI), was calculated. These values are used to calculate the

deflection of each beam as it was initially loaded and confirm the beams' rigidity for the second

part of the analysis process.

To start, the cracking moment must be found using the modulus of rupture. The cracked

moment of inertia for the beam is then calculated. Both of these values are then used to find

the effect moment of inertia for the shallow beam sections, which when multiplied by the

elastic modulus of the concrete gives the beam stiffness.

$$M_{cr} = \frac{I_g}{h-y} f_r \qquad (6.15)$$

Where I_g is the gross moment of inertia

h is the height of the beam

y is the depth of the neutral axis

f_r is the modulus of rupture

$$I_{cr} = \frac{b(k_d)^3}{3} + (n-1)A'_s(k_d - d')^2 + nA_s(d - k_d)^2 + n_f A_f(h - k_d)^2 \qquad (6.16)$$

Where b is the width of the beam

k_d is the depth of the neutral axis

N is the ratio of the modulus of steel to the modulus of the concrete

A_s is the total area of the tension steel

d is the distance from the extreme compression fiber to the centroid of the tension steel

A'_s is the total area of the compression steel

d' is the distance from the extreme compression fiber to the centroid of the compression steel

n_f is the ratio of the modulus of the fiber to the concrete modulus

A_f is the total area of the fibers

$$I_e = I_{cr} + (I_g - I_{cr})(\frac{M_{cr}}{M})^3 \qquad (6.17)$$

Where M is the moment at which the deflection is being evaluated

For this calculation, the method presented by Klein in his confirmation testing was followed.

Klein derived an analysis method from the moment area theorem for point source heating,

noting differential expansion in the beam generating curvature beyond its initial deflected

shape. From this prior research we will assume the actual heat in surface of the beam is 950°F,

the coefficient of thermal expansion is 5.70 X 10-6/°F, and the strain just under the heat source

is 0.0045in/in (Klein 2013).

Klein proposed using classical elastic-beam theory but treating the depth of the neutral axis as

the lowest temperature measured directly under the heat source on the beam. This distance is

referred to as ds which expands to ds' when the heat is applied. The strain in the beam due to

the temperature gradient was defined as:

$$\varepsilon = \frac{(ds' - ds)}{ds} = \alpha \Delta T \qquad (6.18)$$

This equation can be combined with Hooke's law by using Elastic modulus ratios to treat the

beam as a homogeneous material. This combination results in:

$$\frac{1}{\rho} = \frac{\alpha \Delta T}{h} \qquad (6.19)$$

Where ρ is the curvature of the beam

h is the distance to the lowest temperature below the heating elements

Graphing the solutions of a series of elements, dx, from the maximum value under the heat source creates an equivalent curve to M/EI. The second moment-area theorem can then be used to find the deflections in each beam. The following equations can be used to calculate the additional deflection in a heated simply supported beam such as the ones used in this research. Traditional deflection equations can then be used to calculate the expected loss in load due to heating. The equations generated from the second moment-area method are presented below, where tA/B and tC/B are locations of tangent lines from the first locations, A and C, with respect to a second, B.

$$\Delta_c = \frac{t_{\frac{A}{B}}}{2} - t_{\frac{C}{B}} \qquad (6.20)$$

$$t_{\frac{A}{B}} = \bar{x} \int_A^B \frac{\alpha \Delta T}{h} dx \qquad (6.21)$$

$$t_{\frac{C}{B}} = \bar{x} \int_C^B \frac{\alpha \Delta T}{h} dx \qquad (6.22)$$

6.3 Recommendations for Practical Application

The most important recommendation that can be given when using an SRiP composite in an area with the chance of fire exposure would be to avoid any kind of backing material that may hold the selected steel together. While a mesh backing can keep fibers well aligned and provide even spacing for the strands, the presence of the backing can have adverse effects when temperatures start to increase.

Weight of steel wires can be an issue when installing an SRiP system in situ. During lab testing,

beams were able to be placed upside down so steel wires could easily be laid in the matrix

applied to the tension face of the beams. In an in use situation, the wires will have to be held up

onto the tension face of the beam as the geopolymer sets. Anchorages may be necessary

depending on the length of steel wire for the repair. It should be noted, however, that steel

strands are easier to manipulate than traditional fibers and can save time in that respect.

While using two layers of reinforcement can reduce some of the heat damage experienced in

the inner layer, outer layers can have more bonding issues. This can be especially true with steel

wires being much thicker than traditional fibers. If at all possible, use one layer of SRiP

composite and be sure to coat in generous number of thin layers of geopolymer.

A more detailed cost analysis would be needed to assess any economic benefits stemming from

materials and labor.

6.4 Summary

- Traditional equations for FRP reinforced RC beams are able to accurately calculated the

  flexural strength of FRP.

- A strain of 0.006 in/in appears accurate in calculating strength for SRiP beams and

  further confirmation and investigations into impact on code should be pursued.

- The temperature gradient present in the heated beams can make traditional linear

  analysis less accurate in determining induced curvature and loss of load. Utilizing an

  non-linear method, such as with the moment are method, allows for the M/EI graph to

  be substituted with one based on the changing temperature and in turn give a more

  accurate representation of the heat's effects.

- Important considerations for practical use include: weight of steel wires for attaching to the underside of existing structures, tradeoff between bonding issues and more protection when using multiple layers of reinforcement, and further economic study given the newness of the material.

CHAPTER 7 – CONCLUSIONS

The following paragraphs detail the major findings of this dissertations. To start a review of available state-of-the-art materials for FRP and fire and steel reinforced inorganic polymers.

- o The increase in shipping of flammable chemicals and liquids via trucks has led to more issues with fires on roadways. When these events occur near bridges or overpasses. These events can be especially catastrophic when traditional FRP composites are present.

- o Traditional FRP composites are highly susceptible to failure at increased temperatures. This is mostly due to the use of organic resins and epoxies as a matrix to affix fibers to concrete surfaces. These organic matrixes can quickly deteriorate in temperatures below that achieved by vehicle fires.

- o While carbon, glass, and other traditional fiber types can maintain strength in higher temperature, direct exposure to fire or other heating elements can still result in damage to the fibers themselves.

- o Inorganic matrixes, such as aluminosilicate geopolymer, have the ability to behave like a ceramic when in the presence of high temperatures. These properties allow for aluminosilicate geopolymer to prevent the common debonding issues of traditional polymer matrixes.

- o Though steel is not initially an obvious choice for use in fire related applications, the insulating properties of geopolymer, similar to concrete, and the ductility of steel compared to carbon or glass fibers can allow for much more controlled failures and more easily repaired beams.

The following observations were made from the research presented in this dissertation:

- SRiP composites maintain flexural load in a predictable fashion comparable to other FRP methods. SRiP can maintain bond with concrete without the need for lengthy and costly surface preparation techniques common to most FRP's. The testing also shows the potential for increasing the strain limits of SRiP code calculations to approximately 0.006 in/in. Further research would be recommended to see how code could adapt to this new material.

- While the use of steel wire "tape" can make the application of SRiP composite more efficient, the mesh backing used in some tapes can compromise the composite when exposed to high temperature events. If it is planned that in the instance of a fire, composite should be replaced no matter the damage, it may be beneficial to use the tapes and save cost on installation time.

- The addition of chopped carbon fiber can result in a better bond of the SRiP composite. The shorter fibers are sealed in the geopolymer and well protected from fire damage. These fibers tend to work better when mixed into the dry ingredients and blended before the edition of liquid components.

- Application of the coating must be done in relatively thin layers. Thicker layers can compromise bond due to increased odds of shrinkage cracking in the polymer. Shrinkage cracks are easily avoidable as long as layer thickness is maintained.

- Further exploration is needed to determine the true effects of iron oxide in these composites. Though improved bond with the concrete was hypothesized,

simple flexural repair tests were not enough to show one way or another that iron oxide impacted the bond strength.

- o SRiP reinforced beams were able to achieve a significant portion of their predicted flexural load even when debonding was the method of failure in the fibers, as opposed to failing completely through the composite wires.

- o Unlike traditional FRP composites, SRiP can maintain load even after it has been exposed to upwards of 1000°F. Even in cases where this is not enough to maintain full load of traffic, SRiP systems could prevent catastrophic failures that result in more costly repairs.

- o Nonlinear analysis through the moment area theorem provides a more accurate representation of the curvature and load losses that beams experiences with temperature gradients generated inside the beams.

- o Utilizing multiple layers of steel wire reinforcement can significantly improve the flexural capacity of a normal RC beam. The second layer potentially has the risk of debonding sooner as the beam will be stiffer with multiple layers of the comparably thick steel wire.

- o The aluminosilicate geopolymer can be ground off to allow for the replacement or composite with new layers. This could again allow more successful replacement of an existing system in the case of fire damage.

REFERENCES

ACI 211. 2014. Design of Normal Weight Concrete. Farmington Hills: American Concrete Institute.

ACI 318. 2014. Building Code Requirements for Reinforced Concrete. Farmington Hills: American Concrete Institute.

ACI Committee 440. 2002. Guide for the Design and Construction of Externally Bonded FRP Systems for Strengthening Concrete Structures. Guide, Farmington Hills: ACI.

Ahmed, Aqeel, and Kodur, Venkatesh. 2011. "Effect of bond degradation on fire resistance of FRP-strengthened reinforced concrete beams." Composites: Part B. 226-237.

Ahmed, Aqeel, and Kodur, Venkatesh. 2011. "The experimental behavior of FRP-strengthened RC beams subjected to design fire exposure." Engineering Structures. 2201-2211.

ASTM C882. 2012. "Standard Test Method for Bond Strength of Epoxy-Resin Systems Used With Concrete By Slant Shear." American Society for Testing and Materials

ASTM D6944. 2009. "Standard Practice for Resistance of Cured Coatings to Thermal Cycling." American Society for Testing and Materials

Avila, Melissa B., Dembsey, Nicholas A., and Dore, Charles. 2008. "Effect of type and glass content on the reaction to fire characteristics of typical FRP composites." Composites: Part A. 1503-1511.

Balaguru, Perumalsamy N. "Inorganic Polymer Composites for Protection of Aging Infrastructures." National Science Foundation. Arlington, VA, USA.

Balaguru P.N.; Kurtz S. 1998. "Use of inorganic polymer-fiber composites for repair and rehabilitation of infrastructures." Proceedings of the International Seminar on Repair and Rehabilitation of Reinforced Concrete Structures. 155-168

Balaguru, Perumalsamy, Antonio Nanni, and James Giancaspro. 2009. FRP Composites for Reinforced and Prestressed Concrete Structures. New York: Taylor and Francis.

Bakis C.E.; Bank L.C.; Brown V.L.; Cosenza E.; Davalos J.F.; Lesko J.J.; Machida A.; Rizkalla S.H.; Triantafillou T.C. "Fiber-Reinforced Polymer Composites for Construction—State-of-the-Art Review." Journal of Composites for Construction. 73-87.

Barton, B., Wobbe, E., Dharani, L.R., Silva, P., Birman, V., Nanni, A., Alkhrdaji, T., Thomas, J., and Tunis, G. 2005. "Characterization of reinforced concrete beams strengthened by steel reinforced polymer and grout (SRP and SRG) composites." Material Science and Engineering. 129-136.

Bisby, Luke, Green, Mark, and Kodur, Venkatesh K.R. 2005. "Response to fire of concrete structures that incorporate FRP." Prog. Struct. Engng. Mater. 136-149.

Blontrock H.; Taerwe L.; Vandevelde P. "Fire testing of concrete slabs strengthened with fibre composite laminates." Proceedings 5th Annual Symposium of Fibre-Reinforced-Plastic Reinforcement for Concrete Structures. London. 547-556

Brownstein, Jeremy. 2010. "Inorganic Polymer Fiber Composites for Protection of Structures." Thesis. New Brunswick, NJ: Rutgers, The State University of New Jersey, May.

Burke, Paul J., Bisby, Luke A., and Green, Mark F. 2013. "Effects of elevated temperature on near surface mounted and externally bonded FRP strengthening systems for concrete." Cement & Concrete Composites. 190-199.

Casadei, Paolo. 2005. "Steel-reinforced polymer: An innovative and promising material for strengthening infrastructures." Concrete Engineering International. 54-56.

Casadei, Paolo, Nanni, Antonio. "Steel reinforced polymer: An innovative and promising material for strengthening the infrastructures."

Casadei, Paolo, Nanni, Antonio, Alkhrdaji, Tarek, and Thomas, Jay. 2005. "Performance of Double-T Prestressed Concrete Beams Strengthened with Steel Reinforcement Polymer." Advances in Structural Engineering. 427-442.

Correla, Joao Ramoa. 2013. "The New FRP Materials for Civil Engineering Structural Applications." 57th Meeting of the European Council of Civil Engineers. May.

Cree, D., Chowdhury, E.U., Green, M.F., Bisby, L.A., and Benichou, N. 2012. "Performance in fire of FRP-strengthened and insulated reinforced concrete columns." Fire Safety Journal. 86-95.

Davidovits, J. 1991. "Geopolymers: Inorganic Polymeric New Materials." Journal of Thermal Analysis 1633-1656.

Davis, Martha, Paul Tremel, and Alex Pedrego. 2008. "Bill Williams River Concrete Bridge Fire Damage Assessment." Structure Magazine 30-32.

Del Prete, Iolanda, Bilotta, Antonio, and Nigro, Emidio. 2015. "Performances at high temperature of RC bridge decks strengthened with EBR-FRP." Composites Part B. 27-37.

El-Hacha, R., Rizkalla, S.H., and Kotynia R. "Modelling of Reinforced Concrete Flexural Members Strengthened with Near-Surface Mounted FRP Reinforcement. FRPRCS-7. 1681-1700.

Foden, Andrew J. 1999. "Mechanical Properties and Material Characterization of Polysialate Structural Composites." Dissertation. New Brunswick, NJ: Rutgers, The State University of New Jersey, January

Garon, Ronald J. 2000. "Effectiveness of High Strength Composites as Structural and Protective Coatings for Structural Elements." Dissertation. New Brunswick, New Jersey: Rutgers, The State University of New Jersey, May.

Giancaspro, James, Balaguru, P.N., and Lyon, Richard E. 2003. "Recent Advances in Inorganic Polymer Composites." Proceedings of the Thirteenth International Offshore and Polar Engineering Conference. Honolulu, Hawaii, USA. 263-270.

Hardwire LLC, 2013, What is Hardwire? www.hardwirellc.com. Pocomoke City, MD.

Hashemi, Siavash, and Riadh Al-Mahaidi. 2008. "Cement Based Bonding Material for FRP." Inorganic-Bonded Fiber Composites Conference. Madrid: Department of Civil Engineering, Monash University. 267-271.

Hashemi, Siavash, and Riadh Al-Mahaidi. 2012. "Experimental and finite element analysis of flexural behavior of FRP-strengthened RC beams using cement-based adhesives." Construction and Building Materials. 268-273.

Huang, X., Birman, V., Nanni, A., and Tunis, G. 2005. "Properties and potential for application of steel reinforced polymer and steel reinforced grout composites." Composites Part B. 73-82.

Ji, Gefu, Li, Guoquiang, and Alaywan, Walid. 2013. "A new fire resistant FRP for externally bonded concrete repair." Construction and Building Materials. 87-96.

Kamal, Osama A., Hamdy, Gehan A., and Abou-Atteya, Mohamed A. 2014. "Efficiency of coating layers used for thermal protection of FRP strengthened beams." Housing and Building National Research Center Journal. 183-190.

Katakalos, Konstantinos and Papkonstantinou, Christos G. 2009. "Fatigue of Reinforced Concrete Beams Strengthened with Steel-Reinforced Inorganic Polymers." Journal of Composites for Construction. 103-112.

Keller, Thomas. 2010. "Structural Performance of FRP Composites in Fire." Advances in Structural Engineering. 793-804.

Klein, Matthew J. 2013. "Nondestructive Repair and Rehabilitation of Structural Elements Using High Strength Inorganic Polymer Composites." Dissertation. New Brunswick, New Jersey: Rutgers, The State University of New Jersey, May.

Kodur, Venkatesh, and Aqeel Ahmed. 2011. "Behavior of FRP-Strengthened Reinforced Concrete Members Under Fire Conditions." Fire Protection Engineering, 1-13.

Kodur, V.K.R., and Naser, M.Z. 2013. "Importance factor for design of bridges against fire hazard." Engineering Structures. 207-220.

Kodur, Venkatesh, and Yu, B. 2014. "Fire behavior of concrete T-beams strengthened with near-surface mounted FRP reinforcement." Engineering Structures, 350-361.

Kurtz S.; Balaguru P.N. "Comparison of Inorganic and Organic Matrices for Strengthening of RC Beams with Carbon Sheets." Journal of Structural Engineering. 35-42.

Lopez, Alexis, Galati, Nestore, Alkhrdaji, Tarek, and Nanni, Antonio. 2007. "Strengthening of a reinforced concrete bridge with externally bonded steel reinforced polymer (SRP)." Composites Part B. 429-436.

Lyon, Richard E., P. N. Balaguru, Andrew Foden, Usman Sorathia, Joseph Davidovits, and Michel Davidovics. 1997. "Fire Resistant Aluminosilicate Composites." Fire and Materials 67-73.

Marston, N.J. 2007. "Fibre Reinforced Polymer Composites." BRANZ Study Report 172. BRANZ Ltd. Judgeford, New Zealand.

Menna, Costantino, Asprone, Domenico, Ferone, Claudio, Colangelo, Francesco, Balsamo, Alberto, Prota, Andrea, Cioffi, Raffaele, and Manfredi, Gaetano. 2013. "Use of geopolymers for composite external reinforcement of RC members." Composites: Part B. 1667-1676.

Nazier, Mohamed. 2004. "Evaluation of High Strength Composites and New Construction Techniques for Their Effective Use." Dissertation. New Brunswick, New Jersey: Rutgers, The State University of New Jersey, October.

Ng, Tian Sing, Foster, Stephen J., and Amin, Ali. 2013. " The behavior of steel-fibre-reinforced geopolymer concrete beams in shear." Magazine of Concrete Research. 308-318.

Nigro, Emidio, Cefarelli, Giuseppe, Bilotta, Antonio, Manfredi, Gaetano, and Cosenza, Edoardo. 2014. "Guidelines for flexural resistance of FRP reinforced concrete slabs and beams in fire." Composites: Part B. 103-112.

Papakonstantinou, Christios G. 2009. "Flexural behavior of reinforced concrete beams strengthened with a hybrid inorganic matrix-steel fiber retrofit system." Structural Engineering and Mechanics. 567-582.

Papakonstantinou C.G.; and Balaguru P.N. 2007. "Geopolymer protective coatings for concrete, International SAMPE Symposium and Exhibition." Baltimore, MD. 13.

Prota, Andrea, Tan, Kah Yong, Nanni, Antonio, Pecce, Marisa, and Manfredi, Gaetano. 2006. "Performance of Shallow Reinforced Concrete Beams with Externally Bonded Steel-Reinforced Polymer." ACI Structural Journal. 163-170

Rafi, Muhammad Masood, and Nadjai, Rafi. 2011. " Behavior of hybrid (steel-CFRP) and CFRP bar-reinforced concrete beams in fire." Journal of Composite Materials. 1573-1584.

Rizkalla, S., Dawood, M., and Shahawy, M. "FRP for Transportation and Civil Engineering Infrastructure: Reality and Vision."

Sasmal, S. 2013. "Nonlinear Finite Element Analysis of FRP Strengthened Reinforced Concrete Beams." Journal of The Institution of Engineers (India): Series A. 241-249.

Williams, B., L. Bisby, V. Kodur, J. Su, and M. Green. 2005. "An Investigation of Fire Performance of FRP-Strengthened RC Beams." International Symposium on Fire Safety Science. Beijing: National Research Council Canada. 247-258.

Won J.P.; Kang H.B.; Lee S.J.; Kang J.W. 2012. "Eco-friendly fireproof high-strength polymer cementitious composites." Construction and Building Materials. 406-412.

Wu, Hong-Chun, Chang, Ri-Cheng, Ou, Hsin-Jung, and Peng, Deng-Jr. 2010. "Case study on prevention of fire hazards in coating epoxy-based FRP work with illumination." 346-350.

Yu, B. and Kodur, Venkatesh. 2014. "Effect of high temperature on bond strength of near-surface mounted FRP reinforcement." Composite Structures. 88-97.

Yu, Baolin and Kodur, Venkatesh. 2014. "Effect of temperature on strength and stiffness of near-surface mounted FRP reinforcement." Composite Part B. 510-517.

Zhou, Le, Liu, Xiaoxing, Li, Ying, and Yan, Dong. 2012. "Nonlinear Analysis of FRP SRC Concrete Beams." Biotechnology, Chemical, and Materials Engineering. 201-204.